On the stability of periodic billiard paths in triangles

A Dissertation, Presented

by

W. Patrick Hooper

to

The Graduate School

in Partial Fulfillment of the

Requirements

for the Degree of

Doctor of Philosophy

in

Mathematics

Stony Brook University

May 2006

Abstract of the Dissertation

On the stability of periodic billiard paths in triangles

by

W. Patrick Hooper

Doctor of Philosophy

in

Mathematics

Stony Brook University

2006

A periodic billiard path in a triangle is considered stable if it persists under sufficiently small perturbations of the triangle. Several results pertaining to the question, "which triangles have stable periodic billiard paths?" are proved. Right triangles do not have stable periodic billiard paths. Further, periodic billiard paths in acute triangles and obtuse triangles are combinatorially different. All but countably many obtuse isosceles triangles have stable periodic billiard paths. On the other hand, there is a list of countably many isosceles triangles which do not have stable periodic billiard paths.

Stability of periodic billiard paths in triangles seems to be related to Veech's lattice property for triangles. We describe a previously unknown triangle with the lattice property.

Contents

List of Figures

Acknowledgements

First and foremost, I would like to thank my advisor, Yair Minsky, for the beautiful mathematics he has taught and for the support he has given. Speaking with Yair about mathematics has been a great clarifying experience for me. Through Yair, I have learned discipline and the power of carefully constructed logical arguments.

It was Rich Schwartz who realized that a computational approach to the triangular billiards conjecture could lead to new results. Rich deserves great thanks for allowing me to contribute to the McBilliards program, and giving me the freedom to do my own research within the context of triangular billiards. More importantly, Rich has been an unfailing source of mathematical inspiration since I was an undergraduate.

Both Yair and Rich deserve thanks for wading through early versions of this thesis.

I would like to thank Barak Weiss for the idea of searching for obtuse Veech triangles, and Curt McMullen for his encouragement to write this result down. Curt also deserves thanks for pointing out a significant logical error in an early version of chapter 8.

Giving an enlightening talk is one of the most difficult tasks faced by a mathematician faces. Thankfully, I have received helpful feedback on my talks from Bill Goldman, John Smillie, Barak Weiss, and others. I am grateful for such constructive critisism.

I would like to thank Stony Brook and Yale Universities for providing wonderful environments for learning mathematics. I have been fortunate to learn from so many great mathematicians.

Finally, I would also like to thank several of my friends: Daniel An, Matt Bainbridge, Jason Behrstock, Hrant Hakobyan, Hossein Namazi, and the late Candida Silveira.

Chapter 1

Introduction

We are concerned with the stability of periodic billiard paths in triangles under perturbation of the triangle. Interest in this question derives from the following:

Open Question 1.1. *Does every triangle have a periodic billiard path?*

A periodic billiard path in a triangle Δ is a piecewise linear closed loop which bends only at points in the boundary $\partial\Delta$. The angle of incidence must equal the angle of reflection.

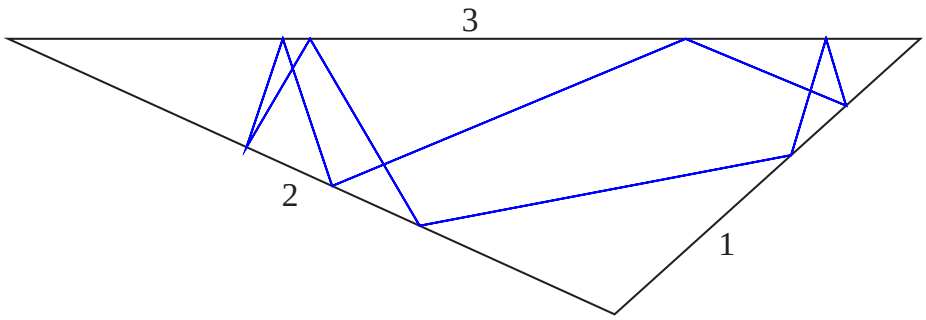

Figure 1.1: A periodic billiard path in a triangle. For this example $s_{\widehat{\gamma}} = \overline{123232313}$ repeating.

We mark the sides of our triangle with the integers in $\{1, 2, 3\}$. A periodic billiard path $\widehat{\gamma}$ in a triangle gives rise to the bi-infinite periodic sequence of marked edges it hits. We call this sequence the *symbolic dynamics of* $\widehat{\gamma}$ and denote it by $s_{\widehat{\gamma}}$. Formally, we say that a periodic billiard path in a triangle Δ is *stable* if there is an open set U of marked triangles up to similarity containing Δ, so that every Δ' has a periodic billiard path $\widehat{\gamma}'$ with the same symbolic dynamics ($s_{\widehat{\gamma}} = s_{\widehat{\gamma}'}$).

The relationship between the open question above and stability of periodic billiard paths stems from

Proposition 1.2. *If the angles (in radians) of the triangle Δ are linearly independent over the integers, then all periodic billiard paths in Δ are stable.*

We will prove this proposition in chapter 3. Equivalent statements appear in [Tab95] and [VGS92]. Motivated by this relationship we pose a related open question.

Open Question 1.3. *Which triangles admit stable periodic billiard paths?*

Perhaps surprisingly, some triangles do and some triangles do not. Let us now summarize what is known and what we will prove.

In the 1700's, Fagnano demonstrated that every acute triangle admits a periodic billiard path $\widehat{\gamma}$ with symbolic dynamics $s_{\widehat{\gamma}} = \langle \ldots, 1, 2, 3, 1, 2, 3, \ldots \rangle$.

As for right triangles, we will show that right triangles never admit stable periodic billiard paths (See also [Hoo06]). This answers a question posed by Vorobets, Gal′perin, and Stëpin, who proved it for a countable set of right triangles [VGS92]. We will demonstrate the stronger result:

Theorem A. *If $\widehat{\gamma}_{ob}$ is a stable periodic billiard path in an obtuse triangle Δ_{ob} and $\widehat{\gamma}_{ac}$ is a stable periodic billiard path in an acute triangle Δ_{ac} then their symbolic dynamics differ ($s_{\widehat{\gamma}_{ob}} \neq s_{\widehat{\gamma}_{ac}}$).*

Proof of this fact constitutes chapter 4 of this thesis. Let us sketch the argument now.

We give the space of marked triangles, $\mathcal{T}$, up to similarity the structure of a Euclidean 2-simplex in $\mathbb{R}^3$ by identifying each triangle with the ordered triple consisting of the angles of the triangle in radians. We say that the *tile of a periodic billiard path* $\widehat{\gamma}$, *tile*$(s_{\widehat{\gamma}})$, is the collection of all triangles that have periodic billiard paths with symbolic dynamics $s_{\widehat{\gamma}}$. It is known that if $\widehat{\gamma}$ is stable than *tile*$(s_{\widehat{\gamma}})$ is an open set with piecewise smooth boundary. However, *tile*$(s_{\widehat{\gamma}})$ might be a complicated. For example, it is unknown if *tile*$(s_{\widehat{\gamma}})$ is always connected or simply connected.

In chapter 4, we use topological ideas to define finite union of lines $UF(s_{\widehat{\gamma}}) \subset \mathcal{T}$ so that *tile*$(s_{\widehat{\gamma}})$ and $UF(s_{\widehat{\gamma}})$ are disjoint. We call this union the *unfriendly set*. We prove

Theorem B. *If $\widehat{\gamma}$ is a stable periodic billiard path in a triangle, then tile$(s_{\widehat{\gamma}})$ is contained in a single component of $\mathcal{T} \smallsetminus UF(s_{\widehat{\gamma}})$.*

We can compute this component explicitly. This gives us a convex polygonal bounding box for the tile. We then demonstrate that regardless of the choice of a stable periodic billiard path $\widehat{\gamma}$, the right triangles are all contained in $UF(s_{\widehat{\gamma}})$. Then theorem A follows.

Recently, Richard Schwartz has demonstrated that if Δ is an obtuse triangle with largest angle less or equal to 100 degrees than Δ has a stable periodic billiard path. See [Sch06a], and [Sch06b].

The story for isosceles triangles is interesting.

Theorem C. *There are obtuse isosceles triangles with and without stable periodic billiard paths.*

1. *All but countably many obtuse isosceles triangles have stable periodic billiard paths.*

2. *Countably many obtuse isosceles triangles do not have stable periodic billiard paths.*

The two statements of this theorem have distinct proofs. We prove the existence of stable periodic billiard paths in all but countably many obtuse isosceles triangles in chapter 5. We prove the existence of a countable collection of obtuse isosceles triangles that do not have stable periodic billiard paths in chapter 7.

Interestingly, the countably many obtuse triangles which do not have stable periodic billiard trajectories are triangles with *Veech's lattice property.* That is, these triangles unfold into translation surfaces with an affine automorphism group which is a lattice. Veech's lattice property can be defined for polygons with arbitrarily many sides. One amazing consequence of Veech's work is that if a polygon has Veech's lattice property, then the countably infinite collection of periodic billiard paths in the polygon can be listed off in a simple manner. A precise definition of Veech's lattice property will be given in chapter 6, as well as a brief introduction to the implications of this property. See also [MT02], [Vee89].

The list of known triangles with the lattice property consists of

1. The acute isosceles triangles with angles $(\frac{(n-1)\pi}{n}, \frac{(n-1)\pi}{n}, \frac{\pi}{2n})$ for $n \geq 3$. (due to Veech [Vee89]).

2. The acute triangles $(\frac{\pi}{4}, \frac{\pi}{3}, \frac{5\pi}{12})$, $(\frac{\pi}{5}, \frac{\pi}{3}, \frac{7\pi}{15})$, $(\frac{2\pi}{9}, \frac{\pi}{3}, \frac{4\pi}{9})$. (due to Veech [Vee89], Vorobets [Vor96], and Kenyon and Smillie [KS00] respectively).

3. The right triangles with angles $(\frac{\pi}{n}, \frac{(n-2)\pi}{2n}, \frac{\pi}{2})$ for $n \geq 4$. (due to Veech [Vee89]).

4. The obtuse isosceles triangles with angles $(\frac{\pi}{n}, \frac{\pi}{n}, \frac{(n-2)\pi}{n})$ with $n \geq 5$. (due to Veech [Vee89]).

5. The obtuse triangles with angles $(\frac{\pi}{2n}, \frac{\pi}{n}, \frac{(n-3)\pi}{2n})$ with $n \geq 4$. (due to Ward [War98]).

It is known that this list is complete in the case of acute, right, and isosceles triangles. See [Puc01] and [KS00]. In chapter 8, we add a new obtuse triangle to this list.

Theorem D. *The obtuse triangle with angles* $(\frac{\pi}{12}, \frac{\pi}{3}, \frac{7\pi}{12})$ *has Veech's lattice property.*

Chapter 2

McBilliards

Motivated by the large number of unanswered questions concerning billiards in triangles whose angles are irrational multiples of π, Rich Schwartz wrote a computer program called *McBilliards* [1]. Later, I collaborated with Rich to make the program faster and more featured.

With McBilliards, the user is able to select a triangle Δ. McBilliards can then do a search, returning all periodic billiard paths which hit less than N sides of the triangle in a period, for any given N. Suppose the search returns a periodic billiard path $\widehat{\gamma}$ in the triangle Δ. Given this information, McBilliards is capable of rigorously computing the collection of all triangles Δ' for which there is a periodic billiard path $\widehat{\gamma}'$ in Δ' with the same symbolic dynamics $s_{\widehat{\gamma}'} = s_{\widehat{\gamma}}$. We call this set $\mathit{tile}(s_{\widehat{\gamma}})$.

Using McBilliards, it has been possible to explore the parameter space of triangles and experimentally investigate questions about billiards. Theorem A was first an obvious conjecture which could be formulated after playing with very early versions of McBilliards. As McBilliards improved, it became reasonable to expect theorem C to be true. Several of Rich Schwartz's results on billiards in triangles are similarly motivated by observations gained by experimenting with McBilliards. See [Sch06a] and [Sch06b].

Using McBilliards, it seems that the following strengthening of theorem C should be true.

Conjecture 2.1. *The obtuse isosceles triangles which do not have stable periodic billiard paths are those with angles* $(\frac{\pi}{2^{k+1}}, \frac{\pi}{2^{k+1}}, \pi - \frac{\pi}{2^k})$ *for* $k \geq 2$.

The discovery of a new triangle with the lattice property (theorem D) also has roots in McBilliards. Kenyon and Smillie discovered a necessary condition for a triangle to satisfy the lattice property [KS00]. This condition is defined given a periodic billiard trajectory. Since McBilliards is capable of finding periodic billiard trajectories in triangles, it can check this condition. A search unveiled the $(\frac{\pi}{12}, \frac{\pi}{3}, \frac{7\pi}{12})$ triangle.

[1] McBilliards is freely available online at `http://www.math.sunysb.edu/~pat/` or `http://www.math.brown.edu/~res/`.

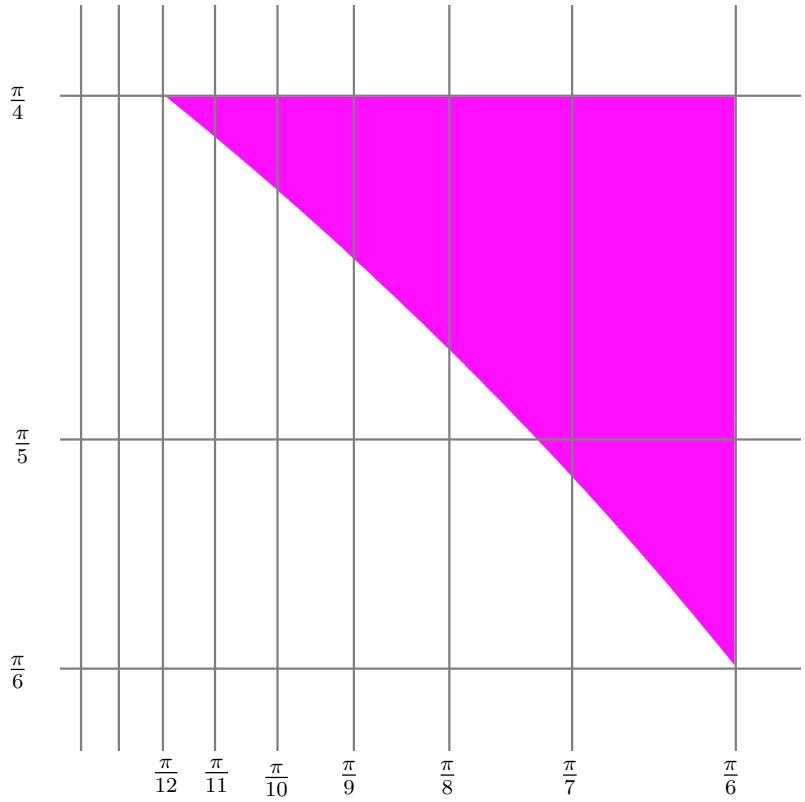

Figure 2.1: An example $tile(s_{\widehat{\gamma}})$.

Chapter 3

Euclidean cone surfaces and stability

Let us first define a *cone*. Consider the plane with the origin removed, $\mathbb{R}^2 \setminus 0$. Points are identified by their polar coordinates (r, θ) with $r > 0$ and θ defined $\pmod{2\pi}$. We lift to the universal cover $\widetilde{\mathbb{R}^2 \setminus 0}$, where points are identified by (r, θ) with $r > 0$ and $\theta \in \mathbb{R}$. The *cone* C_α with cone angle $\alpha > 0$ is the surface

$$\left(\widetilde{\mathbb{R}^2 \setminus 0}/\sim\right) \cup \{0\}$$

Where $\sim$ is the equivalence relation on $\widetilde{\mathbb{R}^2 \setminus 0}$ defined

$$(r_1, \theta_1) \sim (r_2, \theta_2) \text{ if } r_1 = r_2 \text{ and } \theta_1 - \theta_2 \text{ is an integer multiple of } \alpha$$

A *cone surface* is an surface S with a finite singular set $\Sigma \subset S$, so $S \setminus \Sigma$ is locally isometric to the plane, and each point $p \in \Sigma$ has a neighborhood $U_p \subset S$ which is isometric to a subset of a cone C_α under a map sending p to the apex of the cone.

A relevant example cone surface $\mathcal{D}_\Delta$ can obtained by doubling a triangle Δ across its boundary as in figure 3.1. In this case, there are three cone angles of magnitude twice the angles of the triangle.

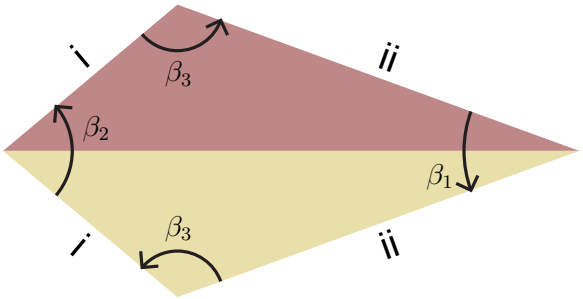

Figure 3.1: The cone surface $\mathcal{D}_\Delta$ can be built by doubling a triangle Δ across its boundary. The singular set Σ consists of the vertices.

The *billiard flow* on a triangle is the standard geodesic flow on unit tangent

vectors based in the interior of the triangle. Tangent vectors on the boundary of the triangle are glued so that the angle of incidence is equal to the angle of reflection. Then the billiard flow "bounces" a vector pointed at an edge of the triangle off the edge, just as you expect the velocity vector of a billiard ball to change when it bounces. In general, the billiard flow can not be well defined at the vertices. A *periodic billiard path* on a triangle is a loop with speed 1 on the interior of a triangle whose derivative (a loop on the unit tangent space of the triangle with identifications) is invariant under the billiard flow. We do not allow periodic billiard paths to pass through the vertices of the triangle.

There is folding map $\mathcal{D}_\Delta \to \Delta$ which is 2-1 except along the boundary of the triangle. The billiard flow on Δ can be pulled back under the folding map to the standard geodesic flow on $\mathcal{D}_\Delta \smallsetminus \Sigma$. Thus, a periodic billiard path $\widehat{\gamma}$ on Δ lifts to a closed geodesic γ on $\mathcal{D}_\Delta \smallsetminus \Sigma$. Conversely, a closed geodesic on $\mathcal{D}_\Delta \smallsetminus \Sigma$ can be pushed down to a billiard path on Δ.

We use $\mathcal{T}$ to denote the space of marked triangles up to similarity. The marking allows us to differentiate angles and edges. All of our triangles will lie in this space.

In the introduction, we mentioned that the symbolic dynamics of a periodic billiard path $\widehat{\gamma}$ is the bi-infinite sequence of marked edges the billiard ball hits. Let γ be the pull back to a closed geodesic on $\mathcal{D}_\Delta$. Then, this same sequence is realized by the sequence of marked edges of the triangulation of $\mathcal{D}_\Delta$ that γ hits. We call this sequence the *symbolic dynamics* of γ and denote it s_γ.

We say that a geodesic γ on $\mathcal{D}_\Delta \smallsetminus \Sigma$ is *stable* if there is an open set of triangles $U \subset \mathcal{T}$ containing Δ so that for all $\Delta_2 \in U$ there is a geodesic γ_2 on $\mathcal{D}_{\Delta_2} \smallsetminus \Sigma$ with the same symbolic dynamics ($s_\gamma = s_{\gamma_2}$). By the discussion above, this definition of stability for γ is equivalent to the definition of stability of $\widehat{\gamma}$ introduced in the introduction.

We now provide a necessary and sufficient algebraic condition for the stability of a geodesic on $\mathcal{D}_\Delta$. Equivalent forms of this fact appear in [Tab95, lemma 3.3.1] and [VGS92, equation 3].

Theorem 3.1 (Stability Theorem). *The closed geodesic $\gamma \subset \mathcal{D}_\Delta \smallsetminus \Sigma$ is stable if and only if γ is null-homologous in $\mathcal{D}_\Delta \smallsetminus \Sigma$.*

To prove this, we break the proof into two pieces.

Proof of the stability theorem; necessity: We will prove that if γ is a stable closed oriented geodesic in $\mathcal{D}_\Delta \smallsetminus \Sigma$ then it is null-homologous. Let γ' denote the loop contained in the unit tangent bundle $T_1(\mathcal{D}_\Delta \smallsetminus \Sigma)$ obtained by taking the unit tangent at every point of γ that agree with the orientation. To save breath, we call this the *lift of γ to the unit tangent bundle*.

Let $T_1\mathbb{R}^2$ denote the unit tangent bundle to the plane, and $\theta : T_1\mathbb{R}^2 \to \mathbb{R}/2\pi\mathbb{Z}$ denote the usual measure of directions in the plane in terms of angle. Note that θ is invariant under the geodesic flow in the plane. We will be concerned with $d\theta$ which is the closed differential 1-form on $T_1\mathbb{R}^2$ obtained by differentiating the multi-valued function θ.

Because $\mathcal{D}_\Delta \smallsetminus \Sigma$ is locally isometric to the plane and $d\theta$ is invariant under isometries of the plane, the $d\theta$ form on $T_1\mathbb{R}^2$ pulls back to closed differential 1-form on $T_1(\mathcal{D}_\Delta \smallsetminus \Sigma)$. We will denote this pull-back form by $d\theta_\Delta$. Further, γ' is invariant under the geodesic flow on $T_1(\mathcal{D}_\Delta \smallsetminus \Sigma)$ and θ is invariant under the geodesic flow on $T_1\mathbb{R}^2$, so

$$\int_{\gamma'} d\theta_\Delta = 0 \tag{3.1}$$

But since $d\theta$ is a closed form, this integral is only dependent on the homology class $[\![\gamma']\!]$ in $H_1\big(T_1(\mathcal{D}_\Delta \smallsetminus \Sigma), \mathbb{Z}\big)$.

In fact, $[\![\gamma']\!]$ is determined by the symbolic dynamics of the geodesic γ. Take two oriented geodesics γ_1 and γ_2 with the same symbolic dynamics in $\mathcal{D}_{\Delta_1} \smallsetminus \Sigma$ and $\mathcal{D}_{\Delta_2} \smallsetminus \Sigma$ respectively. Lift each loop to the universal cover. (That is, take a single geodesic in the pre-image.) The lifts $\widetilde{\gamma}_i \subset \widetilde{\mathcal{D}_{\Delta_i} \smallsetminus \Sigma}$ are geodesics and are therefore simple. There is a homeomorphism $\phi : \widetilde{\mathcal{D}_{\Delta_1} \smallsetminus \Sigma} \to \widetilde{\mathcal{D}_{\Delta_2} \smallsetminus \Sigma}$ which

1. takes the triangulation of $\widetilde{\mathcal{D}_{\Delta_1} \smallsetminus \Sigma}$ by copies of Δ_1 to the triangulation of $\widetilde{\mathcal{D}_{\Delta_2} \smallsetminus \Sigma}$ by copies of Δ_2
2. and takes $\widetilde{\gamma}_1$ to $\widetilde{\gamma}_2$.

Item 1 tells us that ϕ is homotopic to the identity as a map $T_1(\widetilde{\mathcal{D}_{\Delta_1} \smallsetminus \Sigma}) \to T_1(\widetilde{\mathcal{D}_{\Delta_2} \smallsetminus \Sigma})$. For each $\widetilde{\gamma}_i$, let $\widetilde{\gamma}'_i \subset T_1(\widetilde{\mathcal{D}_{\Delta_i} \smallsetminus \Sigma})$ be the corresponding lift to the unit tangent bundle of $\widetilde{\mathcal{D}_{\Delta_i} \smallsetminus \Sigma}$. Then $\gamma'_2 \subset T_1(\mathcal{D}_{\Delta_1} \smallsetminus \Sigma)$ can be obtained from $\gamma'_1 \subset T_1(\mathcal{D}_{\Delta_1} \smallsetminus \Sigma)$ by

1. lifting γ'_1 to $\widetilde{\gamma}'_1 \subset T_1(\widetilde{\mathcal{D}_{\Delta_1} \smallsetminus \Sigma})$, then
2. mapping $\widetilde{\gamma}'_1$ to $\widetilde{\gamma}'_2$ under the homotopically trivial map ϕ, and
3. pushing $\widetilde{\gamma}'_2$ down to γ'_2 under the covering $T_1(\widetilde{\mathcal{D}_{\Delta_2} \smallsetminus \Sigma}) \to T_1(\mathcal{D}_{\Delta_2} \smallsetminus \Sigma)$.

Because ϕ is homotopically trivial on the unit tangent bundles of the universal covers, γ'_1 and γ'_2 are homotopic on the homeomorphic spaces $T_1(\mathcal{D}_{\Delta_1} \smallsetminus \Sigma)$ and $T_1(\mathcal{D}_{\Delta_2} \smallsetminus \Sigma)$. Therefore, their homology classes are identical ($[\![\gamma'_1]\!] = [\![\gamma'_2]\!]$). A related argument appears in section 4.2 as one of the central ideas of the chapter.

Assume γ is a stable geodesic on $\mathcal{D}_\Delta$. Then there is an open neighborhood $U \subset \mathcal{T}$ containing Δ of triangles with closed geodesics with the same symbolic dynamics. By the previous argument, all the lifts of these geodesics to the unit tangent bundle lie in the same homology class as $[\![\gamma']\!]$. Therefore,

$$\int_{[\![\gamma']\!]} d\theta_T = 0 \qquad \text{for all triangles } T \in U \tag{3.2}$$

We will prove in proposition 3.3 below that $H_1\big(T_1(\mathcal{D}_\Delta \smallsetminus \Sigma), \mathbb{Z}\big)$ is generated by the homology classes of three loops β'_1, β'_2, and β'_3 on $T_1(\mathcal{D}_\Delta)$ which wrap around

the cone points of Σ. The loops are shown in figure 3.1. If α_1, α_2 and α_3 are the respective angles of the triangle Δ (and half the respective cone angles on $\mathcal{D}_\Delta$), it follows from the Gauss-Bonnet formula that

$$\int_{[\![\beta_i']\!]} d\theta_\Delta = 2\alpha_i \qquad \text{for } i = 1, 2, 3 \tag{3.3}$$

By proposition 3.3, we can write $[\![\gamma']\!] = n_1[\![\beta_1']\!]+n_2[\![\beta_2']\!]+n_3[\![\beta_3']\!]$ for some $n_1, n_2, n_3 \in Z$. Therefore,

$$\int_{[\![\gamma']\!]} d\theta_\Delta = 2n_1\alpha_1 + 2n_2\alpha_2 + 2n_3\alpha_3 \tag{3.4}$$

But for generic triangles, the angles of the triangle are linearly independent over the integers. For equation 3.4 to be zero on an open set U as required by equation 3.2, it must be true that $n_1 = n_2 = n_3 = 0$ and so γ' must be null-homologous in $H_1\big(T_1(\mathcal{D}_\Delta \smallsetminus \Sigma), \mathbb{Z}\big)$.

Finally, we observe that the projection to the base of the unit tangent bundle $T_1(\mathcal{D}_\Delta \smallsetminus \Sigma) \to \mathcal{D}_\Delta \smallsetminus \Sigma$ induces a homomorphism on homology. This sends γ' to γ and therefore γ is null-homologous on $\mathcal{D}_\Delta \smallsetminus \Sigma$. $\diamondsuit$

Remark 3.2. *The above proof also demonstrates half of the proof of proposition 1.2. If the angles (in radians) of the triangle Δ are linearly independent over the integers, then all periodic billiard paths in Δ are null-homologous. When we prove null-homologous implies stable, we will have demonstrated proposition 1.2.*

In the proof above we skipped the step of proving the generators of $H_1\big(T_1(\mathcal{D}_\Delta \smallsetminus \Sigma), \mathbb{Z}\big)$ were as claimed.

Proposition 3.3 (Homological Generators). *The homology class $H_1\big(T_1(\mathcal{D}_\Delta \smallsetminus \Sigma), \mathbb{Z}\big)$ is generated by the loops β_1', β_2', and β_3' which are the derivatives of the three loops which wrap once around each of the three points in Σ.*

Proof: Since $T_1\mathcal{D}_\Delta \smallsetminus \Sigma$ is a circle bundle over $\mathcal{D}_\Delta \smallsetminus \Sigma$, we know

$$0 \to H_1(S^1) \to H_1(T_1\mathcal{D}_\Delta \smallsetminus \Sigma) \to H_1(\mathcal{D}_\Delta \smallsetminus \Sigma) \to 0 \tag{3.5}$$

is an exact sequence. These maps are induced by the inclusion $S^1 \to T_1\mathcal{D}_\Delta \smallsetminus \Sigma$ as a unit tangent circle to a single point P and the projection to the base $p : T_1\mathcal{D}_\Delta \smallsetminus \Sigma \to \mathcal{D}_\Delta \smallsetminus \Sigma$. Because $H_1(\mathcal{D}_\Delta \smallsetminus \Sigma)$ is free abelian, the sequence splits

$$H_1(T_1\mathcal{D}_\Delta \smallsetminus \Sigma) \cong H_1(S^1) \oplus H_1(\mathcal{D}_\Delta \smallsetminus \Sigma)$$

The homology group of the three punctured sphere, $H_1(\mathcal{D}_\Delta \smallsetminus \Sigma)$, is isomorphic to $\mathbb{Z}^2$ and generated by $[\![\beta_1]\!]$ and $[\![\beta_2]\!]$ of figure 3.1. Since, $p : \beta_i' \mapsto \beta_i$, we have the $H_1(\mathcal{D}_\Delta \smallsetminus \Sigma)$ factor in the group $\langle [\![\beta_1']\!], [\![\beta_2']\!], [\![\beta_3']\!] \rangle$. Next, we must show that the $H_1(S^1)$ factor is included.

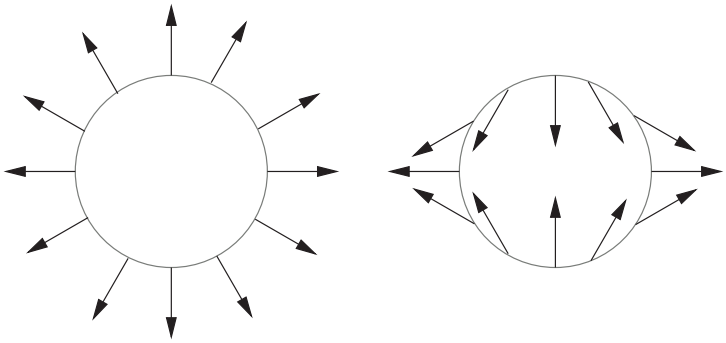

Figure 3.2: $\sigma : S^1 \to T_1\mathcal{D}_\Delta$ is an assignment of unit vectors to points in the circle. This map is depicted on the left. The loop $-\sigma$ with opposite orientation is depicted to the right.

Let $\sigma : S^1 \to T_1\mathcal{D}_\Delta \setminus \Sigma$ be a loop which travels once around the tangent circle to a single point P. See figure 3.2. We will show that

$$[\![\beta_1']\!] + [\![\beta_2']\!] + [\![\beta_3']\!] = [\![\sigma]\!] \tag{3.6}$$

Essentially, this is the Poincaré-Hopf index theorem. We will prove this by explicitly showing that the set of loops $\{\beta_1', \beta_2', \beta_3', -\sigma\}$ bound a surface in $T_1\mathcal{D}_\Delta \setminus \Sigma$. This surface is a vector field on the sphere with four singularities coming from the boundaries of this surface. See figure 3.3. $\diamondsuit$

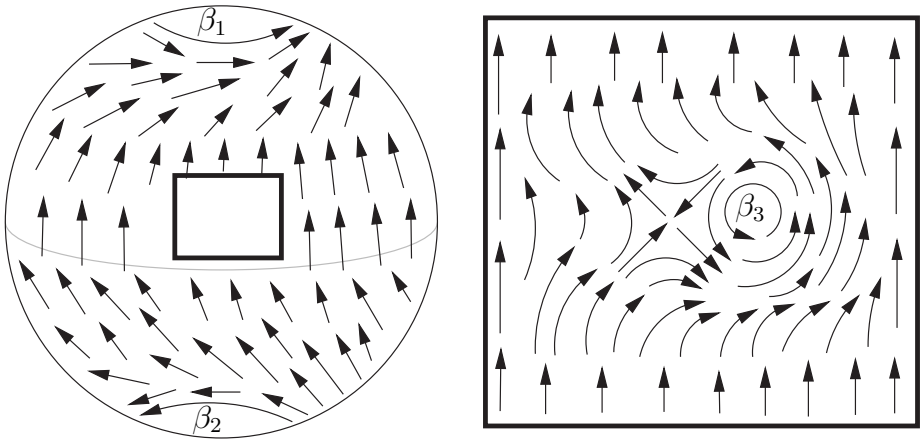

Figure 3.3: There is a vector field on the sphere with two singularities each with index 1. Singularities of indices 1 and -1 "cancel" and can be added to the vector field.

Proof of the stability theorem; sufficiency: We will now demonstrate that if γ is a null-homologous closed geodesic on $\mathcal{D}_\Delta \setminus \Sigma$, then it is stable under small perturbations of Δ.

We begin by describing the general process of developing a curve into the plane. Note that this construction works for any smooth curve, not only geodesics.

The surface $\mathcal{D}_\Delta \setminus \Sigma$ is locally isometric to the plane. We think of the loop γ as a map $[0,1] \to \mathcal{D}_\Delta \setminus \Sigma$ with $\gamma(0) = \gamma(1)$. Suppose we find a simply connected open set U, together with a path $f : [0,1] \to U$ and a local homeomorphism $g : U \to \mathcal{D}_\Delta \setminus \Sigma$ so that $\gamma = g \circ f$. Then the pull-back metric induced by g on U makes U locally isometric to the plane, and since U is simply connected, it immerses isometrically into the plane.

We will consider a particular open set U which is related to the triangulation of $\mathcal{D}_\Delta$. Lift $\gamma : [0,1] \to \mathcal{D}_\Delta \setminus \Sigma$ to the universal cover $X_\Delta = \widetilde{\mathcal{D}_\Delta \setminus \Sigma}$. This gives a path $\widetilde{\gamma} : [0,1] \to X_\Delta$. Take U_Δ to be the interior of the union of triangles that $\widetilde{\gamma}$ hits. This construction relates to the above paragraph by $f = \widetilde{\gamma}$ and $g = X_\Delta \to \mathcal{D}_\Delta \setminus \Sigma$ is the covering map. The result is a simply connected open set U_Δ which decomposes into triangles isometric to Δ. U_Δ can be immersed into the plane as in figure 3.4. We call U_Δ the *unfolding* of γ.

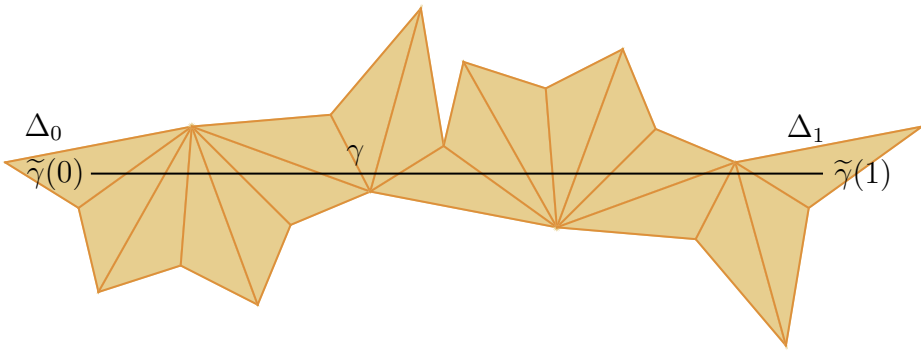

Figure 3.4: An unfolding of a periodic billiard path in a triangle

The triangle $\Delta_0 \subset U_\Delta$ which contains $\gamma(0)$ and the triangle $\Delta_1 \subset U_\Delta$ which contains $\gamma(1)$ project to the same triangle in $\mathcal{D}_\Delta$. Therefore, there is an isometry of the plane which takes the immersed image of Δ_0 in the plane to the image of Δ_1. This is the *holonomy*, hol_Δ, around γ.

Since U_Δ is a finite chain of triangles isometric to the marked triangle Δ, we can build the same combinatorial object out of any marked triangle T. Just replace each copy of Δ in U_Δ with T. Call this object U_T. Again, there is a holonomy map, hol_T sending the first triangle T_0 to the last triangle T_1.

The curve $\widetilde{\gamma}$ is a line segment in U_Δ joining a point $P \in \Delta_0$ to $hol_\Delta(P) \in \Delta_1$. Since the locations of the vertices of U_Δ deform continuously with the deformation of Δ, we can find an open set of triangles N containing Δ so that for all $T \in \Delta$, there

is a line segment $\widetilde{\eta}$ joining a point $Q \in T_0$ and its holonomy image $hol_T(Q) \in T_1$.

I claim that for all $T \in N$, $\widetilde{\eta}$ projects to a closed geodesic η in $\mathcal{D}_T$ under $g_T : U_T \to \mathcal{D}_T$. We must check that there is no angle at the point $g_T(Q) = \eta(0) = \eta(1)$. We will measure the angle α between $\eta'(0)$ and $\eta'(1)$. We define a loop $\eta' : S^1 \to T_1(\mathcal{D}_T \smallsetminus \Sigma)$. η' starts by following the derivative of η from 0 to 1, and then it connects $\eta'(1)$ to $\eta'(0)$ by rotating the vector based at $g_T(Q)$. See figure 3.5. In doing so, η' rotates the vector by α.

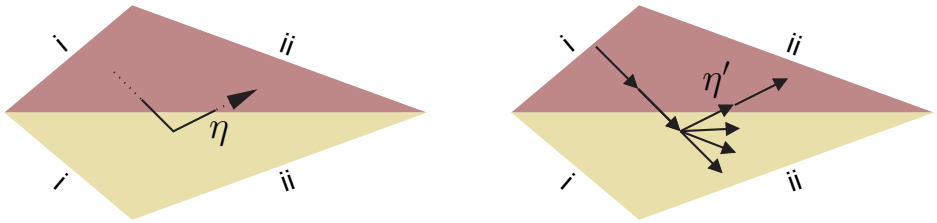

Figure 3.5: The curves η and η'.

Notice that the homology class $[\![\eta']\!]$ projects to $[\![\eta]\!]$ under the map induced on homology by projection to the base of the unit tangent bundle,

$$H_1\big(T_1(\mathcal{D}_T \smallsetminus \Sigma)\big) \to H_1(\mathcal{D}_T \smallsetminus \Sigma)$$

Furthermore, $[\![\eta]\!] = [\![\gamma]\!]$ based on the identification of the two marked triangles. Since $[\![\gamma]\!]$ is null-homologous, $[\![\eta]\!] = 0 \in H_1(\mathcal{D}_T \smallsetminus \Sigma)$. By the remarks above (equations 3.5 and 3.6) this implies that the homology class $[\![\eta']\!]$ is of the form

$$[\![\eta']\!] = n[\![\sigma]\!] = n([\![\beta_1']\!] + [\![\beta_2']\!] + [\![\beta_3']\!]) \tag{3.7}$$

for some integer n. Because all the turning of η' happens when interpolating between $\eta'(0)$ and $\eta'(1)$ by rotating by α, we know

$$\alpha = \int_{\eta'} d\theta_T = 2n\pi \equiv 0 \pmod{2\pi} \tag{3.8}$$

Therefore, there is no angle formed at the point $g_T(Q) = \eta(0) = \eta(1)$ and η is a geodesic. $\diamondsuit$

Chapter 4

Billiard-like paths in triangles

In this chapter, we prove theorem A from the introduction. First we will restate this theorem more carefully.

We parameterize the space of all marked triangles $\mathcal{T}$, by the angles of the triangle. Thus, we identify points in $\mathcal{T}$ with elements of the 2-simplex

$$\mathcal{T} = \{(\alpha_1, \alpha_2, \alpha_3) | \alpha_i > 0 \text{ and } \alpha_1 + \alpha_2 + \alpha_3 = \pi\} \tag{4.1}$$

In this parameterization, the space of all right triangles consists of three lines:

$$\alpha_1 = \frac{\pi}{2} \qquad \alpha_2 = \frac{\pi}{2} \qquad \alpha_3 = \frac{\pi}{2} \tag{4.2}$$

Let us denote these three lines by ℓ_1, ℓ_2, and ℓ_3. See figure 4.1.

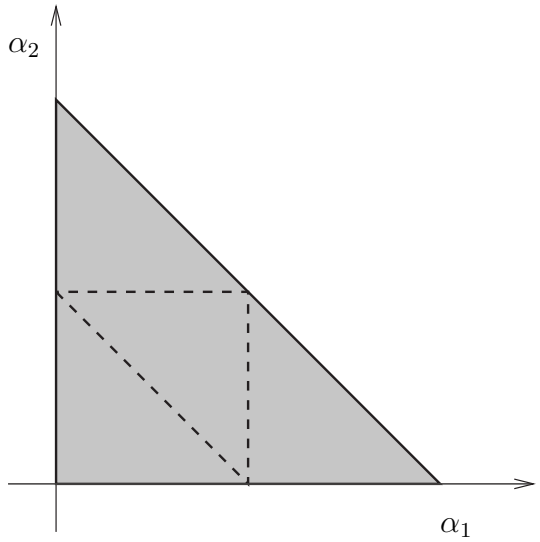

Figure 4.1: Points in $\mathcal{T}$ can be identified by two of their angles, α_1 and α_2. The right triangles split the parameter space of marked triangles into four components.

Recall that if $\widehat{\gamma}$ is a periodic billiard path in a triangle Δ, we define $\mathit{tile}(s_{\widehat{\gamma}})$ to be the set of all triangles that have a periodic billiard path with the same symbolic dynamics as $\widehat{\gamma}$.

The following is a restatement of theorem A from the introduction:

Theorem A. *If $\widehat{\gamma}$ is a stable periodic billiard path in a triangle, then $\mathit{tile}(s_{\widehat{\gamma}})$ is contained in one of the four connected components of $\mathcal{T} \smallsetminus (\ell_1 \cup \ell_2 \cup \ell_3)$.*

This theorem is proved using a technique to confine $\mathit{tile}(s_{\widehat{\gamma}})$. In section 4.5, we define a set of triangles $\mathit{UF}(s_{\widehat{\gamma}}) \subset \mathcal{T}$, called the unfriendly set, which consists of a finite union of lines in $\mathcal{T}$. Topological techniques demonstrate that $\mathit{UF}(s_{\widehat{\gamma}})$ and $\mathit{tile}(s_{\widehat{\gamma}})$ are disjoint. We go on to prove that

Theorem B. *If $\widehat{\gamma}$ is a stable periodic billiard path in a triangle, then $\mathit{tile}(s_{\widehat{\gamma}})$ is contained in a single component of $\mathcal{T} \smallsetminus \mathit{UF}(s_{\widehat{\gamma}})$.*

Then we use the topological ideas defining $\mathit{UF}(s_{\widehat{\gamma}})$ to prove that regardless of the choice of a stable periodic billiard path $\widehat{\gamma}$, the right triangles lines are in the unfriendly set ($\ell_1 \cup \ell_2 \cup \ell_3 \subset \mathit{UF}(s_{\widehat{\gamma}})$). This directly implies theorem A.

The title of this chapter derives from the idea that the component of $\mathcal{T} \smallsetminus \mathit{UF}(s_{\widehat{\gamma}})$ containing $\mathit{tile}(s_{\widehat{\gamma}})$ have closed billiard-like paths. Vaguely, we do not require that a billiard-like path be geodesic. It only must be smooth and bounce of the edges so that the angle of incidence equals the angle of reflection. But, the curve must satisfy certain topological angle conditions at self-intersections and intersections with boundary edges of Δ. The conditions are "obviously true" for billiard paths. We define the *billiard-like tile*, $\mathit{bl\text{-}tile}(s_{\widehat{\gamma}})$, to be the set of all triangles with a billiard-like path with symbolic dynamics $s_{\widehat{\gamma}}$. The billiard-like tile is the component mentioned in theorem A, so it satisfies $\mathit{tile}(s_{\widehat{\gamma}}) \subset \mathit{bl\text{-}tile}(s_{\widehat{\gamma}})$.

Relatively, speaking $\mathit{bl\text{-}tile}(s_{\widehat{\gamma}})$ is much easier to compute and understand than $\mathit{tile}(s_{\widehat{\gamma}})$. $\mathit{bl\text{-}tile}(s_{\widehat{\gamma}})$ is a convex rational polygon, while $\mathit{tile}(s_{\widehat{\gamma}})$ is a region with piecewise smooth boundary. It is unknown if $\mathit{tile}(s_{\widehat{\gamma}})$ is always connected and simply connected.

Heuristically, when trying to understand $\mathit{tile}(s_{\widehat{\gamma}})$, first we would hope to be able to localize the problem by restricting analysis to a small subset of the parameter space of triangles. In fact, the component of $\mathcal{T} \smallsetminus \mathit{UF}(s_{\widehat{\gamma}})$ that contains $\mathit{tile}(s_{\widehat{\gamma}})$ can be computed explicitly (see definition 4.25). This algorithm is implemented as part of *McBilliards*. The algorithm that computes the relevant component of $\mathcal{T} \smallsetminus \mathit{UF}(s_{\widehat{\gamma}})$ operates quite quickly and is used to localize the computations that yield approximations to $\mathit{tile}(s_{\widehat{\gamma}})$.

4.1 Translation Surfaces

A Euclidean cone surface S has a holonomy homomorphism defined by developing a loop into the plane using analytic continuation:

$$\mathit{hol} : \pi_1(S \smallsetminus \Sigma) \to \mathit{Isom}_+(\mathbb{R}^2) \tag{4.3}$$

Here, the holonomy homomorphism is defined after noticing that if X is an open simply connected space which is locally isometric to the plane, then it immerses isometrically into the plane. First choose a base point P and an open neighborhood $U_P \ni P$ together with an isometry $\phi : U_p \to \mathbb{R}^2$. Suppose we are given a smooth loop $\alpha : [0,1] \to S$ with $\alpha(0) = \alpha(1) = P$. We extend α by taking an open 2-disk $D \supset [0,1]$ together with an immersion $\widehat{\alpha} : D \to S$ so that $\widehat{\alpha}|_{[0,1]} = \alpha$. Choose components $U_0, U_1 \subset \widehat{\alpha}^{-1}(U_P)$ so that $0 \in U_0$ and $1 \in U_1$. When endowed with the pull back metric, D becomes locally isometric to the plane. Then because D is simply connected, there is an isometric immersion $\psi : D \to R^2$. We make the unique choice for ψ so that $\psi|_{U_0} = \phi \circ \widehat{\alpha}|_{U_0}$. Choose $hol(\alpha)$ so that $hol(\alpha) \circ \phi \circ \widehat{\alpha}|_{U_1} = \psi|_{U_1}$. This construction is invariant under homotopies of α preserving the condition that $\alpha(0) = \alpha(1) = P$. Further, *hol* defines a group homomorphism.

A *translation surface* is an Euclidean cone surface where the image $hol(\pi_1(S \setminus \Sigma))$ consists only of translations. This implies that the surface can be constructed by gluing subsets of the plane together by translations. The cone angles of translation surfaces must be integer multiples of 2π. In particular, directions make sense on a translation surface. In other words,

Proposition 4.1. *There is a fibration from the unit tangent bundle of a translation surface S to the unit circle in the plane,*

$$\theta : T_1 S \to S^1$$

which is an isometry when restricted to the unit tangent circle at any non-singular point and is invariant under the geodesic flow.

For example, suppose $\gamma : [0,1] \to S$ is an oriented geodesic arc. Let $\gamma' : [0,1] \to T_1$ denote the canonical lift to the unit tangent bundle T_1. That is γ' sends x to the unit tangent of γ at $\gamma(x)$ in the direction of the orientation of γ. Then $\theta \circ \gamma'(x)$ is a constant independent of x. Call this constant $\theta(\gamma')$.

Proposition 4.2. *Geodesics on a translation surface S satisfy the following:*

1. *Geodesics have no self intersections.*
2. *Two distinct geodesics γ and η traveling in the same direction ($\theta(\gamma') = \theta(\eta')$) never intersect. The same is true for geodesics traveling in opposite directions ($\theta(\gamma') \equiv \theta(\eta') + \pi \pmod{2\pi}$).*
3. *Let γ and η be two geodesics on S. The absolute value of the algebraic intersection number between γ and η is equal to the geometric intersection number. The sign of the algebraic intersection number is determined*

$$sign(\gamma \cap_{alg.} \eta) = \begin{cases} 1 & \text{if } 0 < \theta(\gamma') - \theta(\eta') < \pi \\ -1 & \text{if } \pi < \theta(\gamma') - \theta(\eta') < 2\pi \end{cases}$$

Proof: This is just a tautology based on the fact that a local picture of any intersection is determined by the (constant) directions the geodesics are traveling in. $\diamondsuit$

In this paper we will allow our translation surfaces to be non-compact. We will allow our cone singularities to have infinite cone angle.

Remark 4.3 (On notation). *In this chapter, the singular set Σ of our Euclidean cone surfaces and translation surfaces will become a notational nuisance. We introduce the notation $\mathcal{E}_\Delta = \mathcal{D}_\Delta \setminus \Sigma$. So, $\mathcal{E}_\Delta$ is a locally Euclidean cone surface homeomorphic to a 3-punctured sphere. We will also remove the singularities from our translation surfaces.*

Given our locally Euclidean surface $\mathcal{E}_\Delta$, we can construct covers branched over the singular set which are translation surfaces. A trivial example is the universal cover, $\widetilde{\mathcal{E}}_\Delta$. Another translation surface covering is the universal abelian cover,

$$AC_\Delta = \widetilde{\mathcal{E}}_\Delta / [\pi_1(\mathcal{E}_\Delta), \pi_1(\mathcal{E}_\Delta)] \tag{4.4}$$

Here, $[\pi_1(\mathcal{E}_\Delta), \pi_1(\mathcal{E}_\Delta)]$ is the commutator subgroup of $\pi_1(\mathcal{E}_\Delta)$. The universal abelian cover is a translation surface because the commutator subgroup of $Isom_+(\mathbb{R}^2)$ is the group of translations. There is always a *minimal translation surface covering*, which we define as

$$MT_\Delta = \widetilde{\mathcal{E}}_\Delta / hol_\Delta^{-1}(\mathbb{R}^2)$$

where $hol_\Delta^{-1}(\mathbb{R}^2)$ is the preimage of the group of translations of the plane in $\pi_1(\mathcal{E}_\Delta)$. We call MT_Δ minimal because every translation surface which covers $\mathcal{E}_\Delta$ also covers MT_Δ.

Remark 4.4. *MT_Δ can also be built directly out of copies of Δ. Consider the group action of $\mathbb{Z}_2 * \mathbb{Z}_2 * \mathbb{Z}_2$ generated by reflections in the sides of Δ. Take all images of Δ under this group and identify any two triangles which differ by a translation. Identify two triangles along an edge if they differ by reflection in that edge, up to a translation. This tautologically builds MT_Δ.*

In summary, we have discussed the following sequence of covers:

$$\widetilde{\mathcal{E}}_\Delta \to AC_\Delta \to MT_\Delta \to \mathcal{E}_\Delta \tag{4.5}$$

It should be noted that each cover is regular. The cover $AC_\Delta \to \mathcal{E}_\Delta$ is regular because the commutator subgroup of the fundamental group is normal. Thus the automorphism group of this cover is

$$H_1(\mathcal{E}_\Delta, \mathbb{Z}) = \pi_1(\mathcal{E}_\Delta, \mathbb{Z}) / [\pi_1(\mathcal{E}_\Delta), \pi_1(\mathcal{E}_\Delta)] \cong \mathbb{Z}^2 \tag{4.6}$$

Since this group is abelian, the intermediate covers, $AC_\Delta \to MT_\Delta \to \mathcal{E}_\Delta$, will be regular as well.

4.2 Geodesics on translation surfaces

If we develop a geodesic on $\mathcal{E}_\Delta$ into the plane, we see a line. The holonomy around this geodesic must preserve this line and is therefore a translation. A loop γ on $\mathcal{E}_\Delta$ whose holonomy is a translation must lift to a loop $\widetilde{\gamma}$ on the minimal translation surface MT_Δ. The main idea of this paper is to use this to build obstructions to the existence of geodesics on $\mathcal{E}_\Delta$.

Proposition 4.2 implies that a collection of geodesics which all are traveling the same direction on a translation surface are simple and disjoint. Using objects called train-tracks, Thurston discovered a technique to list collections of disjoint simple closed curves on surfaces. See [PH92] for more on train tracks. We follow this idea in spirit here.

$\mathcal{E}_\Delta$ comes equipped with the geodesic triangulation which cuts the surface into two copies of Δ. The pull-back of this triangulation gives a geodesic triangulation on any of our translation surface covers of $\mathcal{E}_\Delta$.

A second look at proposition 4.2 reveals that a collection of geodesics which all are traveling the same direction on a translation surface cover of $\mathcal{E}_\Delta$ have at most one algebraic sign of intersection with each edge of the triangulation. In particular, the magnitude of the algebraic intersection number between this curve family and any edge of the triangulation of MT_Δ equals the geometric intersection number. This algebraic intersection number is a homological invariant.

We will be considering topological (smooth) curves on our locally Euclidean surface, $\mathcal{E}_\Delta$, and on the translation surfaces that cover $\mathcal{E}_\Delta$. We say the *symbolic dynamics* of a topological curve γ on S is the sequence of edges of the triangulation of S that γ hits together with the orientation at which the curve crosses the edge. We will always assume that our topological curves intersect transversely with the edges of the triangulation (and with each other, when relevant). We say that the *symbolics class* of γ, denoted $[\gamma]_s$, is the collection of all topological curves on S that have the same symbolic dynamics as γ. A symbolics class is a stricter notion than a homotopy class.

Just like a homotopy class, we can define the symbolics class of a finite set of geodesics to be the collection of all symbolics classes of the curves in the set.

Now let S be a translation surface. Let $X = \{\gamma_1, \ldots, \gamma_n\}$ be a collection of geodesics on S which are all traveling in the same direction. Let $[\![X]\!]$ be the collection's homology class

$$[\![X]\!] = [\![\gamma_1]\!] + \ldots + [\![\gamma_n]\!]$$

We will show that we can recover the symbolics classes, $\{[\gamma_i]_s\}$, of the curves in X from the homology class $[\![X]\!]$.

The homology class $[\![X]\!]$ is determined by its intersection numbers with the edges of the triangulation of S. Because the triangulation of S is by saddle connections (which are properly embedded arcs, since the vertices have been removed), S is homotopic to the dual graph to this triangulation. Let Γ be the dual graph to the triangulation. A homology class in a graph is an assignment of orientations and

positive integral weights to finitely many edges of the graph subject to a vertex condition. The vertex condition is that the sum of the weights of edges oriented inward at a vertex is equal to the sum of weights of edges oriented outward. Given such an assignment of orientations and weights, for each triangle there is a unique topological way to draw disjoint oriented arcs connecting the edges of the triangle so that

1. orientations of arcs crossing an edge of a triangle match the orientation of the edge of Γ crossing the same edge of the triangle, and
2. the number of arcs crossing an edge of a triangle equals the weight of the edge of Γ crossing that same edge.

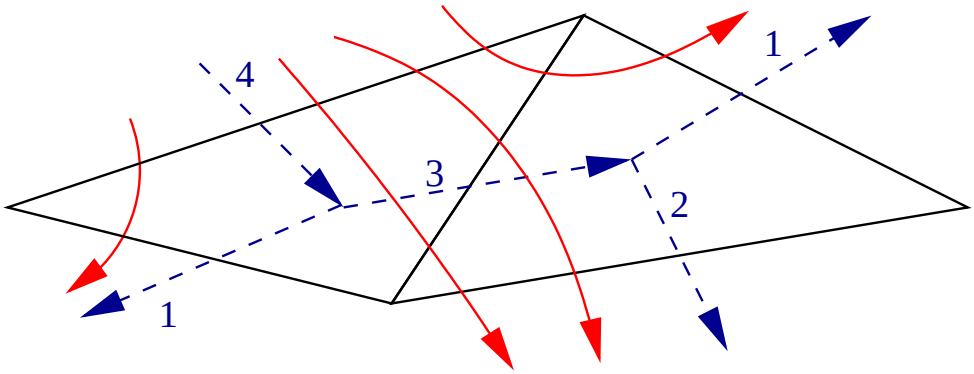

Figure 4.2: Turning a homology class into simple curves

There is a unique way to glue together the arcs of two adjacent triangles. See figure 4.2 for a local picture. The result of gluing the arcs together is a finite union of disjoint oriented simple closed curves in the right homology class. We call this construction "combing out the homology class."

Now let us summarize this situation. Let $H_1(S)$ denote the first homology group with coefficients in $\mathbb{Z}$. Let $\mathcal{H}(S)$ denote the collection of all finite sets of symbolics classes of (non-homotopically trivial) oriented curves. This construction gives us a map

$$\Psi : H_1(S) \to \mathcal{H}(S)$$

which sends a homology class $[\![X]\!]$ to a set of symbolics classes of curves $[X]_s$ in that homology class. Furthermore $[X]_s$ can always be realized by disjoint simple curves which intersect each edge of the triangulation of S with the same algebraic sign. By uniqueness of the construction,

Proposition 4.5. *Let $[X]_s$ be finite set of (nontrivial) symbolics classes of oriented curves on S. Then $[X]_s$ can be realized by disjoint simple curves which intersect*

each edge of the triangulation of S with the same algebraic sign if and only if $[X]_s = \Psi(\llbracket X \rrbracket)$.

The purpose for this is

Corollary 4.6. *If X is a collection of closed geodesics that are all traveling in the same direction on S then $[X]_s = \Psi(\llbracket X \rrbracket)$ or equivalently $[X]_s \in img(\Psi)$.*

Proof: Combine propositions 4.2 and 4.5. $\diamondsuit$

To apply this corollary to our situation, we will need to better understand the translation surfaces AC_Δ and MT_Δ.

4.3 The universal abelian cover

Note that $\mathcal{E}_\Delta$ is a three punctured sphere, and thus is homotopic to the Θ-graph, which we will think of as embedded in $\mathcal{E}_\Delta$. See the left side of figure 4.3. Because $\mathcal{E}_\Delta$ is a thickening of the Θ-graph, AC_Δ will be a thickening of the universal abelian cover of the Θ-graph, AC_Θ.

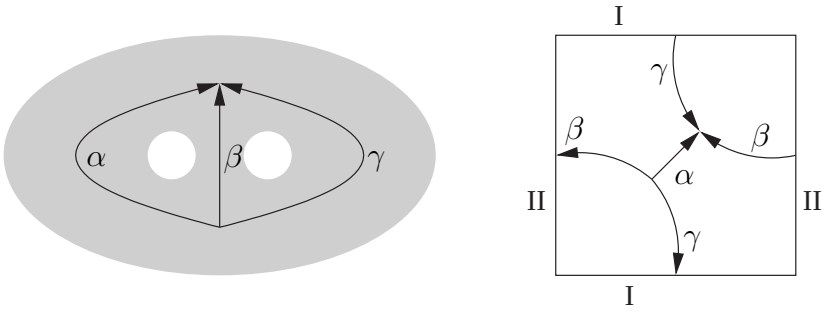

Figure 4.3: *Left:* Edge markings on the theta graph. *Right:* The Θ-graph embedded inside the torus with a hexagon in the complement. Roman numerals indicate edge identifications on the torus.

The universal abelian cover of the Θ-graph, AC_Θ, is the graph consisting of the edges of the usual tiling of the plane by hexagons. To see this, mark and orient the edges of the theta graph as in figure 4.3. Then we can glue a hexagonal 2-cell to the theta graph by using the concatenation of paths, $\alpha\beta^{-1}\gamma\alpha^{-1}\beta\gamma^{-1}$, as a boundary curve. This builds an embedding of the theta graph into the torus, $i : \Theta \hookrightarrow T^2$. The loop bounding this hexagon is inside the commutator because

$$[\alpha\beta^{-1}, \gamma\beta^{-1}] = (\alpha\beta^{-1})(\gamma\beta^{-1})(\beta\alpha^{-1})(\beta\gamma^{-1}) = \alpha\beta^{-1}\gamma\alpha^{-1}\beta\gamma^{-1} \tag{4.7}$$

This together with the fact that the commutator $[\pi_1(T^2), \pi_1(T^2)]$ is trivial implies that the commutator $[\pi_1(\Theta), \pi_1(\Theta)]$ is precisely the kernel of the induced map $i_* :$

$\pi_1(\Theta) \to \pi_1(T^2)$. Hence the universal abelian cover of the Θ-graph is the cover of the theta graph induced by the universal cover of T^2. As claimed, the universal abelian cover of the theta graph is the graph consisting of edges of the usual tiling of the plane by hexagons. The automorphisms of this cover act by translations of the plane.

We mentioned that $\mathcal{E}_\Delta$ is a thickening of the Θ-graph. We now understand that the Θ-graph is the graph coming from the tiling of the plane by hexagons modulo the set of translations preserving the tiling. We redraw the embedding of the Θ-graph into $\mathcal{E}_\Delta$ in figure 4.4 to make our two pictures more clearly compatible.

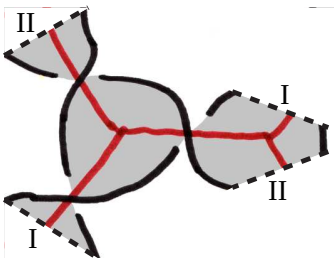

Figure 4.4: The embedding $\Theta \hookrightarrow \mathcal{E}_\Delta$. This surface is just the thrice punctured sphere. Each edge of the Θ-graph is thickened to a half twisted band.

Translations of figure 4.4 glue up the surface to a thrice punctured sphere. We lift this thickening of the Θ-graph to the universal abelian cover. We see AC_Δ is homeomorphic to the surface shown in figure 4.5. Each edge of AC_Θ is thickened to a half twisted band.

4.4 The minimal translation surface cover

MT_Δ is always an intermediate cover between AC_Δ and $\mathcal{E}_\Delta$. Recall, the cover $AC_\Delta \to \mathcal{E}_\Delta$ is regular and has an automorphism group $H_1(\mathcal{E}_\Delta)$ isomorphic to $\mathbb{Z}^2$. Since MT_Δ is intermediate, it is regular and arises as

$$MT_\Delta = AC_\Delta / K_\Delta \tag{4.8}$$

for some subgroup $K_\Delta \subset H_1(\mathcal{E}_\Delta)$.

By definition, $MT_\Delta = \widetilde{\mathcal{E}}_\Delta / hol_\Delta^{-1}(\mathbb{R}^2)$. Thus K_Δ is the image of the subgroup $hol_\Delta^{-1}(\mathbb{R}^2) \subset \pi_1(\mathcal{E}_\Delta)$ inside $H_1(\mathcal{E}_\Delta)$. K_Δ can be understood as the kernel of the abelianization of the holonomy map, hol_Δ. Consider the commutative diagram,

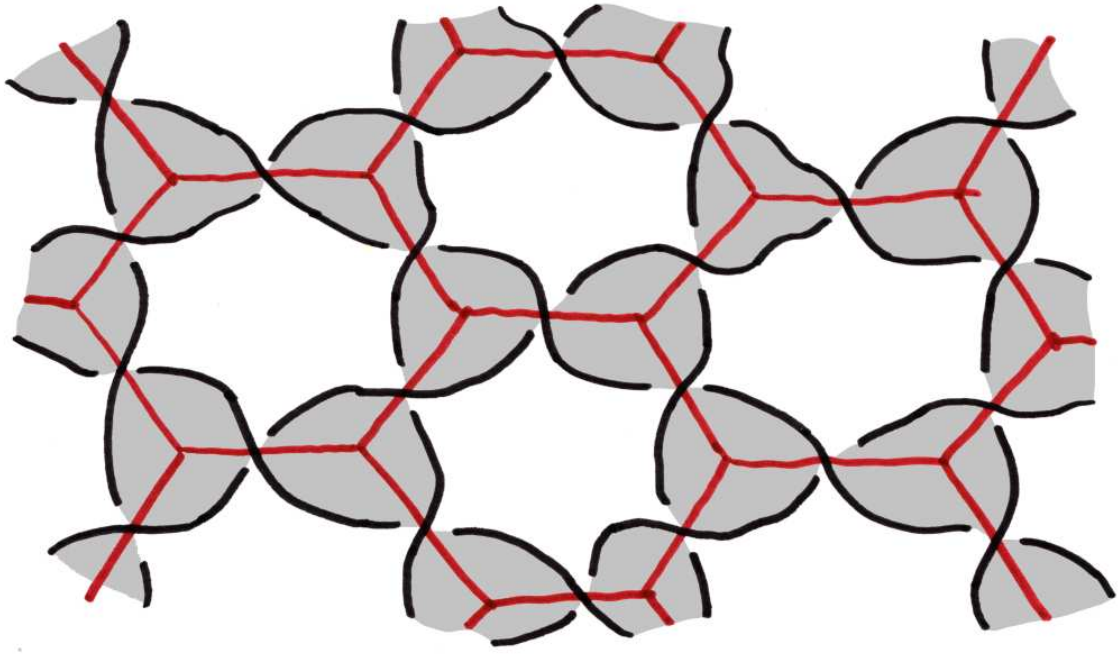

Figure 4.5: The embedding $AC_\Theta \hookrightarrow AC_\Delta$

where the down arrows correspond to abelianizations,

$$\begin{array}{ccc} \pi_1(\mathcal{E}_\Delta) & \xrightarrow{hol_\Delta} & Isom_+(\mathbb{R}^2) \\ \downarrow & & \downarrow \\ H_1(\mathcal{E}_\Delta) & \xrightarrow{hol_\Delta^{ab}} & Isom_+(S^1) \end{array} \tag{4.9}$$

Here $Isom_+(S^1)$ is the abelianization of $Isom_+(\mathbb{R}^2)$, because the commutator subgroup of $Isom_+(\mathbb{R}^2)$ is precisely the subgroup of translations. We can think of the abelianization of an isometry of the plane as its rotational part. Now,

$$K_\Delta = ker(hol_\Delta^{ab}) \quad \text{and} \quad MT_\Delta = AC_\Delta / ker(hol_\Delta^{ab}) \tag{4.10}$$

Using the direction map θ of proposition 4.1, we can give a clean geometric interpretation of the abelianized holonomy map hol_Δ^{ab}. Consider an automorphism ζ of the cover $AC_\Delta \to \mathcal{E}_\Delta$. Because ζ preserves the local Euclidean structure, it must act as a rotation on the direction map. $hol_\Delta^{ab}(\zeta)$ describes this rotation. In other words, the following diagram commutes

$$\begin{array}{ccc} T_1AC_\Delta & \xrightarrow{\theta} & S^1 \\ {\scriptstyle\zeta}\downarrow & & \downarrow{\scriptstyle hol_\Delta^{ab}(\zeta)} \\ T_1AC_\Delta & \xrightarrow{\theta} & S^1 \end{array} \tag{4.11}$$

So, MT_Δ is AC_Δ modulo those automorphisms which act trivially on the directions in AC_Δ. Therefore, to understand MT_Δ, we will first need to understand $hol_\Delta^{ab} : H_1(\mathcal{E}_\Delta) \to Isom_+(S^1)$. The group $H_1(\mathcal{E}_\Delta)$ is the free abelian group generated by the homology classes of the curves β_1 and β_2 which travel around the punctures as in figure 3.1. If α_i is the angle in radians of the triangle Δ at the vertex surrounded by β_i, then it is clear that the holonomy around β_i acts as a rotation by $2\alpha_i$ around the puncture surrounded by β_i. Consequently,

$$hol_\Delta^{ab} : r[\![\beta_1]\!] + s[\![\beta_2]\!] \mapsto 2r\alpha_1 + 2s\alpha_2 \in \mathbb{R}/2\pi\mathbb{Z} = Isom_+(S^1) \tag{4.12}$$

There is another way we could have arrived at the map hol_Δ^{ab}. If $[\![\gamma]\!] \in H_1(\mathcal{E}_\Delta)$ and $\gamma \in [\![\gamma]\!]$ is a smooth curve, then hol_Δ^{ab} measures the total turning angle of γ modulo 2π. In other words,

$$hol_\Delta^{ab}([\![\gamma]\!]) = \Big(\int_{\gamma'} d\theta \Big) \ (mod\ 2\pi) = \Big(\int_\gamma \kappa_g ds \Big) \ (mod\ 2\pi) \tag{4.13}$$

Here γ' represents the curve on the unit tangent bundle, $T_1\mathcal{E}_\Delta$, obtained by taking the unit tangents at each point of γ. The form $d\theta$ on $T_1 s_\Delta$ measures change in angle of a tangent vector using the locally Euclidean structure of s_Δ. This idea was

introduced in the proof of the stability theorem in chapter 3. This integral is related to a classical idea from differential geometry. $\kappa_g ds$ denotes the geodesic curvature with respect to arc length. Since our surface is locally Euclidean, this just measures the rate at which the unit tangents change directions.

The *(mod* 2π*)* term is needed for these integrals to yield homological invariants over $H_1(\mathcal{E}_\Delta)$. Consider for example, a homotopically trivial simple closed loop with total curvature 2π. Nonetheless, we would like to remove *(mod* 2π*)* from the equation. Note that $d\theta$ is a closed form on $T_1\mathcal{E}_\Delta$. Therefore integrating $d\theta$ over a curve ξ in $T_1\mathcal{E}_\Delta$ is a homological invariant. We define the "lift" of hol_Δ^{ab} to be the map

$$\widetilde{hol}_\Delta^{ab} : H_1(T_1\mathcal{E}_\Delta) \to \mathbb{R} : [\![\xi]\!] \mapsto \int_\xi d\theta \tag{4.14}$$

Let $\pi : T_1\mathcal{E}_\Delta \to \mathcal{E}_\Delta$ be projection to the base of the unit tangent bundle and let $\pi_* : H_1(T_1\mathcal{E}_\Delta) \to H_1(\mathcal{E}_\Delta)$ be the map induced on homology. Then $\widetilde{hol}_\Delta^{ab}$ is a lift of hol_Δ^{ab} in the sense of the following commuting diagram:

$$\begin{array}{ccc} H_1(T_1\mathcal{E}_\Delta) & \xrightarrow{\widetilde{hol}_\Delta^{ab}} & \mathbb{R} \\ {\scriptstyle \pi_*}\downarrow & & \downarrow{\scriptstyle (mod\ 2\pi)} \\ H_1(\mathcal{E}_\Delta) & \xrightarrow{hol_\Delta^{ab}} & \mathbb{R}/2\pi\mathbb{Z} \end{array} \tag{4.15}$$

We now go about understanding the map $\widetilde{hol}_\Delta^{ab}$. Let β_1, β_2, and β_3 be loops which travel around each puncture of $\mathcal{E}_\Delta$ as depicted in figure 3.1. Let β_i' be their respective derivatives. It is easy to see that

$$\widetilde{hol}_\Delta^{ab}([\![\beta_i']\!]) = \int_{\beta_i'} d\theta_\Delta = 2\alpha_i \tag{4.16}$$

Where α_i is angle of the triangle at the vertex that β_i surrounds. This in fact determines the map $\widetilde{hol}_\Delta^{ab}$, because of proposition 3.3 (appearing in chapter 3)

Using proposition 3.3, we know that there are $n_1, n_2, n_3 \in \mathbb{Z}$ so that

$$[\![\gamma']\!] = n_1[\![\beta_1']\!] + n_2[\![\beta_2']\!] + n_3[\![\beta_3']\!]$$

By equation 4.16, the integral of $[\![\gamma']\!]$ with respect to $d\theta$ depends on the angles of the triangle. If $(\alpha_1, \alpha_2, \alpha_3)$ denotes the triangle with the given angles,

$$\widetilde{hol}_{(\alpha_1,\alpha_2,\alpha_3)}^{ab}([\![\beta_i']\!]) = \int_{[\![\gamma']\!]} d\theta_{(\alpha_1,\alpha_2,\alpha_3)} = 2n_1\alpha_1 + 2n_2\alpha_2 + 2n_3\alpha_3 \tag{4.17}$$

We consider $\mathcal{T}$ to be the subspace of $\mathbb{R}^3$ determined by the angles of the triangles.

That is, we identify $\mathcal{T}$ with points in the simplex

$$\{(\alpha_1, \alpha_2, \alpha_3) \text{ such that } \alpha_i > 0 \text{ and } \alpha_1 + \alpha_2 + \alpha_3 = \pi\}$$

Equation 4.12 tells us that the map hol^{ab} is the restriction of a bilinear map from $\mathbb{R}^3 \times H_1(\mathcal{E}_\Delta)$ to $\mathbb{R}/2\pi$. Let us change notation, to make this bilinear map look more standard. We will use $\mathcal{E}$ to refer to the triangulated three punctured sphere when we only care about topology. We can denote the map $hol^{ab} : \mathbb{R}^3 \times H_1(\mathcal{E}) \to \mathbb{R}/2\pi\mathbb{Z}$ as

$$hol^{ab}((\alpha_1, \alpha_2, \alpha_3), r[\![\beta_1]\!] + s[\![\beta_2]\!]) = 2r\alpha_1 + 2s\alpha_2 \in \mathbb{R}/2\pi\mathbb{Z} \tag{4.18}$$

Likewise, $\widetilde{hol}^{ab}$ is a restriction of a bilinear map from $\mathbb{R}^3 \times H_1(T_1\mathcal{E})$ to $\mathbb{R}$. By equation 4.17, we write

$$\widetilde{hol}^{ab} : \big((\alpha_1, \alpha_2, \alpha_3), r[\![\beta_1']\!] + s[\![\beta_2']\!] + t[\![\beta_3']\!]\big) \mapsto 2r\alpha_1 + 2s\alpha_2 + 2t\alpha_3 \tag{4.19}$$

Our non-degenerate bilinear map, $\widetilde{hol}^{ab}$, induces a duality between $H_1(T_1\mathcal{E})$ and even integer linear functions $\mathbb{R}^3 \to \mathbb{R}$. Let $\widetilde{hol}^{ab}(\star, \zeta)$ denote the even integer linear map $(\alpha_1, \alpha_2, \alpha_3) \mapsto \widetilde{hol}^{ab}((\alpha_1, \alpha_2, \alpha_3), \zeta)$, where $\zeta \in H_1(T_1\mathcal{E})$. Note that every even integer linear map from $\mathcal{T}$ to $\mathbb{R}$ can be written in a unique way as $\widetilde{hol}^{ab}(\star, \zeta)$.

Theorem 4.7. *Consider the map ϕ from the space of even integer linear functions on $\mathbb{R}^3$ to $H_1(\mathcal{E})$ given by*

$$\phi : \widetilde{hol}^{ab}(\star, \zeta) \mapsto \pi_*(\zeta) \tag{4.20}$$

Fixing any $\Delta \in \mathcal{T}$, the restricted map

$$\phi : \{\widetilde{hol}^{ab}(\star, \zeta) \big| \widetilde{hol}^{ab}(\Delta, \zeta) = 0\} \to H_1(S) \tag{4.21}$$

is a bijection to $ker(hol^{ab}_\Delta)$.

Proof: First we will check that this map does indeed send even integer functions which kill Δ to elements in $ker(hol^{ab}_\Delta)$. Assume $\widetilde{hol}^{ab}(\Delta, \zeta) = 0$. Then because $\widetilde{hol}^{ab}$ is a lift of hol^{ab},

$$hol^{ab}(\Delta, \pi_*(\zeta)) = \widetilde{hol}^{ab}(\Delta, \zeta) \ (mod\ 2\pi) = 0 \in \mathbb{R}/2\pi\mathbb{Z} \tag{4.22}$$

Second, we will check that the restricted ϕ is 1-1. Consider any ζ_1 and ζ_2 with $\pi_*(\zeta_1) = \pi_*(\zeta_2)$. We will show that the $\widetilde{hol}^{ab}(\Delta, \zeta_i)$ can not both be zero unless $\zeta_1 = \zeta_2$. We know that $\zeta_1 - \zeta_2 \in ker(\pi_*)$, so by proposition 3.3, $\zeta_1 - \zeta_2$ lies in the subgroup generated by $[\![\beta_1']\!] + [\![\beta_2']\!] + [\![\beta_3']\!]$. Therefore, there exists an integer n so that

$$\zeta_1 - \zeta_2 = n\big([\![\beta_1']\!] + [\![\beta_2']\!] + [\![\beta_3']\!]\big) \tag{4.23}$$

Using linearity and the definition of equation 4.19, we see

$$\widetilde{hol}^{ab}(\Delta, \zeta_1) - \widetilde{hol}^{ab}(\Delta, \zeta_2) = 2n\alpha_1 + 2n\alpha_2 + 2n\alpha_3 = 2n\pi \tag{4.24}$$

So, $\widetilde{hol}^{ab}(\Delta,\zeta_1) = \widetilde{hol}^{ab}(\Delta,\zeta_2)$ implies $\zeta_1 = \zeta_2$.

Finally, we must check that the restricted ϕ is onto. Assume $\pi_*(\zeta) \in ker(hol^{ab}_\Delta)$. Then because $\widetilde{hol}^{ab}$ is a lift of hol^{ab}, there is an integer n so that $\widetilde{hol}^{ab}(\Delta,\zeta) = 2n\pi$. Then

$$\widetilde{hol}^{ab}(\Delta, \zeta - n\big([\![\beta_1']\!] + [\![\beta_2']\!] + [\![\beta_3']\!]\big)) = 0 \tag{4.25}$$

But of course, $[\![\beta_1']\!] + [\![\beta_2']\!] + [\![\beta_3']\!] \in ker(\pi_*)$, so

$$\pi_*(\zeta - n\big([\![\beta_1']\!] + [\![\beta_2']\!] + [\![\beta_3']\!]\big)) = \pi_*(\zeta) \tag{4.26}$$

Therefore $\pi_*(\zeta)$ is the image of $\widetilde{hol}^{ab}(\star, \zeta - n\big([\![\beta_1']\!] + [\![\beta_2']\!] + [\![\beta_3']\!]\big))$ which kills Δ as desired. $\diamondsuit$

Essentially, theorem 4.7 tells us that even integer linear functions which vanish on Δ and elements in $ker(hol^{ab})$ are dual under the bilinear map $\widetilde{hol}^{ab}$. Recall that $ker(hol^{ab}_\Delta) \subset H_1(\mathcal{E}_\Delta) \cong \mathbb{Z}^2$. Therefore, $ker(hol^{ab}_\Delta)$ is isomorphic to either 0, $\mathbb{Z}$, or $\mathbb{Z}^2$. We can use theorem 4.7 to determine the isomorphism class of $ker(hol^{ab}_\Delta)$ by looking at the angles of Δ. One way to differentiate between these groups is by looking at the number of maximal non-trivial one-generator subgroups (0, 1, or ∞ respectively). Maximal non-trivial one-generator subgroups of $\mathbb{Z}^2$ correspond to sets of elements of $\mathbb{Z}^2$ which lie on a line with rational slope. In other words, maximal non-trivial one-generator subgroups are in one to one correspondence with the projectivization of $\mathbb{Z}^2$. We now define a dual notion:

Definition 4.8. *A* rational line ℓ *in* $\mathcal{T}$ *is a subset determined by three integers* n_1, n_2, n_3*, not all zero:* $\ell = \{(\alpha_1,\alpha_2,\alpha_3) | n_1\alpha_1 + n_2\alpha_2 + n_3\alpha_3 = 0\} \subset \mathcal{T}$.

Note that a rational line is a projective notion, in the sense that the line determined by the integers n_1, n_2, n_3 is the same as the line determined by the integers kn_1, kn_2, kn_3. Also, we can assume the n_i are all even and we get the same set of lines. The duality of theorem 4.7 gives us a bijection between maximal non-trivial one-generator subgroups of $ker(hol^{ab}_\Delta)$ and rational lines containing Δ. We introduce

Definition 4.9 (A classification of triangles). We say a triangle is *irrational* if it lies on no rational lines, and *generic in a rational line* ℓ if ℓ is the unique rational line it lies on. Otherwise, the triangle lies on infinitely many rational lines. In this case, each angle of the triangle is a rational multiple of π and we call it a *rational* triangle.

According to the duality just mentioned, this classification of triangles also classifies the isomorphism class of $ker(hol^{ab}_\Delta)$. In particular, $ker(hol^{ab}_\Delta) = \{0\}$ if Δ is irrational, $ker(hol^{ab}_\Delta) \cong \mathbb{Z}$ if Δ is generic in a rational line, and $ker(hol^{ab}_\Delta) \cong \mathbb{Z}^2$ if Δ is rational.

AC_Δ was described as a twisted thickening of the graph coming from the tiling of the plane by regular hexagons. The cover automorphisms of $AC_\Delta \to \mathcal{E}_\Delta$ act by translations of the plane preserving the hexagonal tiling. We deduce that MT_Δ can

be described as a twisted thickening of the hexagonal tiling of the Euclidean surface, $\mathbb{R}^2$ modulo the action of $ker(hol^{ab}_\Delta)$. To summarize, we give a vague description of MT_Δ corresponding to the classification of Δ.

Corollary 4.10 (Topology of MT_Δ). *MT_Δ is homeomorphic to a twisted thickening of the graph coming from a regular hexagonal tiling of an Euclidean surface $E_\Delta = \mathbb{R}^2/ker(hol^{ab}_\Delta)$. The topology of E_Δ and the isomorphism class of $ker(hol^{ab}_\Delta)$ depend on the classification of Δ:*

1. *If Δ is* irrational*, then $ker(hol^{ab}_\Delta) = \{0\}$ and E_Δ is the plane. Thus, we know $MT_\Delta = AC_\Delta$.*
2. *If Δ is* rational*, then $ker(hol^{ab}_\Delta) \cong \mathbb{Z}^2$ and E_Δ is a torus. The covering $MT_\Delta \to \mathcal{E}_\Delta$ is finite.*
3. *Otherwise, Δ is* generic in some rational line ℓ*, $ker(hol^{ab}_\Delta) \cong \mathbb{Z}$, and E_Δ is an Euclidean cylinder.*

Remark 4.11. *If ℓ is a rational line, then each MT_Δ is homeomorphic for a generic $\Delta \in \ell$. We will denote this homeomorphism class by MT_ℓ, and use $MT_{\ell,\Delta}$ as an alternate notation for MT_Δ when Δ is generic in ℓ. We think of MT_ℓ only as a topological surface with a triangulation and $MT_{\ell,\Delta}$ as that topological surface rigidified by setting the geometry of each triangle to match Δ. Then if Δ is rational triangle contained in ℓ, $MT_{\ell,\Delta}$ is a translation surface which covers MT_Δ.*

Figure 4.6 shows some examples of MT_Δ.

4.5 A bounding box

The first goal of this section is to understand the ramifications of corollary 4.6. Sets of symbolics classes of curves on MT_Δ which can be realized by geodesics all traveling in the same direction lie in the image of the comb-out map $\Psi : H_1(MT_\Delta, \mathbb{Z}) \to \mathcal{H}(MT_\Delta)$. To make discussing this notion easier we introduce a definition:

Definition 4.12. *Let S be a surface which is triangulated by saddle connections (such as MT_Δ or AC_Δ). Let $\{[\eta_1]_s, \ldots, [\eta_n]_s\}$ be a set of symbolics classes of oriented curves on S. We say that $\{[\eta_1]_s, \ldots, [\eta_n]_s\}$ is* friendly *if*

$$\{[\eta_1]_s, \ldots, [\eta_n]_s\} = \Psi\Big([\![\eta_1]\!] + \ldots + [\![\eta_n]\!]\Big)$$

By proposition 4.5, this is equivalent to the statement that $\{[\eta_1]_s, \ldots, [\eta_n]_s\}$ can be realized by a set of curves $\{\eta_1, \ldots, \eta_n\}$ with $\eta_i \in [\eta_i]_s$ so that

1. *no η_i has a self-intersection,*
2. *the $\{\eta_1, \ldots, \eta_n\}$ are all disjoint, and*

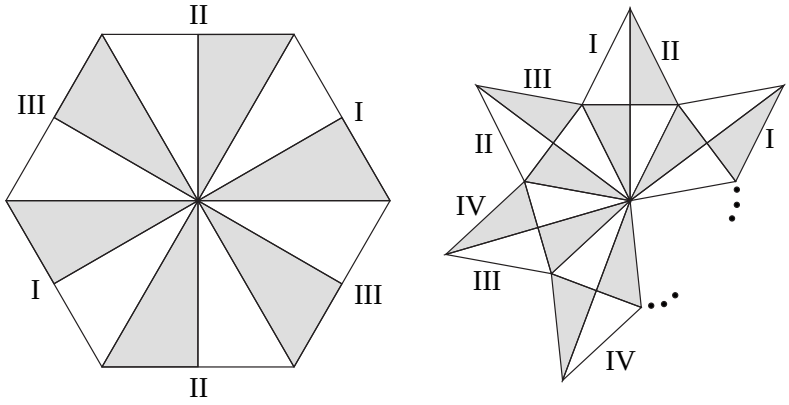

Figure 4.6: This figure describes some examples of minimal translation surfaces. If Δ is the 30-60-90 triangle, then the associated translation surface is a torus obtained by gluing opposite sides of a hexagon. If Δ is generic in the line of right triangles, then the translation surface can be decomposed into rhombi which spiral around a single vertex. The edges on the boundary of this spiral of rhombi can be identified in parallel pairs.

3. *the set of curves $\{\eta_1, \ldots, \eta_n\}$ intersect each edge of the triangulation of S with at most one algebraic sign.*

If $\{[\eta_i]_s\}$ is not friendly, then we call it unfriendly*.*

Remark 4.13. *The second definition of friendliness uses only topological notions of intersections. Therefore, if $\phi_1 : S_1 \to S_2$ is a homeomorphism between surfaces which respects the triangulation, then $\{[\eta_i]_s\}$ is friendly on S_1 if and only if $\{\phi_1([\eta_i]_s)\}$ is friendly on S_2. Further, if $\phi_2 : S_3 \to S_4$ is a covering map respecting the triangulations, then if $\{\phi_2([\eta_i]_s)\}$ is friendly, then so is $\{[\eta_i]_s\}$. To see this, realize the $\{\phi_2([\eta_i]_s)\}$ by curves on S_4 which satisfy the definition and lift them back to S_3. Since, there were no faulty intersections on S_4, there can be none on S_3.*

We are interested in applying this concept to the study of stable geodesics on $\mathcal{E}_\Delta$. By theorem 3.1 , stable geodesics must lift to the universal abelian cover AC_Δ. Since each AC_Δ is homeomorphic, we use AC to denote this homeomorphism class. Let $[\widetilde{\gamma}]_s$ be a symbolics class of curves on AC. Let $\phi_\Delta : AC \to MT_\Delta$ be the covering map. There might (depending on the choice of Δ) be an automorphism $\rho : MT_\Delta \to MT_\Delta$ of the cover $MT_\Delta \to \mathcal{E}_\Delta$ which acts on the direction map by a rotation by π. That is, ρ also acts on $T_1 MT_\Delta$, and the map $\theta \circ \rho \circ \theta^{-1}$ is well defined and rotates elements in S^1 by π. We call ρ a *rotation by π*. If x is a geodesic on MT_Δ, and ρ is a rotation by π, then x and $-\rho(x)$ (the image of x under ρ with the opposite orientation) both travel in the same direction.

Remark 4.14. *A minimal translation surface can admit at most one rotation by π. Suppose ρ_1 and ρ_2 are both rotations by π. Then $\rho_1 \circ \rho_2^{-1}$ acts trivially on directions*

in the minimal translation surface, and hence must be the trivial automorphism of the cover.

Definition 4.15. *Let ϕ_Δ be the covering $AC \to MT_\Delta$. Given a symbolics class of curves $[\widetilde{\gamma}]_s$ on AC, the* unfriendly set of $[\widetilde{\gamma}]_s$ *is*

$$UF([\widetilde{\gamma}]_s) = \left\{ \Delta \in \mathcal{T} \;\middle|\; \begin{array}{l} \{\phi_\Delta([\widetilde{\gamma}]_s)\} \text{ is unfriendly on } MT_\Delta \text{ or} \\ \{\phi_\Delta([\widetilde{\gamma}]_s), -\rho \circ \phi_\Delta([\widetilde{\gamma}]_s)\} \text{ is unfriendly on } MT_\Delta \\ \text{which admits } \rho, \text{ a rotation by } \pi. \end{array} \right\}$$

It is clear by corollary 4.6, that if $[\gamma]_s$ is a symbolics class on $\mathcal{E}$ and $[\widetilde{\gamma}]_s$ is a lift to AC then $UF([\widetilde{\gamma}]_s)$ and $tile([\gamma]_s)$ are disjoint.

Determining whether $\Delta \in UF([\widetilde{\gamma}]_s)$ requires first determining if MT_Δ admits a rotation by π. Recall the definition of the topological surface MT_ℓ given in remark 4.11.

Proposition 4.16 (Existence of ρ). *There is a rotation by π of MT_Δ if and only if Δ lies on a rational line ℓ which can be determined by three odd integers n_1, n_2, and n_3.*

$$\ell = \{(\alpha_1, \alpha_2, \alpha_3) \in \mathcal{T} | n_1\alpha_1 + n_2\alpha_2 + n_3\alpha_3 = 0\}$$

The rotation by π of MT_Δ lifts to an automorphism ρ of the cover $MT_\ell \to \mathcal{E}$, which acts as a rotation by π on $MT_{\ell,\Delta'}$ for all $\Delta' \in \ell$.

Proof: First, if ρ is a rotation by π of MT_Δ, then it lifts to a rotation by π of AC_Δ. Recall equation 4.4. The automorphisms of the cover $AC_\Delta \to \mathcal{E}_\Delta$ are canonically identified with $H_1(\mathcal{E}_\Delta)$. Call this lift $\widetilde{\rho} \in H_1(\mathcal{E}_\Delta)$, and it satisfies $hol^{ab}(\Delta, \widetilde{\rho}) = \pi$. Assume $\widetilde{\rho} = a[\![\beta_1]\!] + b[\![\beta_2]\!]$. Then, there is an integer n so that

$$2a\alpha_1 + 2b\beta_1 = (2n+1)\pi$$

Therefore, $(2a - 2n - 1)\alpha_1 + (2b - 2n - 1)\alpha_2 - (2n+1)\alpha_3 = 0$. The odd integers $n_1 = 2a - 2n - 1$, $n_2 = 2b - 2n - 1$ and $n_3 = -2n - 1$ suffice to determine the rational line ℓ containing Δ.

Now, we will prove that if odd n_1, n_2, and n_3 determining a rational line ℓ containing Δ, then MT_Δ admits a rotation by π. Of course, saying that there exist odd integers with $n_1\alpha_1 + n_2\alpha_2 + n_3\alpha_3 = 0$, is equivalent to say that there exist even integers $e_1 = n_1 + 1$, $e_2 = n_2 + 1$, and $e_3 = n_3 + 1$ with

$$e_1\alpha_1 + e_2\alpha_2 + e_3\alpha_3 = \pi$$

First assume such e_i exist. Let $\zeta = \frac{e_1}{2}[\![\beta_1']\!] + \frac{e_2}{2}[\![\beta_2']\!] + \frac{e_3}{2}[\![\beta_3']\!] \in H_1(T_1\mathcal{E}_\Delta, \mathbb{Z})$, so that $\widetilde{hol}^{ab}(\Delta, \zeta) = \pi$ by equation 4.19. Therefore, $hol^{ab}(\Delta, \pi_*(\zeta)) = \pi$ and $\pi_*(\zeta)$ is a rotation by π of AC_Δ. Because the covers $AC_\Delta \to MT_\Delta \to \mathcal{E}_\Delta$ are abelian, $\pi_*(\zeta)$ descends to an automorphisms of the cover $MT_\Delta \to \mathcal{E}_\Delta$ which also acts by a rotation by π.

Continuing the argument, $\pi_*(\zeta)$ also descends to a rotation by π of $MT_{\ell,\Delta}$. Since we used nothing about Δ besides that $\Delta \in \ell$, $\pi_*(\zeta)$ acts by a rotation by π on $MT_{\ell,\Delta'}$ for all $\Delta' \in \ell$. $\diamondsuit$

In order to deal with the unfriendly set, we also need a technique to show when a self intersection or an intersection between two curves must happen regardless of the choice of loops in a symbolics class of curves. We introduce the following two propositions which follow the philosophy that intersections between geodesics on non-positively curved surfaces are "essential."

Proposition 4.17. *Suppose γ is a geodesic on a locally Euclidean surface S covering $\mathcal{E}_\Delta$. If γ is not simple, then no curve in the symbolics class $[\gamma]_s$ is simple.*

Proposition 4.18. *Suppose γ_1 and γ_2 are geodesics on a locally Euclidean surface S covering $\mathcal{E}_\Delta$. If γ_1 and γ_2 are not disjoint, then no curve taken from the symbolics class $[\gamma_1]_s$ is disjoint from a curve from the symbolics class $[\gamma_2]_s$.*

Proof of Propositions 4.17 and 4.18: We provide the proof of proposition 4.18. The other follows the same logic.

Let P be an intersection point between geodesics γ_1 and γ_2 on S. We lift the geodesics passing through this point to two geodesics, $\widetilde{\gamma_1}$ and $\widetilde{\gamma_2}$ on the universal cover $\widetilde{S}$ so that each passes though a lift of P, which we call $\widetilde{P}$.

We will develop a neighborhood N of this intersection at $\widetilde{P}$ into the plane. First let N be the triangle containing $\widetilde{P}$. Whenever a point in the pair $\partial N \cap \widetilde{\gamma_1}$ lies on the same edge as a point in the pair $\partial N \cap \widetilde{\gamma_2}$, add the triangle on the other side of this edge to N. Eventually, this process must terminate, because the developed images of $\widetilde{\gamma_1}$ and $\widetilde{\gamma_2}$ are lines intersecting in the plane. Therefore, the lines are growing further apart, but the triangles are all isometric and hence have a common bounded diameter. The result is a simply connected chain of triangles similar to the one shown in figure 4.7. We think of this intersection as forced because the end points $\partial N \cap \widetilde{\gamma_1}$ separate $\partial N \cap \widetilde{\gamma_2}$ on ∂N.

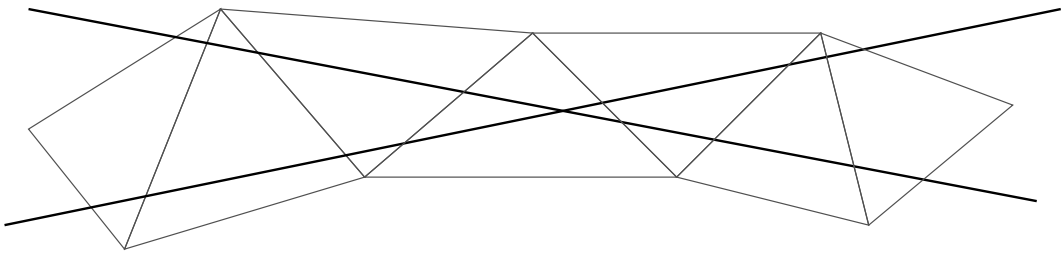

Figure 4.7: An intersection developed into the plane. The intersection is forced because one arc comes in the bottom-left and leaves out the top-right, but the other comes in the top-left and leaves out the bottom-right.

Now suppose $\eta_1 \in [\gamma_1]_s$ and $\eta_2 \in [\gamma_2]_s$. We take the same lifts $\widetilde{\eta_1}$ and $\widetilde{\eta_2}$ to $\widetilde{S}$. By definition of the symbolics class, they must intersect the edges in the same order. Therefore, the end points $\partial N \cap \widetilde{\eta_1}$ separate $\partial N \cap \widetilde{\eta_2}$ on ∂N. Since N is just a disk, $\widetilde{\eta_1}$ and $\widetilde{\eta_2}$ must intersect. We push this intersection back down to S to see an intersection between η_1 and η_2 on S. $\diamondsuit$

We now describe our general approach for working with the unfriendly set, $UF([\widetilde{\gamma}]_s)$. We assume that γ is a geodesic on $\mathcal{E}_\Delta$ for some Δ, and that it lifts to a loop $\widetilde{\gamma}$ on AC_Δ. Now if Δ' is another triangle, then we know there is a covering map $\phi_{\Delta'} : AC_{\Delta'} \to MT_{\Delta'}$. We build a new locally Euclidean surface, $MT_{\Delta'}(\Delta)$, out of copies of Δ by replacing every copy of Δ' in $MT_{\Delta'}$ with Δ. Note that $MT_{\Delta'}(\Delta)$ is not a translation surface for generic choices of Δ and Δ'. We abuse notation by also using $\phi_{\Delta'}$ to denote the covering $AC_\Delta \to MT_{\Delta'}(\Delta)$. Similarly, if the automorphism $\rho : MT_{\Delta'} \to MT_{\Delta'}$ of the cover $MT_{\Delta'} \to \mathcal{E}_{\Delta'}$ is a rotation by π, we also obtain an automorphism $\rho : MT_{\Delta'}(\Delta) \to MT_{\Delta'}(\Delta)$ of the cover $MT_{\Delta'}(\Delta) \to \mathcal{E}_\Delta$.

Propositions 4.17 and 4.18 tell us that

Lemma 4.19 (Witnessing Unfriendliness). *If γ is a geodesic on $\mathcal{E}_\Delta$ which lifts to a loop $\widetilde{\gamma}$ on AC_Δ, then $\Delta' \in UF([\widetilde{\gamma}]_s)$ if and only if one of the following holds:*

1. *$\phi_{\Delta'}(\widetilde{\gamma})$ is not simple on $MT_{\Delta'}(\Delta)$.*
2. *$\phi_{\Delta'}(\widetilde{\gamma})$ intersects the same edge of $MT_{\Delta'}(\Delta)$ twice but with opposite orientations.*
3. *There is a rotation by π, $\rho : MT_{\Delta'} \to MT_{\Delta'}$, and $\phi_{\Delta'}(\widetilde{\gamma})$ is not disjoint from $\rho \circ \phi_{\Delta'}(\widetilde{\gamma})$ on $MT_{\Delta'}(\Delta)$.*
4. *There is a rotation by π, $\rho : MT_{\Delta'} \to MT_{\Delta'}$, and $\phi_{\Delta'}(\widetilde{\gamma})$ and $-\rho \circ \phi_{\Delta'}(\widetilde{\gamma})$ intersect the same edge of the triangulation of $MT_{\Delta'}(\Delta)$ with opposite orientations.*

Proof: It is easier to prove the contrapositive. That is, we will show that all four statements above are false if and only if Δ' is in $\mathcal{T} \setminus UF([\widetilde{\gamma}]_s)$.

First suppose that there is no rotation by π of $MT_{\Delta'}$. Then if statements 1 and 2 are false, then by definition, $\{[\phi_{\Delta'}(\widetilde{\gamma})]_s\}$ is friendly on $MT_{\Delta'}(\Delta)$ which is homeomorphic to $MT_{\Delta'}$, so that $\Delta' \in \mathcal{T} \setminus UF([\widetilde{\gamma}]_s)$.

Now, suppose $\rho : MT_{\Delta'} \to MT_{\Delta'}$ is a rotation by π of $MT_{\Delta'}$. By the negation of statements 1-4, the pair of symbolics classes $\{[\phi_{\Delta'}(\widetilde{\gamma})]_s, [\rho \circ \phi_{\Delta'}(\widetilde{\gamma})]_s\}$ is friendly on $MT_{\Delta'}(\Delta)$ and thus on $MT_{\Delta'}$ as well. Again, $\Delta' \in \mathcal{T} \setminus UF([\widetilde{\gamma}]_s)$.

Now suppose there is no rotation by π of $MT_{\Delta'}$ and $\Delta' \in \mathcal{T} \setminus UF([\widetilde{\gamma}]_s)$. Then by definition of $UF([\widetilde{\gamma}]_s)$, $\{\phi_{\Delta'}[\widetilde{\gamma}]_s\}$ is friendly. This implies that there is a loop $\eta \in \phi_{\Delta'}[\widetilde{\gamma}]_s$ which is simple and intersects each edge of the triangulation with only one orientation. But $\phi_{\Delta'}(\widetilde{\gamma}) \in \phi_{\Delta'}[\widetilde{\gamma}]_s$ as well. Since they lie in the same symbolics class, they must intersect the same sequence of edges, so statement 2 is false. Also, by

proposition 4.17, a self intersection of $\phi_{\Delta'}(\widetilde{\gamma})$ forces a self intersection of η. Therefore, statement 1 is false.

Finally, assume there is a rotation by π of $MT_{\Delta'}$ called ρ and that $\Delta' \in \mathcal{T} \smallsetminus UF([\widetilde{\gamma}]_s)$. By definition, the pair $\{\phi_{\Delta'}[\widetilde{\gamma}]_s, \rho \circ \phi_{\Delta'}[\widetilde{\gamma}]_s\}$ is friendly. Therefore, there exists $\eta_1 \in \phi_{\Delta'}[\widetilde{\gamma}]_s$ and $\eta_2 \in -\rho \circ \phi_{\Delta'}[\widetilde{\gamma}]_s$ which are simple, disjoint, and intersect each edge of the triangulation of $MT_{\Delta'}$ with only one orientation. We conclude that statements 2 and 4 are true because $\phi_{\Delta'}(\widetilde{\gamma})$ and $-\phi_{\Delta'}(\widetilde{\gamma})$ lie in the same symbolics classes as η_1 and η_2 respectively. Again, both must be simple by 4.17, so that statement 1 is false. By 4.18, they must be disjoint. Therefore, statement 3 is false. $\diamondsuit$

In the next section we will use this lemma to prove the following theorem:

Theorem 4.20. *Let γ be a closed geodesic on $\mathcal{E}_\Delta$ which lifts to a closed geodesic $\widetilde{\gamma}$ on AC_Δ. The unfriendly set, $UF([\widetilde{\gamma}]_s)$, is a finite union of rational lines in $\mathcal{T}$.*

We will also connect this set to the $tile([\gamma]_s)$ introduced in the introduction. By corollary 4.6, we know $tile([\widetilde{\gamma}]_s)$ is disjoint from $UF([\widetilde{\gamma}]_s)$. More is true.

Theorem 4.21 (Bounding Box Theorem). *Let γ be a closed geodesic on $\mathcal{E}_\Delta$ which lifts to a closed geodesic $\widetilde{\gamma}$ on AC_Δ. The set $tile([\gamma]_s])$ is contained in one component of $\mathcal{T} \smallsetminus UF([\widetilde{\gamma}]_s)$.*

This theorem will also be proved in the next section.

4.6 Angles at intersections

Given two oriented lines intersecting at a point P in the plane we associate a canonical angle θ_P with measure between 0 and π. This choice of angle is shown in figure 4.8.

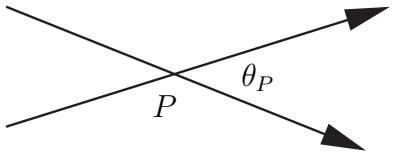

Figure 4.8: An intersection, P, between two oriented lines and the canonical choice of angle θ_P.

Suppose $\widehat{\gamma}$ is a stable periodic billiard on Δ, and γ is its geodesic lift to $\mathcal{E}_\Delta$. Now suppose there is an intersection X of γ on $\mathcal{E}_\Delta$. We can measure the angle of intersection θ_X at this point using a protractor, or alternately using the Gauss-Bonnet formula. Consider the bent geodesic L_X which follows γ until it hits this intersection X, then it makes a left turn and closes up. See figure 4.9. Let L'_X be

the loop on $T_1\mathcal{E}_\Delta$ which follows the derivative of L_X except at the bend, where it interpolates between the tangents by rotating around the unit tangent circle to the left by angle θ_X. Because all the turning of L'_X occurs at this intersection point we see

$$\int_{L'_X} d\theta = \widetilde{hol}^{ab}(\Delta, [\![L'_X]\!]) = \theta_X \tag{4.27}$$

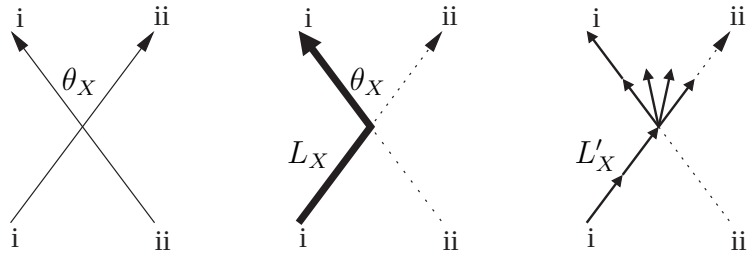

Figure 4.9: *Left:* A local picture of a geodesic self-intersection X on a locally Euclidean surface. θ_X is the angle associated to this intersection. *Center:* The loop L_X on the surface. *Right:* The loop L'_X on the unit tangent bundle of the surface.

Clearly, $0 < \theta_X < \pi$. The value of $\widetilde{hol}^{ab}(\Delta', [\![L'_X]\!])$ varies linearly in the angles of the triangle Δ' as Δ' varies (Recall equation 4.19). More generally,

Lemma 4.22. *Suppose X is a self-intersection of the geodesic γ on $\mathcal{E}_\Delta$. Then if $\mathcal{E}_{\Delta'}$ has a geodesic γ' with the same symbolic dynamics, then*

$$0 < \widetilde{hol}^{ab}(\Delta', [\![L'_X]\!]) < \pi$$

Proof: We prove this by exhibiting an intersection Y of γ' so that $[\![L'_X]\!] = [\![L'_Y]\!]$. This is an application of the general principle that intersections between geodesics on non-positively curved surfaces are essential. It follows much of the logic of the proof of proposition 4.17.

Consider the intersection X of γ. We can lift the two arcs of γ passing through X to the universal cover $\widetilde{\mathcal{E}_\Delta}$ obtaining two geodesic arcs γ_1 and γ_2. We choose the lifts so that they each pass through the lift $\widetilde{X}$ of X. We produce a simply connected union of triangles $U \subset \widetilde{\mathcal{E}_\Delta}$ as in figure 4.7. The union U has the property that the four geodesic rays out of $\widetilde{X}$ leave U out different edges. Their end points $\partial U \cap \gamma_1$ and $\partial U \cap \gamma_2$ separate each other on ∂U. This is forced by the symbolic dynamics.

Since γ' has the same symbolic dynamics, we can find a simply connected union of triangles, $U' \subset \widetilde{\mathcal{E}_{\Delta'}}$, homeomorphic to U and lifts γ'_1 and γ'_2 of γ' which pass through U' in the same manner. Again, their end points separate each other on $\partial U'$ (they are ordered the same on the boundary, because this order is determined by the symbolic dynamics). Therefore γ'_1 and γ'_2 must have an intersection, $\widetilde{Y}$. Name the image of the intersection $\widetilde{Y}$ on $\mathcal{E}_{\Delta'}$ Y.

There is a homeomorphism $U \to U'$ which sends $\gamma_1 \mapsto \gamma_1'$ and $\gamma_2 \mapsto \gamma_2'$. We can build L_X out of the derivative of γ and a local picture about the intersection point X. This local picture lifts to $\widetilde{X} \subset U$. The mentioned homeomorphism tells us that the local picture at Y matches that of X. Moreover, the fact that the symbolic dynamics agree tells us that the constructed curves L_X' and L_Y' are homotopic. Therefore $[\![L_X']\!] = [\![L_Y']\!]$, and

$$\theta_Y = \widetilde{hol}^{ab}(\Delta', [\![L_X']\!]) \tag{4.28}$$

Of course, $0 < \theta_Y < \pi$. $\diamondsuit$

For the next case, suppose that e is an (oriented) edge of the triangulation of $\mathcal{E}_\Delta$. Let γ be a geodesic which intersects the edge e twice but with opposite signs. Call these two intersections A and B and their associated angles θ_A and θ_B respectively. We wish to find a curve in $T_1\mathcal{E}_\Delta$ which when integrated with respect to $d\theta$ yields $\theta_A + \theta_B$.

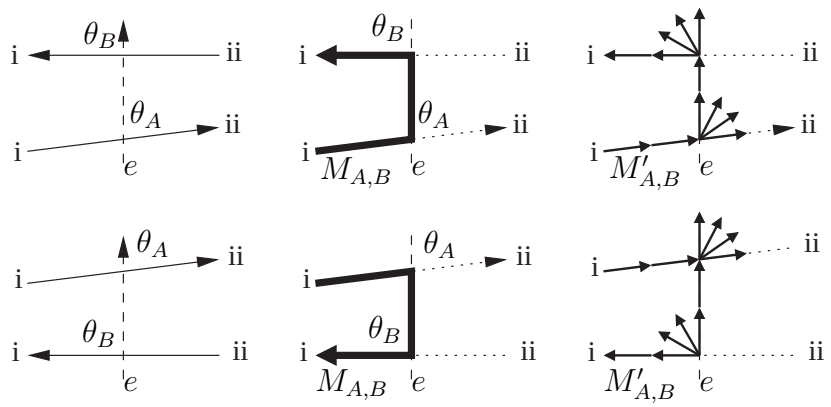

Figure 4.10: *Left:* A local picture of a pair of intersections with opposite orientations, A and B, between a closed geodesic and an edge of the triangulation of $\mathcal{E}_\Delta$. Two possibilities are shown. *Center:* The loop $M_{A,B}$ on the surface. *Right:* The loop $M'_{A,B}$ on the unit tangent bundle of the surface.

In this case there are two distinct pictures which appear, shown as rows in figure 4.10. The differences will not matter for our argument. Rotate the edge e so it is oriented vertically. Assume the arc of γ containing A comes in from the left and the arc of γ containing B comes from the right. We define the loop $M_{A,B}$ which travels along γ until it hits A then travels along e to B and then follows γ again and closes up. We define the loop $M'_{A,B}$ on $T_1\mathcal{E}_\Delta$ to be the loop which agrees with the derivative of γ while $M_{A,B}$ travels along γ and agrees with the derivative of e while $M_{A,B}$ travels along e. It rotates the vectors by θ_A and θ_B at the intersection points. This loop is the derivative of a geodesic except when it rotates by θ_A and

θ_B. We see that

$$\int_{M'_{A,B}} d\theta = \widetilde{hol}^{ab}(\Delta, [\![M'_{A,B}]\!]) = \theta_A + \theta_B \tag{4.29}$$

Of course $0 < \theta_A + \theta_B < 2\pi$. More generally,

Lemma 4.23. *Suppose A and B are intersections with different orientations of the geodesic γ with an edge e on $\mathcal{E}_\Delta$. Then if $\mathcal{E}_{\Delta'}$ has a geodesic γ' with the same symbolic dynamics, then*

$$0 < \widetilde{hol}^{ab}(\Delta', [\![M'_{A,B}]\!]) < 2\pi$$

Proof: The symbolic dynamics of γ determine the sequence of edges it hits and the orientations of these intersections. Therefore, there must be corresponding intersections A' and B' of γ'. The loop $M_{A,B}$ and the corresponding loop $M_{A',B'}$ can be easily verified to be homotopic. Similarly, $M'_{A,B}$ and $M'_{A',B'}$ are homotopic on $T_1\mathcal{E}$. $\diamondsuit$

We will consider one final case of intersection angles. Suppose C and D are intersections on $\mathcal{E}_\Delta$ between a closed geodesic γ and an edge e with the same orientation. We will define a loop $N'_{C,D}$ on $T_1\mathcal{E}_\Delta$, so that when we integrate $d\theta$ over the loop we obtain $\theta_C - \theta_D$.

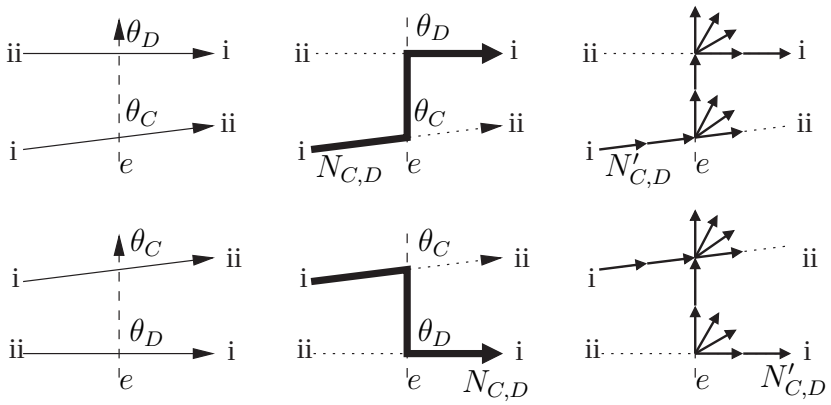

Figure 4.11: *Left:* A local picture of a pair of intersections with the same orientations, C and D, between a closed geodesic and an edge of the triangulation of $\mathcal{E}_\Delta$. *Center:* The loop $N_{C,D}$ on the surface. *Right:* The loop $N'_{C,D}$ on the unit tangent bundle of the surface.

Define $N_{C,D}$ to be the loop which runs along γ to the intersection C, then travels along e to the intersection D, and finally runs along γ again to close up. We define the loop $N'_{C,D}$ to agree with the derivative of γ while $N_{C,D}$ travels along γ and agree with the derivative of e while it travels along e. $N'_{C,D}$ rotates by θ_C at the

intersection C and by $-\theta_D$ at the intersection D. We see

$$\int_{N'_{C,D}} d\theta = \widetilde{hol}^{ab}(\Delta, [\![N'_{C,D}]\!]) = \theta_C - \theta_D \tag{4.30}$$

And $-\pi < \theta_C - \theta_D < \pi$.

Lemma 4.24. *Suppose C and D are intersections with the same orientations of the geodesic γ with an edge e on $\mathcal{E}_\Delta$. Then if $\mathcal{E}_{\Delta'}$ has a geodesic γ' with the same symbolic dynamics, then*

$$-\pi < \widetilde{hol}^{ab}(\Delta', [\![N'_{C,D}]\!]) < \pi$$

Proof: As in the proof of lemma 4.23, there must be corresponding intersections C' and D' of γ'. The loop $N_{C,D}$ on $\mathcal{E}_\Delta$ is homotopic to $N_{C',D'}$ on $\mathcal{E}_{\Delta'}$ and the loop $N'_{C,D}$ on $T_1\mathcal{E}_\Delta$ is homotopic to $N'_{C',D'}$ on $T_1\mathcal{E}_{\Delta'}$. $\diamondsuit$

Definition 4.25. *Given a geodesic loop γ on $\mathcal{E}_\Delta$. We determine a convex subset of $\mathcal{T}$, the space of marked triangles up to similarity parameterized by angles, by considering all such restrictions on the angles of the triangles. Define the* billiard-like tile of γ, *bl-tile(γ), to be the open convex polygon consisting of triangles Δ' satisfying the conditions:*

1. *For each self intersection X of γ,*

$$0 < \widetilde{hol}^{ab}(\Delta', [\![L'_X]\!]) < \pi$$

2. *For each pair of intersections, A and B, between γ and an edge e of opposite orientations,*

$$0 < \widetilde{hol}^{ab}(\Delta', [\![M'_{A,B}]\!]) < 2\pi$$

3. *For each pair of intersections, C and D, between γ and an edge e with the same orientation,*

$$-\pi < \widetilde{hol}^{ab}(\Delta', [\![N'_{C,D}]\!]) < \pi$$

The lemmas 4.22, 4.23, and 4.24 combine to yield:

Theorem 4.26. *Given a geodesic loop γ on $\mathcal{E}_\Delta$, the billiard-like tile bl-tile(γ) contains tile($[\gamma]_s$), the set of all triangles with periodic billiard paths with symbolic dynamics $[\gamma]_s$.*

In order to prove theorems 4.20 and 4.21 we need to recall the connection between $\widetilde{hol}^{ab}$ and hol^{ab}. The projection $p : T_1\mathcal{E}_\Delta \to \mathcal{E}_\Delta$ sends a curve η' on the unit tangent bundle to a curve η on $\mathcal{E}_\Delta$. By diagram 4.15, regardless of the choice of a triangle Δ' we know

$$hol^{ab}(\Delta', [\![\eta]\!]) = \widetilde{hol}^{ab}(\Delta', [\![\eta']\!]) \pmod{2\pi}$$

Essentially, the unfriendly set detects phenomena that occur on the level of hol^{ab} while our definition of the billiard-like tile uses the stronger notion of $\widetilde{hol}^{ab}$.

The following lemma will yield both theorems 4.20 and 4.21.

Lemma 4.27 (The Unfriendly Set). *Suppose γ is a closed geodesic on $\mathcal{E}_\Delta$ which lifts to a closed geodesic $\widetilde{\gamma}$ on AC_Δ. The unfriendly set, $UF([\widetilde{\gamma}]_s)$, is the set of all triangles Δ' so that at least one of the following holds:*

1. *There is a self intersection X of γ so that*

$$hol^{ab}(\Delta', [\![L_X]\!]) = 0 \in \mathbb{R}/2\pi\mathbb{Z}$$

2. *There is a pair of intersections, A and B, between γ and an edge e of opposite orientations so that*

$$hol^{ab}(\Delta', [\![M_{A,B}]\!]) = 0 \in \mathbb{R}/2\pi\mathbb{Z}$$

3. *There is a self intersection X of γ so that*

$$hol^{ab}(\Delta', [\![L_X]\!]) = \pi \in \mathbb{R}/2\pi\mathbb{Z}$$

4. *There is a pair of intersections, C and D, between γ and an edge e with the same orientation so that*

$$hol^{ab}(\Delta', [\![N_{C,D}]\!]) = \pi \in \mathbb{R}/2\pi\mathbb{Z}$$

Proof: There is a correspondence between the conditions of this lemma and those of the Witnessing Unfriendliness Lemma (lemma 4.19). We will show that each statement i from this lemma is equivalent to statement i from the Witnessing Unfriendliness Lemma (we call this statement WUL-i).

Recall that, $MT_{\Delta'}(\Delta)$ is an intermediate cover of $AC_\Delta \to \mathcal{E}_\Delta$ and can be defined as:

$$MT_{\Delta'}(\Delta) = AC_\Delta / \{x \in H_1(\mathcal{E}) \mid hol^{ab}(\Delta', x) = 0 \in S^1\} \tag{4.31}$$

We have the intermediate covers $\phi_{\Delta'} : AC_\Delta \to MT_{\Delta'}(\Delta)$ and $\psi : MT_{\Delta'}(\Delta) \to \mathcal{E}_\Delta$.

(WUL-1 $\implies$ 1): Suppose $\phi_{\Delta'}(\widetilde{\gamma})$ is not simple on $MT_{\Delta'}(\Delta)$. Then it has a self intersection $\widetilde{X}$ on $MT_{\Delta'}(\Delta)$. Call X the self intersection of γ, $\psi(\widetilde{X})$. L_X is built on $\mathcal{E}_\Delta$ by a surgery on γ localized at X. Since this surgery is local, we can also perform it at $\widetilde{X}$ on $\phi_{\Delta'}(\widetilde{\gamma})$, building a new loop $\widetilde{L}_X$. Since L_X lifts to $\widetilde{L}_X$ on $MT_{\Delta'}(\Delta)$, by definition (equation 4.31) it must be that $hol^{ab}(\Delta', [\![L_X]\!]) = 0 \in \mathbb{R}/2\pi\mathbb{Z}$.

(1 $\implies$ WUL-1): If $hol^{ab}(\Delta', [\![L_X]\!]) = 0 \in \mathbb{R}/2\pi\mathbb{Z}$, then L_X lifts to a loop $\widetilde{L}_X$. Since $\psi \circ \phi_{\Delta'}(\widetilde{\gamma}) = \gamma$, this lift $\widetilde{L}_X$ can be chosen to be a subset of $\phi_{\Delta'}(\widetilde{\gamma})$. Therefore,

the point at which $\widetilde{L}_X$ bends is an self intersection of $\phi_{\Delta'}(\widetilde{\gamma})$. So, $\phi_{\Delta'}(\widetilde{\gamma})$ is not simple.

(WUL-2 $\implies$ 2): Suppose that $\phi_{\Delta'}(\widetilde{\gamma})$ intersects an edge $\widetilde{e}$ of the triangulation of $MT_{\Delta'}(\Delta)$ with opposite orientations. Call these intersections $\widetilde{A}$ and $\widetilde{B}$. Call A the intersection $\psi(\widetilde{A})$ and $B = \psi(\widetilde{B})$ which occur between γ and an edge $e = \psi(\widetilde{e})$. We build $M_{A,B}$ and it must lift to a loop $\widetilde{M_{A,B}}$ on $MT_{\Delta'}(\Delta)$. Since this loop lifts, by definition of $MT_{\Delta'}(\Delta)$ we know that $hol^{ab}(\Delta', [\![M_{A,B}]\!]) = 0 \in \mathbb{R}/2\pi\mathbb{Z}$.

(2 $\implies$ WUL-2): Suppose that $hol^{ab}(\Delta', [\![M_{A,B}]\!]) = 0 \in \mathbb{R}/2\pi\mathbb{Z}$. Then, $M_{A,B}$ lifts to a loop $\widetilde{M_{A,B}}$ on $MT_{\Delta'}(\Delta)$. $M_{A,B}$ consists of two pieces, part of the edge e and part of the geodesic γ. We choose the lift $\widetilde{M_{A,B}}$ so that the lifted portion of γ is contained in $\phi_{\Delta'}(\widetilde{\gamma})$. The lifts of the end points of this arc A and B to $\widetilde{A}$ and $\widetilde{B}$ must be contained in the same edge. Therefore, $\phi_{\Delta'}(\widetilde{\gamma})$ intersects this lifted edge with opposite orientations.

Statements 3 and 4 involve loops η with $hol^{ab}(\Delta', [\![\eta]\!]) = \pi$. Now, η no longer lifts to $MT_{\Delta'}(\Delta)$. However, the loop which travels around η twice which we denote by 2η satisfies:

$$hol^{ab}(\Delta', [\![2\eta]\!]) = 0 \in \mathbb{R}/2\pi\mathbb{Z}$$

So 2η lifts to a curve $\widetilde{2\eta}$ on $MT_{\Delta'}(\Delta)$. Furthermore, cover automorphisms of $AC \to \mathcal{E}$ are in bijection with elements of $H_1(\mathcal{E})$. Given a homology class $[\![\eta]\!]$ with $hol^{ab}(\Delta', [\![\eta]\!]) = \pi$, we know that the corresponding cover automorphism $\widetilde{\rho} : AC_{\Delta'} \to AC_{\Delta'}$ is a rotation by π. This cover automorphism descends to the unique rotation by π of the minimal translation surface, $\rho : MT_{\Delta'} \to MT_{\Delta'}$. Of course ρ also acts as a cover automorphism of $MT_{\Delta'}(\Delta) \to \mathcal{E}_{\Delta}$. Since $hol^{ab}(\Delta', [\![\eta]\!]) = \pi$, ρ preserves the loop $\widetilde{2\eta}$, and acts as the non-trivial automorphism of the double cover $\psi : \widetilde{2\eta} \to \eta$.

(WUL-3 $\implies$ 3): Suppose that $\phi_{\Delta'}(\widetilde{\gamma})$ and $\rho \circ \phi_{\Delta'}(\widetilde{\gamma})$ intersect at $\widetilde{X}_1$. Here ρ is a cover automorphism and acts fix point freely. Furthermore, ρ interchanges the two loops. Let, $\widetilde{X}_2 = \rho(\widetilde{X}_1)$ which must be a second distinct intersection point. Now, we build a new loop, called $\widetilde{2L_X}$ which travels along $\phi_{\Delta'}(\widetilde{\gamma})$ from $\widetilde{X}_1$ to $\widetilde{X}_2$ and then travels from $\widetilde{X}_2$ to $\widetilde{X}_1$ along $\rho \circ \phi_{\Delta'}(\widetilde{\gamma})$. We travel along each curve $\phi_{\Delta'}(\widetilde{\gamma})$ and $\rho \circ \phi_{\Delta'}(\widetilde{\gamma})$ along the direction of the orientation. Then $\rho(\widetilde{2L_X}) = \widetilde{2L_X}$ swapping the two arcs of the bi-gon. Let $X = \psi(\widetilde{X}_1) = \psi(\widetilde{X}_2)$ be the self intersection point of γ. The image $\psi(\widetilde{2L_X})$ wraps twice around the curve L_X obtained from this intersection point. The holonomy around L_X can be described by ρ, in the sense that if we try to lift L_X to $MT_{\Delta'}(\Delta)$, we obtain an arc connecting $\widetilde{X}_1$ to $\widetilde{X}_2$. Therefore $hol^{ab}(\Delta', [\![L_X]\!]) = \pi$.

(3 $\implies$ WUL-3): Suppose that $hol^{ab}(\Delta', [\![L_X]\!]) = \pi$. This homology class determines a rotation by π of $AC_{\Delta'}$, which descends to a rotation by π, $\rho : MT_{\Delta'} \to$

$MT_{\Delta'}$. The doubled curve $2L_X$ lifts to a curve $\widetilde{2L_X}$ on $MT_{\Delta'}(\Delta)$ which is preserved by ρ. We can choose this lift to ensure that one arc of the bi-gon is contained in $\phi_{\Delta'}(\widetilde{\gamma})$. Then, because $hol^{ab}(\Delta', [\![L_X]\!]) = \pi$, the other arc is contained in $\rho \circ \phi_{\Delta'}(\widetilde{\gamma})$. Therefore, the two curves $\phi_{\Delta'}(\widetilde{\gamma})$ and $\rho \circ \phi_{\Delta'}(\widetilde{\gamma})$ intersect.

(WUL-4 $\implies$ 4): Suppose that $\phi_{\Delta'}(\widetilde{\gamma})$ and $\rho \circ \phi_{\Delta'}(\widetilde{\gamma})$ intersect the same edge of $MT_{\Delta'}(\Delta)$ with the same orientation. (This is equivalent to $\phi_{\Delta'}(\widetilde{\gamma})$ and $-\rho \circ \phi_{\Delta'}(\widetilde{\gamma})$ intersecting the edge with opposite orientations.) Call this oriented edge $\widetilde{e}_1$. Use $\widetilde{C}_1$ to denote the intersection between $\widetilde{e}_1$ and $\phi_{\Delta'}(\widetilde{\gamma})$, and use $\widetilde{D}_1$ to denote the intersection of $\widetilde{e}_1$ with $\rho \circ \phi_{\Delta'}(\widetilde{\gamma})$. Let $\widetilde{e}_2 = \rho(\widetilde{e}_1$. The intersection $\widetilde{C}_2 = \rho(\widetilde{C}_1$ occurs between $\rho \circ \phi_{\Delta'}(\widetilde{\gamma})$ and $\widetilde{e}_2$, and $\widetilde{D}_2 = \rho(\widetilde{D}_1$ occurs between $\phi_{\Delta'}(\widetilde{\gamma})$ and $\widetilde{e}_2$. Define the loop $\widetilde{2N_{C,D}}$ which travels along $\phi_{\Delta'}(\widetilde{\gamma})$ from $\widetilde{D}_2$ to $\widetilde{C}_1$, then along $\widetilde{e}_1$ to $\widetilde{D}_1$, then along $\rho \circ \phi_{\Delta'}(\widetilde{\gamma})$ to $\widetilde{C}_2$, and finally closes up by traveling along $\widetilde{e}_2$ to $\widetilde{D}_2$. The automorphism ρ preserves the loop $\widetilde{2N_{C,D}}$, swapping the edge contained in $\phi_{\Delta'}(\widetilde{\gamma})$ with that contained in $\rho \circ \phi_{\Delta'}(\widetilde{\gamma})$. The image $\psi(\widetilde{2N_{C,D}})$ wraps twice around the loop $N_{C,D}$ obtained from the intersections of γ $C = \psi(\widetilde{C}_1) = \psi(\widetilde{C}_2)$ and $D = \psi(\widetilde{D}_1) = \psi(\widetilde{D}_2)$ with the edge $e = \psi(\widetilde{e}_1) = \psi(\widetilde{e}_2)$. The holonomy around $N_{C,D}$ is described by ρ so that $hol^{ab}(\Delta', [\![N_{C,D}]\!]) = \pi$.

(4 $\implies$ WUL-4): Suppose that $hol^{ab}(\Delta', [\![N_{C,D}]\!]) = \pi$. We obtain a rotation by π, $\rho : MT_{\Delta'} \to MT_{\Delta'}$, which describes the holonomy of the loop $N_{C,D}$. Its double $2N_{C,D}$ lifts to a loop $\widetilde{2N_{C,D}}$ on $MT_{\Delta'}(\Delta)$, which is preserved by ρ. We choose the lift so that one of the arcs of $2N_{C,D}$ contained in γ lifts to a subset of $\phi_{\Delta'}(\widetilde{\gamma})$. The lift of the other arc must lie in $\rho \circ \phi_{\Delta'}(\widetilde{\gamma})$. The arcs of $2N_{C,D}$ contained in the edge lift to two edges up in $MT_{\Delta'}(\Delta)$. We see that $\phi_{\Delta'}(\widetilde{\gamma})$ and $\rho \circ \phi_{\Delta'}(\widetilde{\gamma})$ intersect each of these edges with the same orientation. Or equivalently, $\phi_{\Delta'}(\widetilde{\gamma})$ and $-\rho \circ \phi_{\Delta'}(\widetilde{\gamma})$ intersect with opposite orientations. $\diamondsuit$

The remaining results from the previous section follow easily.

Proof of Theorem 4.20: Lemma 4.27 places finitely conditions on the unfriendly set each of the form

$$hol^{ab}(\Delta', [\![\eta]\!]) = 0 \ \textit{or} \ \pi \in \mathbb{R}/2\pi\mathbb{Z} \tag{4.32}$$

for some loop η. Equivalently, we could choose a loop η' on $T_1\mathcal{E}$ so that its image under the projection $T_1\mathcal{E} \to \mathcal{E}$ is η and require that

$$\widetilde{hol}^{ab}(\Delta', [\![\eta']\!]) \equiv 0 \ \textit{or} \ \pi \pmod{2\pi}$$

But, for any choice of Δ', $0 < \widetilde{hol}^{ab}(\Delta', [\![\beta_i']\!]) < \pi$. Therefore, the potential values for $\widetilde{hol}^{ab}(\Delta', [\![\eta']\!])$ as Δ' varies are bounded by the size of $[\![\eta]\!]$. Thus, there are only finitely many values of k so that

$$\widetilde{hol}^{ab}(\Delta', [\![\eta']\!]) = (0 \ \textit{or} \ \pi) + 2\pi k \tag{4.33}$$

could be true for some Δ'. Thus each condition in the form of equation 4.32 contributes finitely many lines to the unfriendly set. $\diamondsuit$

Proof of the Bounding Box Theorem: We will show that the billiard-like tile is a single component of $\mathcal{T} \smallsetminus UF([\widetilde{\gamma}]_s)$. Then theorem 4.26 states that $tile([\gamma]_s)$ is contained in this one component.

It is easy to verify that the boundaries of the billiard-like tile (see definition 4.25) are contained in the unfriendly set as described by lemma 4.27. Conversely, each rational line in the unfriendly set is one of a family of parallel rational lines in the form of equation 4.33 and determined by the lemma. Theorem 4.26 forces the billiard-like tile to be contained in one complement of these parallel lines. $\diamondsuit$

4.7 Right triangles are unfriendly

Now that we have proved the bounding box theorem, we can prove theorem A. Let γ be a stable closed geodesic on the surface $\mathcal{E}_\Delta$ (for arbitrary Δ).

Let ℓ be any one of the right triangle lines, say when the angle α_3 is $\frac{\pi}{2}$. This set of right triangles can be described as a rational line:

$$\ell = \{(\alpha_1, \alpha_2, \alpha_3) \in \mathcal{T} | \alpha_1 + \alpha_2 - \alpha_3 = 0\} \tag{4.34}$$

Therefore, by proposition 4.16, MT_ℓ admits a rotation by π which we call ρ. This map simultaneously rotates by π around each lift of the right angled vertex.

By the stability theorem, γ is null-homologous on $\mathcal{E}_\Delta$. Hence, it lifts to a closed geodesic $\widetilde{\gamma}$ on AC_Δ. We let ϕ_ℓ be the covering map $AC \to MT_\ell$.

We need to show that $tile([\gamma]_s)$ is contained in at most one component of $\mathcal{T}$ with the right triangles removed (see figure 4.1). We will have to prove the following lemma:

Lemma 4.28 (Right triangles are unfriendly). *Suppose γ is a stable closed geodesic on $\mathcal{E}_\Delta$ (for arbitrary Δ). It lifts to a closed geodesic $\widetilde{\gamma}$ on AC_Δ. The pair of oriented symbolics class of curves $\{[\phi_\ell(\widetilde{\gamma})]_s, [-\rho \circ \phi_\ell(\widetilde{\gamma})]_s\}$ is unfriendly on MT_ℓ for each right triangle line ℓ.*

In other words, the lemma claims that each right triangle line ℓ is contained in $UF([\widetilde{\gamma}])$. Given this lemma, the proof of Theorem A follows directly from the bounding box theorem.

Let $\gamma_1 = \phi_\ell(\widetilde{\gamma})$ and $\gamma_2 = -\rho \circ \phi_\ell(\widetilde{\gamma})$. To prove this lemma, we suppose by contradiction, that the pair of loops $x = \{\gamma_1, \gamma_2\}$ is friendly on MT_ℓ. Then by proposition 4.5, the symbolics class of the pair of curves is determined uniquely by its homology class $[\![x]\!] = [\![\gamma_1]\!] + [\![\gamma_2]\!]$. We immediately notice two trivial things about this homology class:

1. We can find a homology class $[\![\widetilde{x}]\!]$ on AC so that $\phi_\ell([\![\widetilde{x}]\!]) = [\![x]\!]$. (From hypotheses of the lemma, γ lifts to a curve $\widetilde{\gamma}$ on AC. We can push this back down to MT_ℓ to obtain γ_1. Likewise γ_2 lifts. We can take $[\![\widetilde{x}]\!]$ to be the homology class representing the sum of those lifts.)

2. $\rho([\![x]\!]) = -[\![x]\!]$. (Since ρ maps $\gamma_1 \mapsto -\gamma_2$ and $\gamma_2 \mapsto -\gamma_1$)

First we will use triviality 1. We know that AC is homotopic to the graph corresponding to the hexagonal tiling of the plane, AC_Θ. With hexagonal 2-cells, we can fill in these hexagons to get something simply connected (the plane). Consequently, we can think of a homology class on AC_Θ as the boundary of a finite union of weighted hexagonal 2-cells. MT_ℓ is homotopic to a graph coming from the hexagonal tiling of a cylinder. The hexagonal 2-cells from AC_Θ push down to fill in the hexagons in this graph building a cylinder. In particular, we see that the image of the map $H_1(AC, \mathbb{Z}) \to H_1(MT_\ell, \mathbb{Z})$ is not everything. Instead, $H_1(MT_\ell, \mathbb{Z})$ modulo the image hexagons is isomorphic to $\mathbb{Z}$, generated by a loop which goes once around the cylinder.

We can understand the graph homotopic to MT_ℓ and the action of ρ on this graph by looking at the translation surface itself. The surface decomposes into rhombi consisting of four copies of the triangle as in figure 4.12. In the figure, edges of the dual graph are dashed according to which edge of the triangle they cross. The Θ-graph is the hexagonal tiling graph of the plane modulo translations. So, parallel edges all cross the same type of edge of the triangulation. Indeed, because the dual graph to the triangles in a rhombus is a quadrilateral only crossing two edge types, the dual graph must be the hexagonal graph in the plane modulo a translation by two units upward. Similarly, it can be checked that the rotation by π preserving the rhombus, acts as a translation by one unit upward.

Pictorially, we can describe the homology class of these curves by assigning integral weights (only finitely many nonzero) to the hexagons of the cylinder. These integers represent the weights assigned to the hexagonal 2-cells. Refer to figure 4.13. The hexagonal tiling of the cylinder we mention above is obtained as the quotient of the hexagonal tiling of the plane by the translation by two units upward. Our rotation by π, ρ, acts on a hexagonal 2-cell by translating it one unit upward.

The homology class described by figure 4.13 is a candidate for $[\![x]\!]$. This class lifts to a homology class on AC and $\rho([\![x]\!]) = -[\![x]\!]$. As in the figure, weights assigned to the hexagonal 2-cells in a column are opposites. This forces weights assigned to the horizontal edges in a column to be even and opposite. This is an essential ingredient in the proof.

Figure 4.13 showed the homology class on the hexagonal graph on the cylinder. We would also like to understand what this homology class looks like on the translation surface MT_ℓ. The homology class of figure 4.13 displayed as the dual graph to the triangulation is shown in figure 4.14.

It is important to note that a loop which travels once around the puncture at the center of a rhombus travels once around the cylinder in the other picture. These

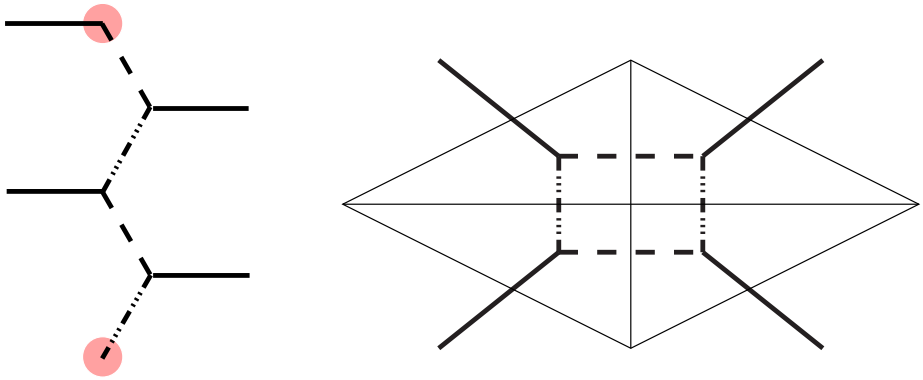

Figure 4.12: On the left, we show a subset of the graph coming from the hexagonal tiling of the cylinder. The two dotted vertices are identified by the translation which we quotient the plane by to get the cylinder. On the right, we show the same graph, the dual graph to the triangulated MT_ℓ.

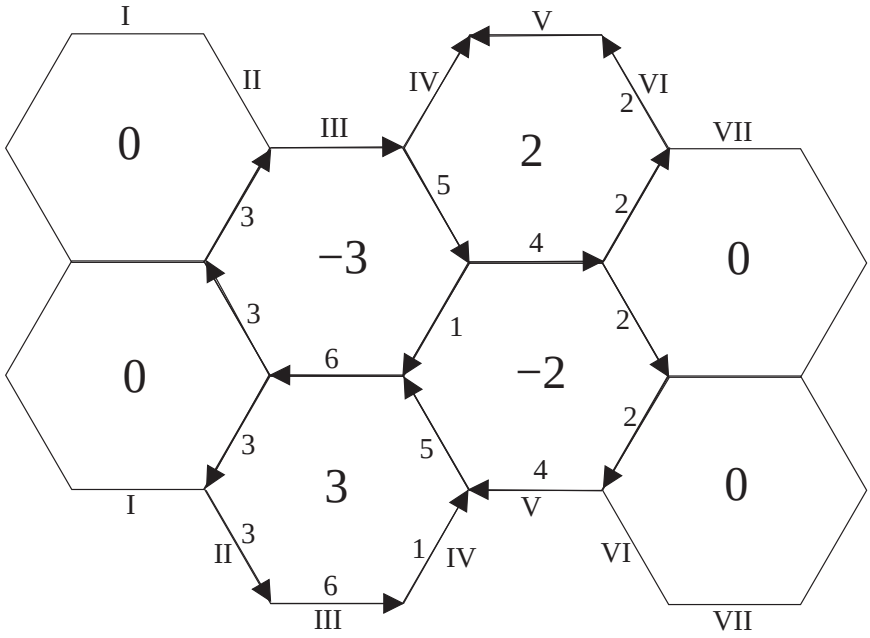

Figure 4.13: A homology class on the graph homotopic to MT_ℓ that lifts to AC_Θ is determined by assigning integer weights to the hexagonal 2-cells in the complement of the graph. This graph is the quotient of the hexagonal graph in the plane by a translation that translates two units upward. Roman numerals indicate identifications used to reconstruct this graph on the cylinder.

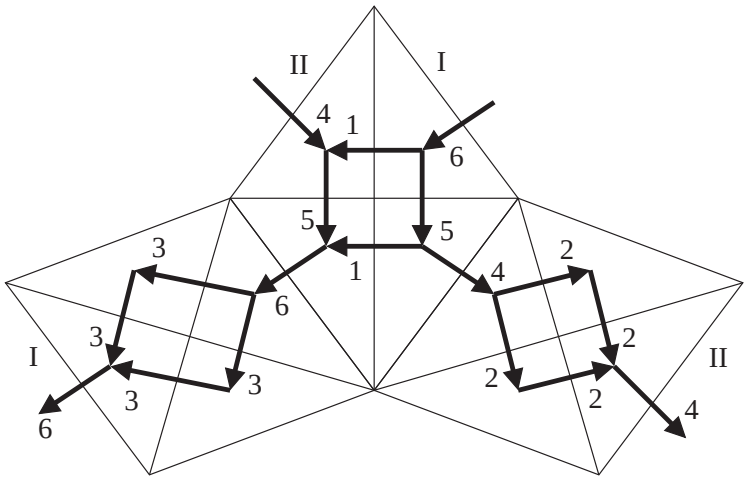

Figure 4.14: This is the same homology class as figure 4.13, only this time it is displayed with the triangulation of MT_ℓ. The roman numerals I and II indicate edge identifications.

curves do not lift to AC.

Let $Y = \Psi([\![x]\!])$ be the set of symbolics classes curves obtained by combing out the homology class $[\![x]\!]$ as in the proof of proposition 4.5.

It is useful to fill in the punctures at the center of each rhombus, constructing a larger surface which we will call $\overline{MT}_\ell$. We have a natural inclusion $i : MT_\ell \hookrightarrow \overline{MT}_\ell$. From what we have already said, we can deduce the following:

Proposition 4.29. *There are an even number of curves in Y. Pushed into $\overline{MT}_\ell$, the curves $i(Y)$ come in homotopic pairs.*

Proof: The push forward $i_*([\![x]\!]) \in H_1(\overline{MT}_\ell, \mathbb{Z})$ can be combed out in a similar manner as in the proof of proposition 4.5. We can see a homology class in $H_1(\overline{MT}_\ell, \mathbb{Z})$ as an assignment of integer weights and orientations to the dual graph to the decomposition of $\overline{MT}_\ell$ into rhombi. The weight assigned by $i_*([\![x]\!])$ to an edge of the dual graph which crosses a boundary of a rhombus is the same as the weight assigned by $[\![x]\!]$ to the edge of the dual graph to the triangulation which crosses that same boundary edge of the rhombus. The edges of the dual graph which cross the hypotenuse of the right triangle are horizontal when the graph is depicted as the hexagonal graph on the cylinder (see figure 4.12). So, all edge weights of $i_*([\![x]\!])$ are even. Weights assigned to edges which cross opposite sides of a rhombus are equal in magnitude but orientations are opposite (one points in, the other out).

Note that if $[\![x]\!]$ assigned orientations to edges as in figure 4.15, then we could not comb out the homology class to arcs in a unique way. Fortunately, because $\rho([\![x]\!]) = -[\![x]\!]$ this assignment of orientations never occurs.

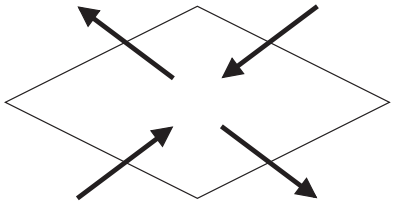

Figure 4.15: $i_*([\![x]\!])$ never assigns orientations to edges crossing the boundary of a rhombus as pictured.

Instead, opposite edges are given opposite orientations. Therefore, we can comb out in a unique way as in figure 4.16.

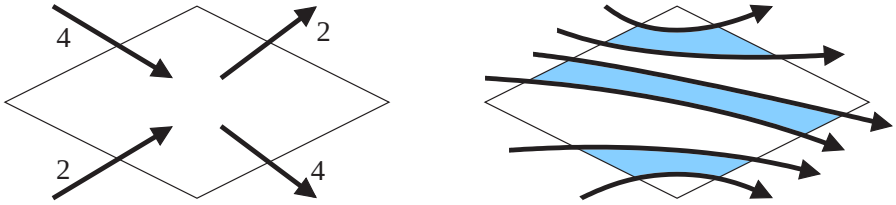

Figure 4.16: Possible edge weights assigned by $i_*([\![x]\!])$ to edges crossing the boundary of a rhombus. On the right, we show the unique comb out.

By uniqueness, the comb out construction constructs a set of curves in the same homotopy class as $i(Y)$. Because an even weight is assigned to each edge, we can partition the arcs which cross a boundary edge of a rhombus into adjacent pairs. (This partition is unique.) The curves travel together across the rhombus and leave as an adjacent pair, since all edge weights are even. Induction tells us that adjacent pairs stay adjacent for all time. Thus, we have partitioned the curves in $i(Y)$ into pairs which are homotopic inside $\overline{MT}_\ell$. We comb out the example homology class of figures 4.13 and 4.14 in figure 4.17. $\diamondsuit$

Proof of Lemma 4.28 We continue to use the notation of this section. Suppose the pair of curves $x = \{\gamma_1, \gamma_2\}$ is friendly on MT_ℓ. Then by proposition 4.5, combing out the homology class $\Psi([\![x]\!])$ yields a pair of curves in the same symbolics class as x. Proposition 4.29 tells us that γ_1 and γ_2 are homotopic inside $\overline{MT}_\ell$. Since they are disjoint, they bound an annulus $\mathcal{A} \subset \overline{MT}_\ell$.

The rotation by π, ρ, preserves the annulus $\mathcal{A}$ and switches its boundary components since $\gamma_2 = -\rho(\gamma_1)$. We claim that ρ fixes two points in $\mathcal{A}$. This follows from Lefshetz's fixed point theorem. Recall that the Lefshetz number associated to

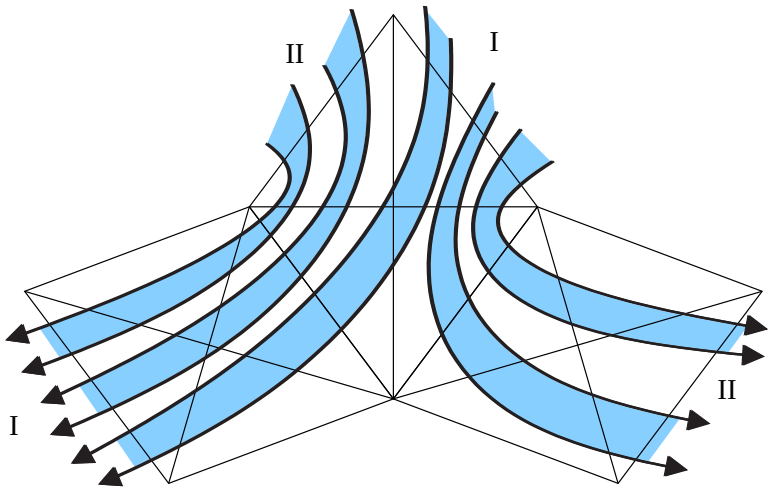

Figure 4.17: The comb out operation applied to the homology class of figures 4.13 and 4.14.

the map $\rho : \mathcal{A} \to \mathcal{A}$ is

$$L(\rho) = \sum_i (-1)^i tr(\rho_{H_i}) \tag{4.35}$$

where $tr(\rho_{H_i})$ is the trace of the map $\rho_{H_i} : H_i(\mathcal{A}, \mathbb{Z}) \to H_i(\mathcal{A}, \mathbb{Z})$ induced by ρ. In our case, the homology of an annulus is

$$H_0(\mathcal{A}, \mathbb{Z}) = H_1(\mathcal{A}, \mathbb{Z}) = \mathbb{Z} \text{ and } H_i(\mathcal{A}, \mathbb{Z}) = 0 \text{ for all } i > 1 \tag{4.36}$$

We see $tr(\rho_{H_0}) = 1$ and $tr(\rho_{H_1}) = -1$, because ρ is homotopic to a homeomorphism from the circle to itself which switches orientation. Thus, $L(\rho) = 2$. Lefshetz's theorem tells us that the Lefshetz number can also be computed as

$$L(\rho) = \sum_{\rho(P)=P} sign(det(I - D_P(\rho))) \tag{4.37}$$

where I and $D_P(\rho)$ are the actions of the identity map and the derivative of ρ on the tangent plane to $\mathcal{A}$ at P respectively. In our case, the only fixed points of the action of ρ on $\overline{MT}_\ell$ are the centers of the rhombi. At the center of each rhombus, ρ acts by a rotation by π. Thus $L(\rho) = 2$ is also the number of centers of rhombi contained in $\mathcal{A}$.

Now we will show that our original curve γ on $\mathcal{E}_\Delta$ could not have been null-homologous, giving us our contradiction. Let ψ denote the cover $MT_\ell \to \mathcal{E}_\Delta$. Because, $\psi(\gamma_1) = \gamma$, we know $\psi([\![\gamma_1]\!]) = 0 \in H_1(\mathcal{E}_\Delta)$. Because ρ was an automorphism

of the cover, we know $\psi(\rho([\![\gamma_1]\!])) = 0$ as well. (Note $\rho(\gamma_1) = -\gamma_2$.) Therefore,

$$\psi([\![\gamma_1]\!] + \rho([\![\gamma_1]\!])) = 0 \in H_1(\mathcal{E}_\Delta)$$

From the previous paragraph, we know $\gamma_1 \cup \rho(\gamma_1)$ is the (oriented) boundary of the annulus $\mathcal{A}$ on $\overline{MT}_\ell$. On MT_ℓ, we know that γ_1 and $\rho(\gamma_1)$ together with two curves α and β which travel around punctures with the same orientations bound a subsurface. See figure 4.18. Then, we know that

$$[\![\gamma_1]\!] + [\![\rho(\gamma_1)]\!] = -([\![\alpha]\!] + [\![\beta]\!]) \in H_1(MT_\ell, \mathbb{Z}) \tag{4.38}$$

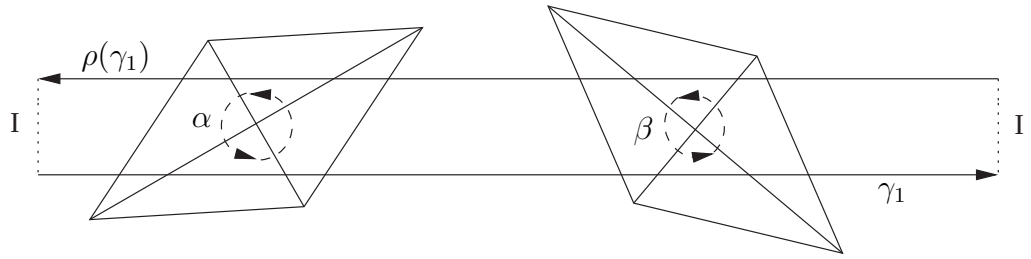

Figure 4.18: In the proof of lemma 4.28, γ_1 and $\rho(\gamma_1)$ bound a punctured annulus. The annulus here is the horizontal strip with vertical dotted lines identified. The punctures come from the centers of rhombi.

Assume $[\![\beta_3]\!]$ represents the homology class of a loop which travels once around the right angled vertex of $\mathcal{E}_\Delta$. (See figure 3.1 and imagine a right triangle.) Then, the covering map $\psi : MT_\ell \to \mathcal{E}_\Delta$ sends both $[\![\alpha]\!]$ and $[\![\beta]\!]$ to $2[\![\beta_3]\!]$. By equation 4.38,

$$\psi([\![\gamma_1]\!] + [\![\rho(\gamma_1)]\!]) = -4[\![\beta_3]\!] \in H_1(MT_\ell, \mathbb{Z}) \tag{4.39}$$

Further, because ρ is an automorphism of the cover ψ, it must be that $\psi([\![\gamma_1]\!]) = \psi([\![\rho(\gamma_1)]\!])$. Therefore, because $\gamma = \psi(\gamma_1)$, we know

$$[\![\gamma]\!] = \psi([\![\gamma_1]\!]) = -2[\![\beta_3]\!] \in H_1(MT_\ell, \mathbb{Z}) \tag{4.40}$$

Thus, $[\![\gamma]\!]$ is not null-homologous. This contradicts the assumption of stability by theorem 3.1. $\diamondsuit$

Chapter 5

Stable periodic billiard paths in obtuse isosceles triangles

We define T_x to be the obtuse isosceles triangle with two acute angles with measure $\alpha = \frac{\pi}{2x}$ and one obtuse angle with measure $(1 - \frac{1}{x})\pi$. In this chapter we prove half of theorem C of the introduction.

Theorem C1. *For every $x > 2$ with $x \notin \mathbb{Z}$ there is a stable periodic billiard path in T_x.*

A *period* of a periodic billiard path is a sub-arc which starts and ends with the billiard ball traveling in the same direction at the same point on the interior of the triangle. A *symbolic period* is a finite sequence of edges hit in a period, that is a finite word in the letters $\{1, 2, 3\}$.

The theorem is proved by studying a two parameter family of billiard paths $Y_{n,m}$. We will mark the long side of the obtuse isosceles triangle 3 and use 1 and 2 for the shorter sides. We define the words

$$X_n = (31)^{n-1}(32)^{n-1} \tag{5.1}$$

We will show the words X_n are symbolic periods for unstable periodic billiard paths in isosceles triangles. We use these words to build a 2-parameter list of new words:

$$Y_{n,m} = 1(X_n)^m 32 \tag{5.2}$$

Theorem C1 is in fact a corollary of the result:

Theorem 5.1. *For every integer $n \geq 2$ and real number x so that $n < x < n + 1$, there is a stable periodic billiard path in T_x with symbolic period $Y_{n,m}$ for some $m \in \mathbb{Z}$.*

5.1 Stability

First we will prove that if in fact we can find a periodic billiard path with a symbolic period given by $Y_{n,m}$, then it must be stable. This follows from theorem 3.1.

Lemma 5.2 (Odd periods are stable). *If $\widehat{\gamma}$ is a periodic billiard path in the triangle T which hits an odd number of edges in its period, then $\widehat{\gamma}$ is stable.*

Proof: Based on theorem 3.1, we only need to prove that the geodesic γ on $\mathcal{D}_T$ corresponding to $\widehat{\gamma}$ is null-homologous in $\mathcal{D}_T \setminus \Sigma$.

The surface $\mathcal{D}_T$ is cut into two triangles by the edges of the triangulation (see figure 3.1). The geodesic γ crosses edges of the triangulation in the same order as $\widehat{\gamma}$, but the period will be twice as long. Each time γ crosses an edge it moves from one triangle in this decomposition to the other. In order to close up, it must cross an even number of edges.

Whenever γ crosses an edge e it must cross it again in half a period with the opposite orientation. Therefore, the total intersection number of γ with each edge of the triangulation is zero. So, γ is null-homologous. $\diamondsuit$

5.2 The unstable family X_n

We need to show that there are periodic billiard paths in these obtuse triangles with combinatorics given by X_n. The fact that these paths are unstable is irrelevant to our arguments.

Proposition 5.3. *For every $x > n-1 \in \mathbb{Z}$ the triangle T_x has a periodic billiard path with symbolic period X_n.*

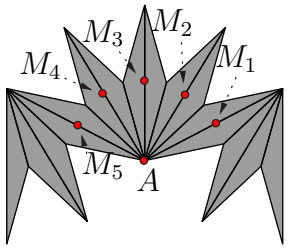

Figure 5.1: An unfolding for the word X_5. One period is shown.

Proof: Let M be the midpoint of the longest side of T_x. By symmetry any billiard path which passes through M twice must close up. As shown in figure 5.2, the measure of angle $M_1AM_n = 2(n-1)\alpha = \frac{(n-1)\pi}{x}$ is less than π precisely when $x > n-1$. In this case the polygon $AM_1M_2 \ldots M_n$ is a convex subset of the unfolding. Therefore, the line segment $\overline{M_1M_n}$ is contained in the unfolding. It is easy to verify that the symbolic period of the resulting billiard path is X_n. $\diamondsuit$

If we unfold a periodic billiard in a triangle T_x, there is a maximal strip of parallel lines contained in the unfolding. Each parallel line folds up to a periodic billiard path with the same symbolic period. The *leading vertices* of an unfolding are the vertices which are contained in the boundary of this maximal strip.

Proposition 5.4. *For every $x > n \in \mathbb{Z}$ the leading vertices of the billiard path with combinatorics X_n are the obtuse vertices of the rhombus containing M_1 and M_n.*

Proof: Note that the unfolding of the word X_n in an isosceles triangle is invariant under a glide reflection which sends M_1 to M_n. Also, a rotation by 180 degrees about M_1 preserves the unfolding. We will slowly go through the vertices of the unfolding (modulo these automorphisms) to show that they are not leaders. It suffices to show that the remaining vertices are further from the axis of the glide reflection. We label the claimed bottom leaders L_1 and L_n and the claimed top vertices L_1' and L_n'. Note that there are automorphisms of the unfolding which take L_1 to each of the other claimed leaders. Therefore, the distance of each to the axis of the glide reflection is the same.

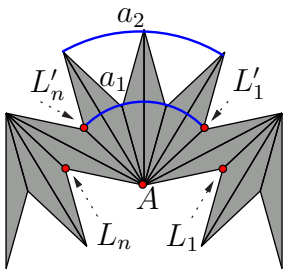

Figure 5.2: The point A and the points on the arcs a_1 and a_2 can not be leaders.

First we will check that the vertex labeled A is not a leader in figure 5.2. The measure of angle $L_1AL_n = 2n\alpha = \frac{n\pi}{x}$, which is less than π whenever $n < x$. When $n < x$, the point A lies further below the line than L_0 and L_n, so A cannot be a leader.

The remaining vertices we need to consider lie on two arcs, a_1 and a_2 of figure 5.2. The arcs are pieces of circles centered at A. The angle associated to the arcs is always less than π when $n < x$. For each i, the convex hull of L_1', L_n', and arc a_i contains the segment $\overline{L_1'L_n'}$ as a boundary component. Therefore all other points on the arc are further from the axis of the glide reflection and cannot be leaders. $\diamondsuit$

We will always normalize lengths so that the short side of the triangle T_x has length 1. We can compute the length translated by the glide reflection preserving the unfolding of the word X_n explicitly (this is the distance between M_1 and M_n in figure 5.2)

$$l = \sin((n-2)\alpha) + \sin(n\alpha) \tag{5.3}$$

We will need this in the next section.

5.3 The stable family $Y_{n,m}$

The word $Y_{n,m}$ has odd length. This tells us that any periodic billiard path with combinatorics $Y_{n,m}$ is stable. Also for odd words, it is easy to compute the direction of the translational holonomy.

Proposition 5.5. *The translation vector of the holonomy of the unfolding of an isosceles triangle by the word $Y_{n,m}$ is parallel to the long side of T_x in the first triangle of the unfolding. See figures 5.3 and 5.4.*

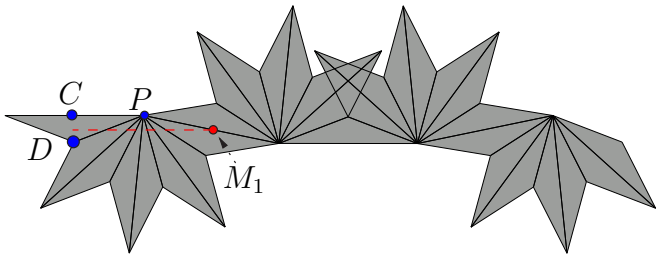

Figure 5.3: An unfolding for the word $Y_{4,1}$

Proof: We will prove that there is reflective symmetry of the unfolding which preserves the first triangle and swaps edges marked 1 with edges marked 2. Such a symmetry of the unfolding induces a symmetry of the symbolic dynamics. The word $Y_{n,m}$ should be invariant under the "symmetry" which reverses order and swaps the letter 2 with the letter 1.

Recall $Y_{n,m} = 1((31)^{n-1}(32)^{n-1})^m 32$. Let $W_{n,m}$ be the word $Y_{n,m}$ written backwards with the letter 1 swapped with the letter 2.

$$W_{n,m} = 13((13)^{n-1}(23)^{n-1})^m 2$$

But this is the same as $W_{n,m} = 1((31)^{n-1}(32)^{n-1})^m 32$. So $W_{n,m} = Y_{n,m}$.

Therefore, the unfolding of an isosceles triangle according to the word $Y_{n,m}$, exhibits this reflective symmetry. The axis of the glide reflection is preserved by this reflection but its orientation is reversed. The same is true for the long side of the first triangle of the unfolding. Therefore, this edge and the line preserved by the glide reflection must be parallel. $\diamondsuit$

A billiard path in an obtuse isosceles triangle that starts parallel to the long side and later hits the midpoint of the long side must close up by symmetry. These are exactly the type of paths we are looking for.

We will break the proof of theorem 5.1 into two cases. This is needed because the leading vertices are different in each case. The first case is easiest.

Lemma 5.6. *For each $n < x \leq n + \frac{1}{2}$ there is a periodic billiard path in T_x with combinatorics $Y_{n,1}$.*

Proof: Given the triangle T_x, unfold the triangle according to the word $Y_{n,1}$. There is a first midpoint of a long side, M_1, so that a rotation by π fixing M_1 preserves the unfolding. See figure 5.3. Let D be the obtuse vertex of the first triangle of the unfolding. Let C be the midpoint of the opposite side. By symmetry, it suffices to show that the line segment connecting M_1 to the segment $\overline{CD}$ orthogonally is contained in the unfolding.

The measure of angle CPM_1 is $2n\alpha = \frac{n\pi}{x} < \pi$ for $n < x$. Thus the orthogonal projection of M_1 to $\overline{CD}$ lies below C.

To see the orthogonal projection of M_1 lies above D, first note that the length $|PM_1|$ is strictly less than $|PD|$. Thus the orthogonal projection of M_1 to $\overline{CD}$ lies above D so long as $2\angle CPD + \angle DPM_1 \geq \pi$. We evaluate the left hand side:

$$2\angle CPD + \angle DPM_1 = (2n+1)\alpha = \frac{(2n+1)\pi}{2x}$$

Therefore, the orthogonal projection of M_1 lies above D when $x \leq \frac{2n+1}{2}$. $\diamondsuit$

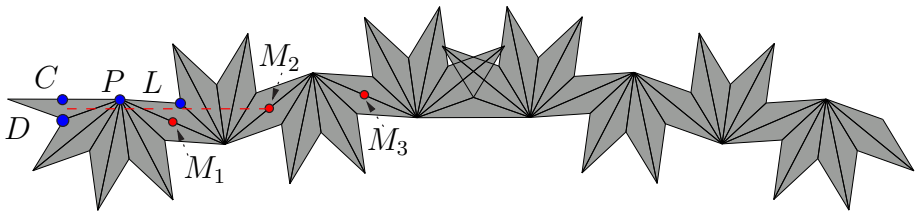

Figure 5.4: An unfolding for the word $Y_{4,2}$

The second case is more complicated. In fact our result is more easily proved non-constructively. A similar proof as the one given above could be given, but I believe this would make the argument far less clear. Consider the case of $Y_{n,2}$. A sample unfolding is shown in figure 5.4. Here, we would show that for some interval of isosceles triangles, the orthogonal projection of M_2 to the segment $\overline{CD}$ is entirely contained in the unfolding. Note that when the measure of angle $\angle CPL < \pi$, the point L becomes a new leader since it is below P. This occurs exactly when $x > n + \frac{1}{2}$ (or $\alpha < \frac{\pi}{2n+1}$). Thus, to show that $Y_{n,2}$ is a symbolic period for billiard path in a particular triangle, we would have to show that the orthogonal projection of M_2 to $\overline{CD}$ passes below L and above D.

Lemma 5.7. *For each $n+\frac{1}{2} < x < n+1$ there is a periodic billiard path in T_x with combinatorics $Y_{n,m}$ for some $m \in \mathbb{N}$.*

Proof: Consider the unfolding of T_x according to the infinite word $1(X_n)^\infty$. See figure 5.5. We will show that there is a M_m so that the orthogonal projection of M_m to $\overline{CD}$ passes below L and above D. A line through M_m and orthogonal to $\overline{CD}$ extends to a periodic billiard path with symbolic dynamics $Y_{n,m}$.

The crucial observation is that, because X_4 is the combinatorics of a periodic billiard path, there is an infinite rectangular strip contained in the unfolding $1(X_n)^\infty$. A beam of light shot orthogonally to $\overline{CD}$ passes below L and above D and then enters this strip. Once inside the strip, the beam of light will continue unobstructed until it hits the line containing $\{M_i\}$. We will show that the beam of light is wider than the vertical change between each M_i and M_{i+1}. It follows that some M_i must be hit by the beam of light. This path generates our desired periodic billiard path.

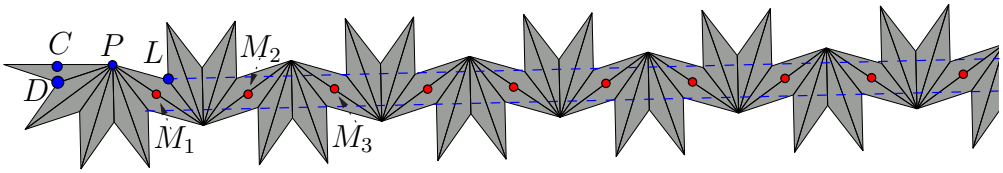

Figure 5.5: An unfolding for the word $1(X_4)^\infty$

Fix coordinates so that $P = (0,0)$. Then $D = (-\cos\alpha, -\sin\alpha)$ and $L = \Big(-\cos\big((2n+1)\alpha\big), -\sin\big((2n+1)\alpha\big)\Big)$. Let π_y be projection to the y-coordinate. Let f be the function which maps the angle α to the difference between the y coordinate of L and D.

$$f(\alpha) = \pi_y(L) - \pi_y(D) = \sin\alpha - \sin\Big((2n+1)\alpha\Big) \tag{5.4}$$

After some extensive trigonometry, we can reduce it into a more convenient form.

$$\begin{aligned} f(\alpha) &= \sin\alpha - (\sin\alpha\cos 2n\alpha + \sin 2n\alpha\cos\alpha) \\ &= \sin\alpha - \sin\alpha(\cos^2 n\alpha - \sin^2 n\alpha) - (2\sin n\alpha\cos n\alpha\cos\alpha) \\ &= 2\sin\alpha\sin^2 n\alpha - 2\sin n\alpha\cos n\alpha\cos\alpha \\ &= -2\sin n\alpha(-\sin\alpha\sin n\alpha + \cos n\alpha\cos\alpha) \\ &= -2\sin n\alpha\cos(n+1)\alpha \end{aligned} \tag{5.5}$$

If $\pi_y(D) < \pi_y(M_1) < \pi_y(L)$ then we can draw a segment connecting M_1 to the segment $\overline{CD}$ orthogonally. As in the previous lemma, this segment would extend to a periodic billiard path with symbolic period $Y_{n,1}$. Let us now check that $\pi_y(M_1) <$

$\pi_y(L)$. We compute

$$\pi_y(M_1) = \frac{-\sin\big((2n+1)\alpha\big) - \sin\big((2n-1)\alpha\big)}{2}$$

So $\pi_y(M_1) < \pi_y(L)$ whenever

$$\sin\big((2n-1)\frac{\pi}{2x}\big) > \sin\big((2n+1)\frac{\pi}{2x}\big)$$

Which is certainly true when $n+\frac{1}{2} < x < n+1$ (these angles are close to π). We will therefore assume that $\pi_y(M_1) < \pi_y(D)$ because otherwise M_1 projects orthogonally to the interval $\overline{CD}$ and we would have a periodic billiard path with symbolic period $Y_{n,1}$.

Now we will use the fact that the word X_n is a periodic billiard path in T_x. In the unfolding of the word $1(X_m)^\infty$, the vector $M_{i+1} - M_i$ is invariant under choice of i. Further $M_{i+1} - M_i$ travels in direction $(n+1)\alpha - \frac{\pi}{2}$. We denote the distance from M_i to M_{i+1} by l. Thus, $\pi_y(M_i)$ is an evenly-spaced increasing sequence. Let $g(\alpha) = \pi_y(M_{i+1}) - \pi_y(M_i)$ which depends on α. Using equation 5.3 we see

$$\begin{aligned} g(\alpha) &= l\sin((n+1)\alpha - \tfrac{\pi}{2}) \\ &= \Big(\sin((n-2)\alpha) + \sin(n\alpha)\Big)\Big(-\cos((n+1)\alpha)\Big) \\ &= -\cos((n+1)\alpha)(2\cos\alpha\sin((n-1)\alpha)) \\ &= -2\cos\alpha\sin((n-1)\alpha)\cos((n+1)\alpha) \end{aligned} \tag{5.6}$$

If $g(\alpha) < f(\alpha)$ then there must be an M_m which projects to $\overline{CD}$ under L as desired. From the formulas above we see that in fact,

$$\frac{f(\alpha)}{g(\alpha)} = \frac{\sin(n\alpha)}{\cos\alpha\sin((n-1)\alpha)} \tag{5.7}$$

The graph of this function of α is depicted in figure 5.6. When $n+\frac{1}{2} < x < n+1$, then $\frac{\pi}{2n+2} < \alpha < \frac{\pi}{2n+1}$. Therefore

$$0 < (n-1)\alpha < n\alpha < \tfrac{\pi}{2} \quad \text{and} \quad \sin(n\alpha) > \sin((n-1)\alpha) \tag{5.8}$$

So that $\frac{f(\alpha)}{g(\alpha)} = \frac{\sin(n\alpha)}{\cos\alpha\sin((n-1)\alpha)} > \frac{1}{\cos\alpha} > 1$. $\diamondsuit$

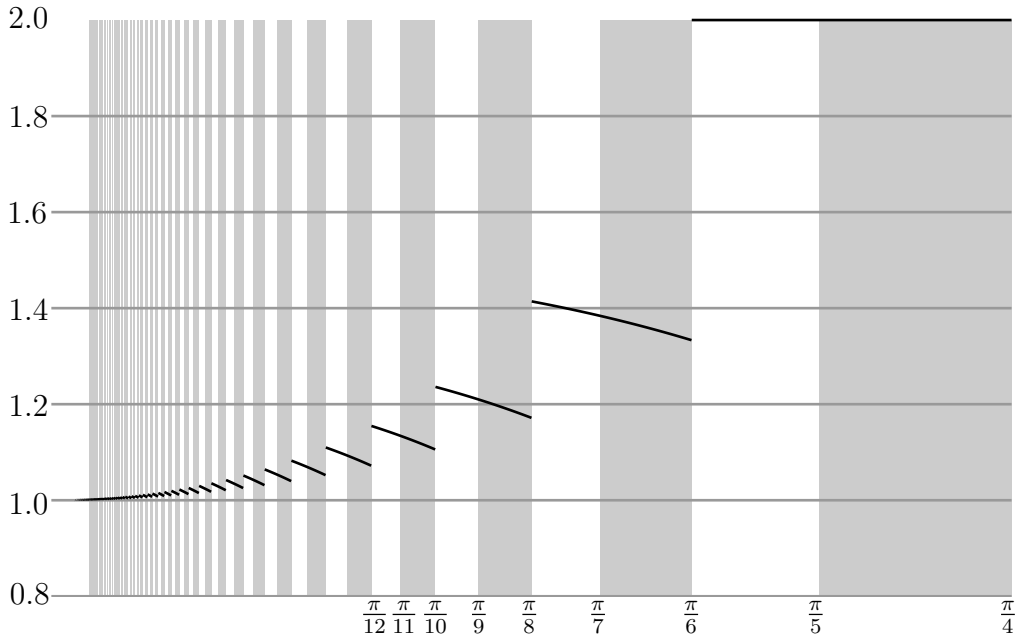

Figure 5.6: The graph of the ratio $\frac{f(\alpha)}{g(\alpha)}$ of equation 5.7 for $0 < \alpha < \frac{\pi}{4}$. We take the integer $n = \mathit{floor}(\frac{\pi}{2\alpha})$. The white regions are the values of α we consider in lemma 5.7.

Chapter 6

Veech's lattice property

Let us briefly review the definition of a translation surface.

A *translation surface* is a surface S together with a singular set Σ and an atlas of charts from $S \setminus \Sigma$ to the plane so that the transition functions are translations. The *singular set* is just a discrete set of cone points that have cone angles which are integer multiples of 2π. The *atlas of charts* is a covering of $S \setminus \Sigma$ by open sets U_i together with local homeomorphisms $\phi_i : U_i \to \mathbb{R}^2$. The *transition functions* are the maps $\phi_i \circ \phi_j^{-1}$ restricted to $\phi_j(U_i \cap U_j)$. The translation surface inherits the pull back metric from the plane and also the notion of direction. In the next chapter, we will be concerned with the translation surfaces of figure 6.1. A thorough discussion of these translation surfaces appears in the next section.

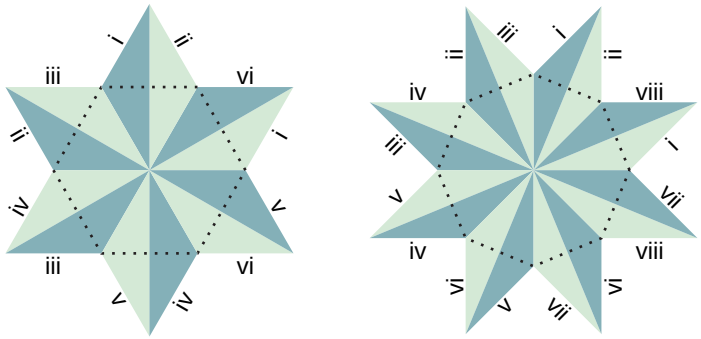

Figure 6.1: Translation surfaces built out of the triangles Δ_{2m} with angles $(\frac{\pi}{2m}, \frac{\pi}{2m}, \frac{(m-1)\pi}{m})$, for $m = 3, 4$. Notice that the same surface can be built out of two regular $2m$-gons, glued so that each edge of the first is glued to the opposite side of the second.

Let $\widehat{SL}(2, \mathbb{R})$ be the subgroup of the affine group of the plane which fixes the origin and preserves unsigned area. That is, $\widehat{SL}(2, \mathbb{R})$ is the Lie group

$$\widehat{SL}(2, \mathbb{R}) = \{M \in GL(2, \mathbb{R}) | Det(M) = \pm 1\} \tag{6.1}$$

This matrix group just acts linearly on points in $\mathbb{R}^2$ in the usual way.

There is an action of $\widehat{SL}(2,\mathbb{R})$ on translation surfaces. If $A \in \widehat{SL}(2,\mathbb{R})$ and S is a translation surface, then we build a new translation surface $A(S)$ by post-composing each chart map $\phi_i : U_i \to \mathbb{R}^2$ with A. The *Veech group* of a translation surface S is the subgroup $\Gamma(S) \subset \widehat{SL}(2,\mathbb{R})$ consisting of those $A \in \widehat{SL}(2,\mathbb{R})$ for which there is an isometry $f_A : S \to A(S)$ which preserves directions. The condition that it preserves directions is essential, since otherwise any rotation would be in the Veech group. Since the surfaces S and $A(S)$ are canonically homeomorphic under the action of A, the elements $\{f_A | A \in \Gamma(S)\}$ are homeomorphisms from the surface to itself. We therefore consider f_A to be an element of the mapping class group of the surface. These elements also permute the points in the singular set and preserve cone angles. We denote the mapping class group of the surface S fixing the singular set Σ by $\mathcal{MCG}(S,\Sigma)$ and use $V(S)$ to denote this particular subgroup.

A parabolic in $\widehat{SL}(2,\mathbb{R})$ is an element which fixes a single direction θ in $\mathbb{R}^2$, so it has a single eigenvector. Veech showed that having a parabolic in the Veech group has implications for the dynamics of the geodesic flow in the direction θ, namely all but finitely many geodesics traveling in the direction θ close up. A *saddle connection* is a geodesic segment which starts at a point on Σ and ends at a point on Σ but hits no elements of Σ on its interior.

Lemma 6.1 (Veech). *If $A \in \Gamma(S)$ is a parabolic preserving the direction θ, then there is a decomposition of the surface into cylinders by cutting along saddle connections in the direction of θ. The corresponding homeomorphism f_A acts as a Dehn twist in each of the cylinders.*

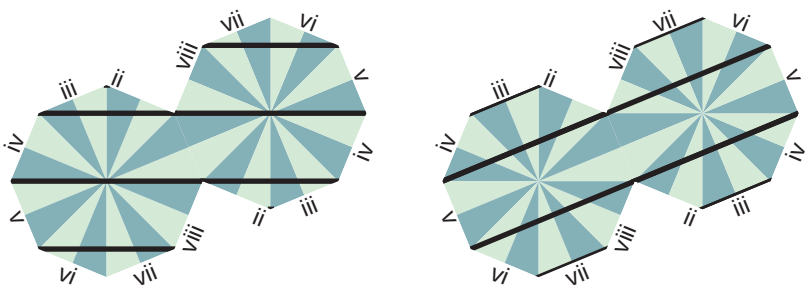

Figure 6.2: There is a parabolic which preserves each of these decompositions of a translation surface into cylinders.

Given a decomposition of a translation surface into parallel cylinders, a necessary and sufficient condition for there to be a parabolic automorphism fixing the direction of the decomposition is that the ratios of the lengths to the widths of the cylinders must be commensurable (differ by multiplication by a rational number). For example, consider the decompositions of the translation surface depicted in figure 6.2.

Assuming the radius of the octagons depicted in figure 6.2 is 1, the lengths and widths of each cylinder shown can be expressed in the form

$$l = 2\Big(\cos\big(\frac{\pi}{8}(k+1)\big) + \cos\big(\frac{\pi}{8}(k-1)\big)\Big)$$
$$w = \sin\big(\frac{\pi}{8}(k+1)\big) - \sin\big(\frac{\pi}{8}(k-1)\big)$$

for some integer k. The angle addition formulas can then be used to show that for each k

$$\frac{l}{w} = \frac{2\cos(\frac{\pi}{8})}{\sin(\frac{\pi}{8})}$$

Since this value is independent of k, it follows that there is are parabolic automorphisms of this surface which fix the directions of the cylinder decompositions. This example is a double cover of one of Veech's original examples. See [Vee89].

Veech showed that if the Veech group $\Gamma(S)$ is a lattice then the dynamics of the billiard flow satisfy a dichotomy. See [MT02] or [Vee89].

Theorem 6.2 (Veech dichotomy). *Suppose $\Gamma(S)$ is a lattice. It can not be cocompact. In every direction θ on the surface S the foliation of geodesics traveling in direction θ is either*

1. *completely periodic. That is, all leaves are closed or saddle connections.*
2. *minimal. Here, every leaf is dense.*

Furthermore, if the direction θ is completely periodic, then there is a parabolic in $\Gamma(S)$ which fixes the direction θ.

We can use these results to list off all the homotopy classes of $S \smallsetminus \Sigma$ containing geodesics.

Corollary 6.3. *Suppose S is a translation surface and $\Gamma(S)$ is a lattice. There is a finite list of homotopy classes of curves containing geodesics $[\gamma_1], \ldots, [\gamma_s]$ so that for every homotopy class $[\eta]$ containing a geodesic, the is an element of the Veech group $f_A \in V(S)$ so that $[\eta] = f_A([\gamma_i])$ for some i.*

Proof: $\widehat{SL}(2,\mathbb{R})/\pm 1$ acts as the isometry group of the hyperbolic plane $\mathbb{H}^2$. We look at the orbifold $X(S) = \mathbb{H}^2/\Gamma^+(S)$, where $\Gamma^+(S)$ is the orientation preserving subgroup of $\Gamma(S)$. (The surface $X(S)$ may have orbifold points coming from finite order elliptics in $\Gamma(S)$.) The orbifold $X(S)$ is known as the Teichmüller curve. $X(S)$ is a finite volume hyperbolic orbifold which must contain punctures, which we list off as $p_1, \ldots, p_s$. Each puncture p_i gives rise to a conjugacy class $[P_i]$ of parabolics in $\Gamma(S)$, realizing the holonomy of a loop traveling around p_i. We make an arbitrary choice of a parabolic $P_i \in [P_i]$ for each i. Veech's dichotomy tells us that in the direction fixed by P_i, there is a decomposition into cylinders $C_{i,j}$. For each cylinder, we get a homotopy class $[\gamma_{i,j}]$ containing a geodesic. Because every parabolic in

the Veech group is conjugate to some P_i, every homotopy class of S containing a geodesic is the image of one the homotopy classes $[\gamma_{i,j}]$ under an element of the Veech group $V(S) \subset \mathcal{MCG}(S, \Sigma)$. Indeed, since $V(S)$ is finitely generated, we can express the set of all closed geodesics on S with a finite amount of information. $\diamondsuit$

Chapter 7

Obtuse isosceles triangles with no stable periodic billiard paths

In this chapter we will prove the second half of theorem C mentioned in the introduction. We will demonstrate that there is a countable list of obtuse isosceles triangles that have no stable periodic billiard paths.

Theorem C2. *The obtuse isosceles triangles with angles*

$$(\pi/2^k, \pi/2^k, \pi - 2\pi/2^k)$$

do not admit any stable periodic billiard paths.

In some sense, this result is quite surprising. Schwartz was able to show that every obtuse triangle with largest angle less than 100 degrees admits a stable periodic billiard path.

7.1 The $(\frac{\pi}{2m}, \frac{\pi}{2m}, \frac{\pi(m-1)}{m})$ triangles

The triangles used in the theorem sit in a larger list of triangles that satisfy Veech's lattice property. Let Δ_{2m} denote the triangle with angles $(\frac{\pi}{2m}, \frac{\pi}{2m}, \frac{\pi(m-1)}{m})$. We build the minimal translation surface associated to these triangles, $MT_{\Delta_{2m}} = MT_{2m}$ as remark 4.4 in section 4.1. There is a natural folding map from $MT_\Delta \to \Delta$. We will say the singular set of MT_Δ is the subset $\Sigma \subset MT_\Delta$ which is mapped to the vertices of the triangle. The first two of these surfaces were shown in figure 6.1.

The surface MT_{2m} can also be constructed by taking two regular $2m$-gons and gluing each edge of the first polygon to the opposite edge of the second polygon. See figure 6.1. The surfaces MT_{2m} are double covers of Veech's original examples of a regular $2m$-gon with opposite edges identified (see [Vee89]).

Recall, $\mathcal{D}_{\Delta_{2m}}$ was the Euclidean cone surface which is the double of the triangle Δ_{2m} along its boundary. We denote $\mathcal{D}_{\Delta_{2m}}$ by $\mathcal{D}_{2m}$. The singular set of $\mathcal{D}_{2m}$ is the collection of cone points, Σ. The surface MT_{2m} is a branched cover of $\mathcal{D}_{2m}$ over the singular set Σ.

Each translation surface MT_{2m} is a Veech surface. In order to use corollary 6.3 to list homotopy classes containing geodesics, we will need to understand the groups $\Gamma(MT_{2m}) \subset \widehat{SL}(2,\mathbb{R})$ and $V(MT_{2m}) \subset \mathcal{MCG}(S,\Sigma)$. These groups are closely related to triangle groups. We define the (∞,∞,∞) triangle group, $\mathcal{T}_\infty$, to be the free product $\mathbb{Z}_2 * \mathbb{Z}_2 * \mathbb{Z}_2$. Each $\mathbb{Z}_2$ factor is reflection one of the sides of a triangle. We specify generators for $\mathcal{T}_\infty$ in an alternate way:

$$\mathcal{T}_\infty = \langle i, j, D | i^2 = j^2 = (iD)^2 = 1 \rangle \tag{7.1}$$

The (m,∞,∞) triangle group, $\mathcal{T}_m$, is the $\mathcal{T}_\infty$ triangle modulo the additional relation, $(i \circ j)^m = 1$.

Proposition 7.1 (The groups $V(\boldsymbol{MT}_{2m})$). *The Veech group $V(MT_{2m})$ is isomorphic to the direct product $\mathcal{T}_{2m} \times \mathbb{Z}_2$. Take generators for $\mathcal{T}_{2m}$ as in equation 7.1 and use h to denote the generator of $\mathbb{Z}_2$. Let $\rho_{2m} : \mathcal{T}_{2m} \times \mathbb{Z}_2 \to V(MT_{2m})$ be this isomorphism. The generators act as follows*

1. *$\rho_{2m}(h)$ is the non-trivial automorphism of the cover mapping MT_{2m} to Veech's original surface obtained by gluing opposite sides of the regular $2m$-gon together by translations. In other words, the generator of the $\mathbb{Z}_2$ factor swaps the decomposition into two regular $2m$-gons shown in figures 7.1-7.3, preserving directions in the translation surface.*
2. *The action of $\rho_{2m}(i)$ is by Euclidean reflection in the horizontal lines shown in figure 7.1.*
3. *The action of $\rho_{2m}(j)$ is by Euclidean reflection in the nearly horizontal lines show in figure 7.2.*
4. *The action of $\rho_{2m}(D)$ is by Dehn twists in the vertical cylinder decomposition. See figure 7.3.*

Consider the surjective group homomorphism

$$V(MT_{2m}) \to \Gamma(MT_{2m}) \subset \widehat{SL}(2,\mathbb{R})$$

which sends an automorphism of the surface MT_{2m} to the corresponding affine transformation of the plane. (This is the map $f_A \mapsto A$ in the notation of the previous chapter.) The kernel of this homomorphism consists of elements of $V(MT_{2m})$ which preserve directions on MT_{2m}. This is exactly the $\mathbb{Z}_2$ factor, since only $\rho_{2m}(h)$ preserves directions on MT_{2m}.

Proposition 7.2 (The Veech groups $\Gamma(\boldsymbol{MT}_{2m})$). *The Teichmüller curve, $X(MT_{2m}) = \mathbb{H}^2/\Gamma^+(MT_{2m})$, is a doubled hyperbolic triangle with two ideal vertices and one vertex with angle $\frac{\pi}{m}$. By corollary 6.3, up to the action of the Veech group, there are exactly two decompositions into parallel cylinders. We can choose the vertical and the slightly off-vertical direction. Figure 7.4 shows one curve in the center of every such cylinder.*

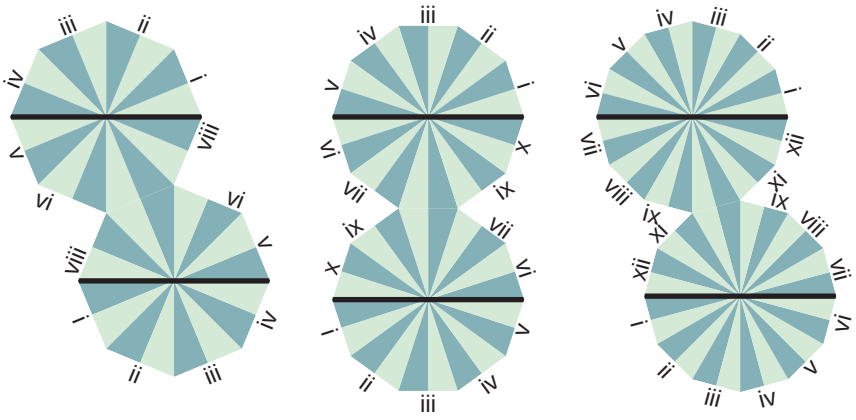

Figure 7.1: The generator $\rho_{2m}(i)$ acts by Euclidean reflection in these vertical lines.

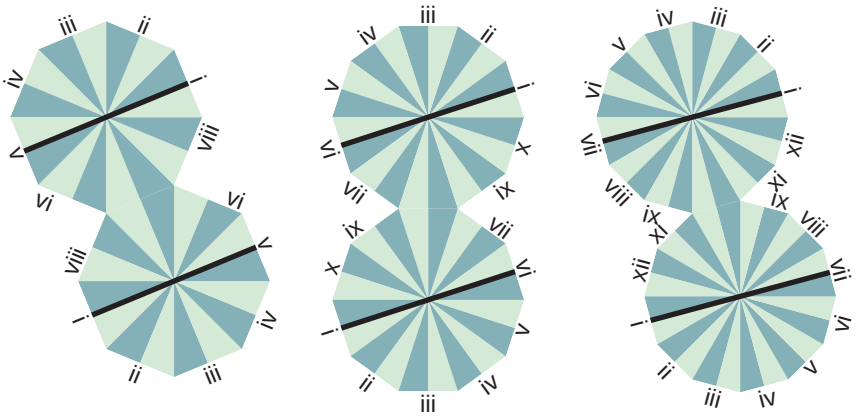

Figure 7.2: The generator $\rho_{2m}(j)$ acts by Euclidean reflection in these slightly off vertical lines.

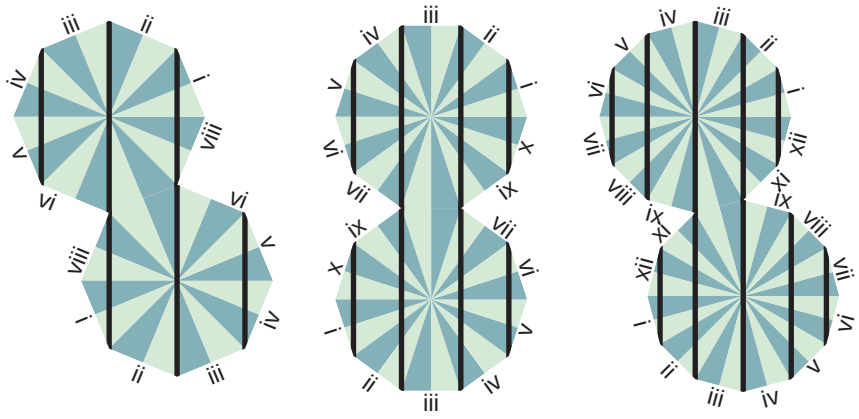

Figure 7.3: The generator $\rho_{2m}(D)$ acts by a Dehn twist in this vertical cylinder decomposition. All the cylinders depicted have the same moduli, so D acts by a single Dehn twist in each cylinder.

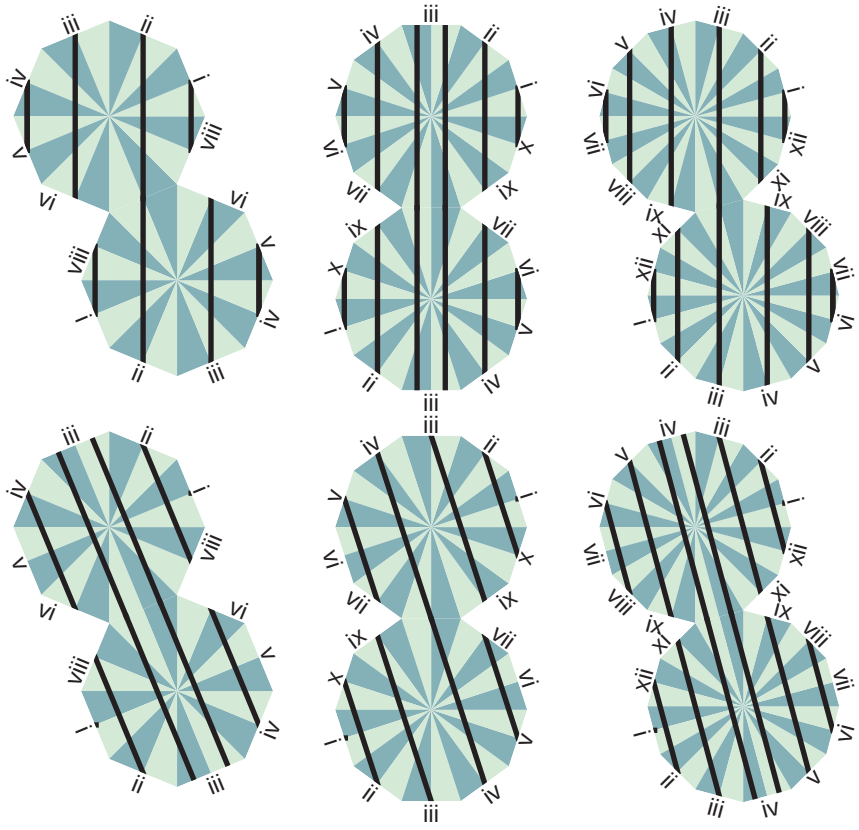

Figure 7.4: Every homotopy class containing a geodesic in MT_{2m} is the image of a homotopy class of curves in one of these two decompositions under $V(MT_{2m})$.

Let us now describe a minimal list of ingredients necessary to prove that Δ_{2m} has no stable periodic billiard paths, for m a power of two.

1. The minimal translation surface MT_{2m} with singular set Σ.
2. The group $V(MT_{2m})$ acting on the first homology group $H_1(MT_{2m} \smallsetminus \Sigma, \mathbb{Z})$.
3. A finite collection of homology classes $F_{2m} = \{[\![\gamma_1]\!], \ldots, [\![\gamma_{2m}]\!]\}$ (shown in figure 7.4). Under the action of $V(MT_{2m})$, this finite collection of curves hits every homology class which contains a geodesic by corollary 6.3.
4. The covering $\phi_{2m} : MT_{2m} \to \mathcal{D}_{2m}$.

Under these circumstances we know by theorem 3.1 corollary 6.3, that

Corollary 7.3. *If there is a stable periodic billiard path in Δ_{2m}, then there is a homology class $[\![\gamma_i]\!] \in F_{2m}$ and an element $f \in V(MT_{2m})$ so that*

$$\phi_{2m} \circ f([\![\gamma_i]\!]) = 0 \in H_1(\mathcal{D}_{2m} \smallsetminus \Sigma, \mathbb{Z})$$

We will use this idea to demonstrate the result that for m a power of two, Δ_{2m} has no stable periodic billiard paths. We break our argument into two cases. The first and easier case deals with the special pair of curves in F_{2m} which bound an annulus. See figure 7.5. In the second case we deal with the remaining curves.

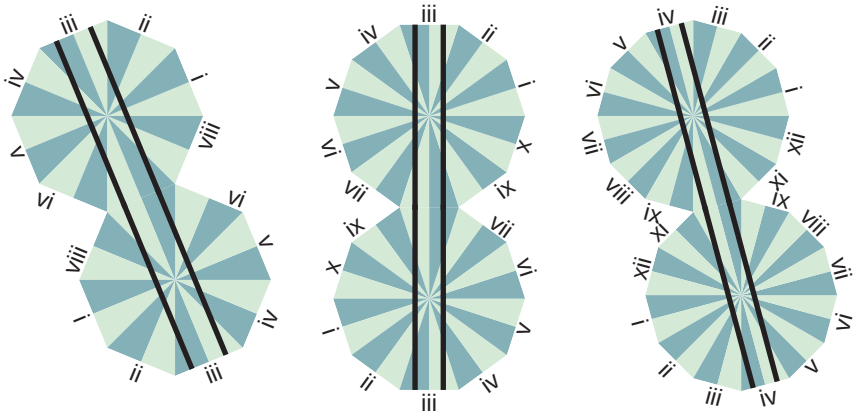

Figure 7.5: These pairs of curves bound an annulus in MT_{2m}.

7.2 Curves that bound an annulus

As in the right side of figure 7.6, we use A, B, and C to denote the cone points of $\mathcal{D}_{2m}$. We use ∂A and ∂B to denote curves in $\mathcal{D}_{2m} \smallsetminus \Sigma$ which travel around A and B respectively in the counter-clockwise direction. Then $[\![\partial A]\!]$ and $[\![\partial B]\!]$ generate $H_1(\mathcal{D}_{2m} \smallsetminus \Sigma, \mathbb{Z}) \cong \mathbb{Z}^2$.

Proposition 7.4. *If $[\![\gamma]\!] \in H_1(\mathcal{D}_{2m} \smallsetminus \Sigma, \mathbb{Z})$ is one of the homology classes of curves coming from figure 7.5 then for all $f \in V(MT_{2m})$*

$$\phi_{2m} \circ f([\![\gamma]\!]) = \pm m([\![\partial A]\!] + [\![\partial B]\!]) \neq 0 \in H_1(\mathcal{D}_{2m} \smallsetminus \Sigma, \mathbb{Z})$$

Proof: Call the two curves of figure 7.5 γ_1 and γ_2 and the annulus they bound $\mathcal{A}$. We orient the curves in opposite directions, so that $\partial\mathcal{A} = \gamma_1 \cup \gamma_2$ is the oriented boundary of the annulus the curves enclose. We label the points in the singular set of MT_{2m} by their images under the map $\phi_{2m} : MT_{2m} \to \mathcal{D}_{2m}$. See figure 7.6.

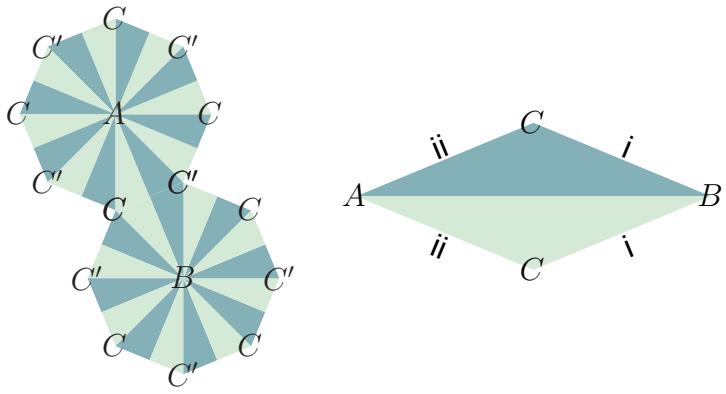

Figure 7.6: The points in the singular set of MT_{2m} labeled the same as their images in $\mathcal{D}_{2m}$. There is only one preimage of A and B, but there are two pre-images of C.

Note that there is an Euclidean isometry of MT_{2m} which acts as a rotation by π preserving the points A and B of figure 7.6. This isometry is an automorphism of the cover $\phi_{2m} : MT_{2m} \to \mathcal{D}_{2m}$. Therefore,

$$\phi_{2m}([\![\gamma_1]\!]) = \phi_{2m}([\![\gamma_2]\!]) \tag{7.2}$$

On MT_{2m}, the pair of curves $\gamma_1 \cup \gamma_2$ is homologically the same as a pair of loops, one of which travels around A once and the other which travels around B once. Therefore, the homology class $\phi_{2m}([\![\gamma_1]\!] + [\![\gamma_2]\!])$ wraps $2m$ times around the vertex A on $\mathcal{D}_{2m}$ and $2m$ times around the vertex B. Therefore, $\phi_{2m}([\![\gamma_1]\!] + [\![\gamma_2]\!])$ is not null homologous. By equation 7.2, it must be that $\phi_{2m}([\![\gamma_1]\!])$ wraps m times around both A and B therefore,

$$\phi_{2m}([\![\gamma_1]\!]) = m([\![\partial A]\!] + [\![\partial B]\!])$$

We can extend this argument to the curves $f(\gamma_1)$ and $f(\gamma_2)$ for all $f \in V(MT_{2m})$ if we can show $A, B \in f(\mathcal{A})$. This follows from the fact that the pair of points $A, B \subset MT_{2m}$ is fixed by the action of $V(MT_{2m})$, which is generated by $\rho_{2m}(h)$, $\rho_{2m}(i)$, $\rho_{2m}(j)$, and $\rho_{2m}(D)$. Recall proposition 7.1. From the description of these

actions, it is easy to verify

1. $\rho_{2m}(h)$ swaps A with B and preserves orientation.
2. $\rho_{2m}(i)$ and $\rho_{2m}(j)$ preserve both A and B, but reverse orientation.
3. If m is even, $\rho_{2m}(D)$ preserves A and B, and preserves orientation. In this case, A and B lie on the boundaries of the cylinders where Dehn twists are being performed. All points on the boundary of a cylinder where a Dehn twist is being preserved are fixed.
4. If m is odd, $\rho_{2m}(D)$ swaps A with B, and preserves orientation. Here, A and B lie in the center of a cylinder and are equally spaced apart. In the center of a cylinder, an affine Dehn twist moves points half way around the cylinder.

Therefore, for all $f \in V(MT_{2m})$, we know that

$$\phi_{2m} \circ f([\![\gamma_1]\!]) = \begin{cases} m([\![\partial A]\!] + [\![\partial B]\!]) & \text{if } f \text{ preserves orientation} \\ -m([\![\partial A]\!] + [\![\partial B]\!]) & \text{if } f \text{ reverses orientation} \end{cases}$$

$\diamondsuit$

7.3 The remaining curves

In this section we deal with curves that appear in figure 7.4, but not in figure 7.5. The central idea is to reduce via topological covering maps to the argument used in the previous section.

The singular set Σ associated to the surface MT_{2m}, has a pair removable singularities. The cone angles at the points A and B of figure 7.6 are 2π. Therefore, we can remove them from the singular set. We define the reduced singular set $\Sigma' = \Sigma \setminus \{A, B\}$.

Unfortunately, there is a cost for removing these singularities. Namely, the curves which travel once around A or B in MT_{2m} are null homologous in $MT_{2m} \setminus \Sigma'$, but not in $MT_{2m} \setminus \Sigma$. The homology classes of these curves are sent by $\phi_{2m} : MT_{2m} \setminus \Sigma \to \mathcal{D}_{2m}$ to $2m[\![\partial A]\!]$ and $2m[\![\partial B]\!]$ respectively. Therefore, we can only define the induced map on homology modulo $2m$. The induced map on homology gives the map:

$$\phi_{2m} : H_1(MT_{2m} \setminus \Sigma', \mathbb{Z}) \to H_1(\mathcal{D}_{2m}, \mathbb{Z}_{2m}) \tag{7.3}$$

The advantage of removing these singularities comes from a covering relationship between the objects involved. For any positive integer k, we can view the topological surface MT_{2km} as a k-fold branched cover of MT_{2m} branched over the points of Σ. Given MT_{2km}, the topological surface MT_{2m} can be obtained as MT_{2km} modulo the action of $(i \circ j)^{2m}$, which acts as a Euclidean rotation by $\frac{2\pi}{k}$ and preserves

the decomposition of MT_{2km} into regular $2km$-gons. Denote this covering map by $\psi_k : MT_{2km} \to MT_{2m}$. See figure 7.7.

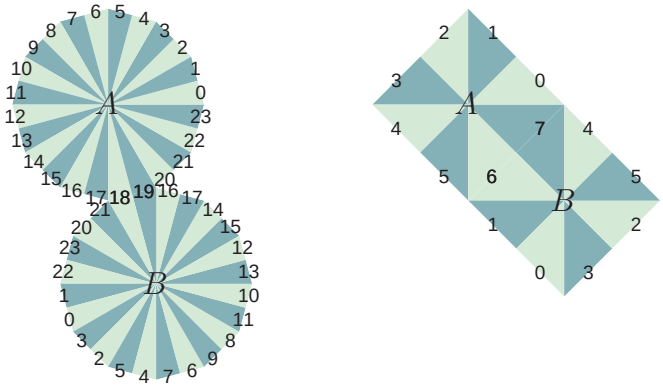

Figure 7.7: The cover $\psi_3 : MT_{12} \to MT_4$ sends triangles marked x to triangles marked $x \pmod 8$.

To carefully define this covering map, we number the triangles of MT_{2km} from 0 to $4km - 1$. We assign the numbers so that they increase as we travel in the counter-clockwise direction around A. We mark the triangles of MT_{2m} in the same manner from 0 to $4m-1$. Then we define the covering map ψ_k to be the map which preserves the labels at the points A and B and sends each triangle labeled t to the triangle labeled $t \pmod{4m}$.

We need to understand how these covering maps act on the objects we care about. Consider the collection of objects:

1. The surface MT_{2m} with singular set Σ'.
2. The group action $\rho_{2m} : \mathcal{T}_\infty \times \mathbb{Z}_2 \to Aut\big(H_1(MT_{2m} \smallsetminus \Sigma', \mathbb{Z})\big)$ generated by the actions $\rho_{2m}(h)$, $\rho_{2m}(i)$, $\rho_{2m}(j)$, and $\rho_{2m}(D)$.
3. The finite collection of homology classes F'_{2m} of curves appearing in figure 7.4, but not in figure 7.5.
4. The map on homology induced by the covering $MT_{2m} \to \mathcal{D}_{2m}$:

$$\phi_{2m} : H_1(MT_{2m} \smallsetminus \Sigma', \mathbb{Z}) \to H_1(\mathcal{D}_{2m} \smallsetminus \Sigma, \mathbb{Z}_{2m})$$

Remark 7.5. *In order to avoid inundating our argument with needless special cases, we note the objects we are considering are not geometric, but are topological. We defined the surfaces MT_{2m} for $m \geq 3$. We can also consider the translation surface surface MT_4 associated to the triangle Δ_4 with angles $(\frac{\pi}{4}, \frac{\pi}{4}, \frac{\pi}{2})$. We can define the surface MT_2 associated to the triangle Δ_2 with angles $(\frac{\pi}{2}, \frac{\pi}{2}, 0)$. Δ_2 is a degenerate triangle, which we can envision as an infinitely long rectangular strip (i.e. $\mathbb{R}_{\geq 0} \times$*

$[0,1]$*). For* MT_4 *everything we have discussed still makes sense.* MT_2 *is a standard infinite Euclidean cylinder with two punctures (A and B). Everything makes sense here except possibly the action of* $\rho_2(D)$*, which acts on homology as a Dehn twist in this cylinder. Even proposition 7.4 makes sense for these surfaces.*

The covering map ψ_k behaves nicely with respect to the collection of objects above.

Lemma 7.6. *The covering map* ψ_k *satisfies the following*

1. ψ_k *sends the singular set* $\Sigma' \subset MT_{2km}$ *to* $\Sigma' \subset MT_{2m}$*.*
2. *For all elements* $x \in \mathcal{T}_\infty \times \mathbb{Z}_2$*, there is an* $x' \in \mathcal{T}_\infty \times \mathbb{Z}_2$ *so that the following diagram commutes:*

$$\begin{array}{ccc} H_1(MT_{2km} \smallsetminus \Sigma', \mathbb{Z}) & \xrightarrow{\rho_{2km}(x)} & H_1(MT_{2km} \smallsetminus \Sigma', \mathbb{Z}) \\ \psi_k \downarrow & & \psi_k \downarrow \\ H_1(MT_{2m} \smallsetminus \Sigma', \mathbb{Z}) & \xrightarrow{\rho_{2m}(x')} & H_1(MT_{2m} \smallsetminus \Sigma', \mathbb{Z}) \end{array} \tag{7.4}$$

3. *We use the identity map* $id : (\mathcal{D}_{2km}, \Sigma) \to (\mathcal{D}_{2m}, \Sigma)$ *to identify the two spheres and the labeled cone points. The following diagram commutes*

$$\begin{array}{ccc} H_1(MT_{2km} \smallsetminus \Sigma', \mathbb{Z}) & \xrightarrow{\phi_{2km}} & H_1(\mathcal{D}_{2km} \smallsetminus \Sigma, \mathbb{Z}_{2km}) \\ \psi_k \downarrow & & id \downarrow \\ H_1(MT_{2m} \smallsetminus \Sigma', \mathbb{Z}) & \xrightarrow{\phi_{2m}} & H_1(\mathcal{D}_{2m} \smallsetminus \Sigma, \mathbb{Z}_{2m}) \end{array} \tag{7.5}$$

Proof: Item 1 is trivial. Item 3 follows from the fact that MT_{2m} is an intermediate branched covering of $MT_{2km} \to \mathcal{D}_{2km} = \mathcal{D}_{2m}$.

Item 2 is much more difficult, and slightly tedious. We postpone the proof of this fact until the next section. $\diamondsuit$

The point of this lemma, is the following

Corollary 7.7. *Suppose* γ *is a curve on* MT_{2km} *and* $\eta = \psi_k(\gamma)$ *is its image in* MT_{2m}*. If for all* $x \in \mathcal{T}_\infty \times \mathbb{Z}_2$*,*

$$\phi_{2m} \circ \rho_{2m}(x)([\![\eta]\!]) \neq 0 \in H_1(\mathcal{D}_{2m} \smallsetminus \Sigma, \mathbb{Z}_{2m}) \tag{7.6}$$

then for all $x \in \mathcal{T}_\infty \times \mathbb{Z}_2$*,*

$$\phi_{2km} \circ \rho_{2km}(x)([\![\gamma]\!]) \neq 0 \in H_1(\mathcal{D}_{2km} \smallsetminus \Sigma, \mathbb{Z}_{2km}) \tag{7.7}$$

Proof: Assume statement 7.6. By the lemma, for all $x \in \mathcal{T}_\infty \times \mathbb{Z}_2$, there is an $x' \in \mathcal{T}_\infty \times \mathbb{Z}_2$ so that the following diagram commutes:

$$\begin{array}{ccccc} H_1(MT_{2km} \setminus \Sigma', \mathbb{Z}) & \xrightarrow{\rho_{2km}(x)} & H_1(MT_{2km} \setminus \Sigma', \mathbb{Z}) & \xrightarrow{\phi_{2km}} & H_1(\mathcal{D}_{2km} \setminus \Sigma, \mathbb{Z}_{2km}) \\ \downarrow{\scriptstyle \psi_k} & & \downarrow{\scriptstyle \psi_k} & & \downarrow{\scriptstyle id} \\ H_1(MT_{2m} \setminus \Sigma', \mathbb{Z}) & \xrightarrow{\rho_{2m}(x')} & H_1(MT_{2m} \setminus \Sigma', \mathbb{Z}) & \xrightarrow{\phi_{2m}} & H_1(\mathcal{D}_{2m} \setminus \Sigma, \mathbb{Z}_{2m}) \end{array} \tag{7.8}$$

Since $\phi_{2m} \circ \rho_{2m}(x')([\![\eta]\!]) \neq 0 \in H_1(\mathcal{D}_{2m} \setminus \Sigma, \mathbb{Z}_{2m})$ for all x', statement 7.7 must hold as well. $\diamondsuit$

Now we can prove theorem C 2. Recall, the theorem stated that the triangles with angles $(\pi/2^k, \pi/2^k, \pi - 2\pi/2^k)$ do not have any stable periodic billiard paths.

Proof of Theorem C 2: Assume m is a power of two. Let $2^k = 2m$. By corollary 7.3, it is sufficient to show that if γ is a curve which shows up in figure 7.4, then for all elements $x \in \mathcal{T}_\infty \times \mathbb{Z}_2$,

$$\phi_{2^k} \circ \rho_{2^k}(x)([\![\gamma]\!]) \neq 0 \in H_1(\mathcal{D}_{2^k} \setminus \Sigma, \mathbb{Z}) \tag{7.9}$$

Proposition 7.4 proved this statement for the special case of the curves appearing in figure 7.5.

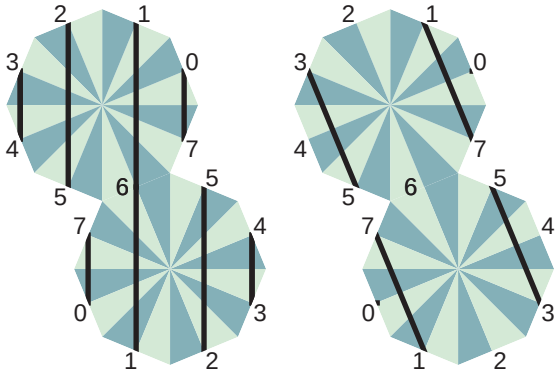

Figure 7.8: The remaining curves dealt with in the proof of Theorem C 2 for $m = 4$.

The remaining curves are depicted in figure 7.8. We organize this list by numbering the midpoint in the long side of the each isosceles triangle in MT_{2^k}. We use elements of $\mathbb{Z}_{2^k}$ and number counter-clockwise around the top 2^k-gon. Our curves are labeled $\gamma(a, b)$ for $a, b \in \mathbb{Z}_{2^k}$. Note that the difference $a - b \pmod{2^k}$ is never equal to 0 or 2^{k-1}. Then we can find an $1 \leq j < k$ so that

$$a - b \equiv 2^{j-1} \pmod{2^j}$$

(Choose $j-1$ to be the biggest power of two dividing $a-b$.)

Consider the branched cover $\psi_{2^{k-j}} : MT_{2^k} \to MT_{2^j}$. The image $\eta = \psi_{2^{k-j}}(\gamma(a,b))$ is a curve which travels from a midpoint marked $a \pmod{2^j}$ to a midpoint marked $a + 2^{j-1} \pmod{2^j}$. After a rotation (of the form $\rho_{2^j}((i \circ j)^n)$ for some n) we can see η is homologically equivalent to one of the special curves of figure 7.5. Then by proposition 7.4, for all $x \in \mathcal{T}_\infty \times \mathbb{Z}_2$,

$$\phi_{2^j} \circ \rho_{2^j}(x)([\![\eta]\!]) = 2^{j-1}([\![\partial A]\!] + [\![\partial B]\!]) \neq 0 \in H_1(\mathcal{D}_{2m} \smallsetminus \Sigma, \mathbb{Z}_{2^j})$$

Finally by corollary 7.7, it follows that for all $x \in \mathcal{T}_\infty \times \mathbb{Z}_2$,

$$\phi_{2^k} \circ \rho_{2^k}(x)([\![\gamma]\!]) \neq 0 \in H_1(\mathcal{D}_{2m} \smallsetminus \Sigma, \mathbb{Z}_{2^k})$$

and therefore $\phi_{2^k} \circ \rho_{2^k}(x)([\![\gamma]\!])$ is not equal to zero in $H_1(\mathcal{D}_{2m} \smallsetminus \Sigma, \mathbb{Z})$ either. $\diamondsuit$

7.4 Proof of Lemma 7.6, item 2

Proof of Lemma 7.6, item 2: We prove the statement on the generators h, i, j, and D.

1. The action of $\rho_{2km}(i)$ on triangles marked as in figure 7.7 sends triangles marked t to a triangle marked $-1-t \pmod{4km}$. If we reduce this map modulo $4m$, then we see $t \mapsto -1-t \pmod{4m}$. Thus, the diagram commutes for $x = i$ and $x' = i$.

2. $\rho_{2km}(j)$ acts on the marked triangles as $t \mapsto 1-t \pmod{4km}$. Again, this reduces to the action of $\rho_{2m}(j)$ modulo $4m$.

3. The action of $\rho_{2km}(h)$ on the marking is

$$t \mapsto \begin{cases} t + 2km + 1 \pmod{4km} & \text{if } t \text{ is even} \\ t + 2km - 1 \pmod{4km} & \text{if } t \text{ is odd} \end{cases}$$

   If k is odd then $2km \equiv 2m \pmod{4m}$ and so if $x = h$ we can choose $x' = h$. If k is even, then we need to find an x' which preserves the triangulation and sends

$$t \mapsto \begin{cases} t + 1 \pmod{4m} & \text{if } t \text{ is even} \\ t - 1 \pmod{4m} & \text{if } t \text{ is odd} \end{cases}$$

   We can choose $x' = h \circ (i \circ j)^m$. The action of the $(i \circ j)^m$ rotates the top $2m$-gon by π about A.

4. We will show for $x = D$ we can take $x' = D$. This argument is longer, so we continue it below:

To analyze the case $x = D$, we introduce a useful organizing proposition:

Proposition 7.8. *Let $\psi : S_1 \to S_2$ be a branched cover between surfaces. Let $\gamma = \{\gamma_1, \ldots, \gamma_n\}$ be a collection of curves on S_1 and let η be a curve on S_2. Let D_γ and D_η denote the action of Dehn twists in the curve families on the homology groups $H_1(S_1)$ and $H_1(S_2)$ respectively. Then the diagram*

$$\begin{array}{ccc} H_1(S_1) & \xrightarrow{D_\gamma} & H_1(S_1) \\ {\scriptstyle\psi}\big\downarrow & & {\scriptstyle\psi}\big\downarrow \\ H_1(S_2) & \xrightarrow{D_\eta} & H_1(S_2) \end{array}$$

commutes if

1. *for all $\gamma_i \in \gamma$, we have $\psi([\![\gamma_i]\!]) = [\![\eta]\!]$, and*
2. *$[\![\gamma]\!] = [\![\psi^{-1}(\eta)]\!]$.*

Proof: Let i denote the algebraic intersection between two homology classes. The action of $D_\eta \circ \psi$ is given by

$$D_\eta \circ \psi([\![x]\!]) = \psi([\![x]\!]) + i([\![\eta]\!], \psi([\![x]\!]))[\![\eta]\!] \tag{7.10}$$

The action of D_γ on homology is

$$D_\eta([\![x]\!]) = [\![x]\!] + \sum_{j=1}^{n} i([\![\gamma_j]\!], [\![x]\!])[\![\gamma_j]\!]$$

When composed with ψ, by item 1 we see

$$\psi \circ D_\eta([\![x]\!]) = \psi([\![x]\!]) + \Big(\sum_{j=1}^{n} i([\![\gamma_j]\!], [\![x]\!])\Big)[\![\eta]\!] \tag{7.11}$$

By item 2,

$$\sum_{j=1}^{n} i([\![\gamma_j]\!], [\![x]\!]) = i([\![\gamma]\!], [\![x]\!]) = i([\![\psi^{-1}(\eta)]\!], [\![x]\!]) = i([\![\eta]\!], \psi([\![x]\!])) \tag{7.12}$$

Thus, equations 7.11 and 7.12 can be combined and compared to 7.10 to see that $\psi \circ D_\eta([\![x]\!]) = D_\eta \circ \psi([\![x]\!])$. $\diamondsuit$

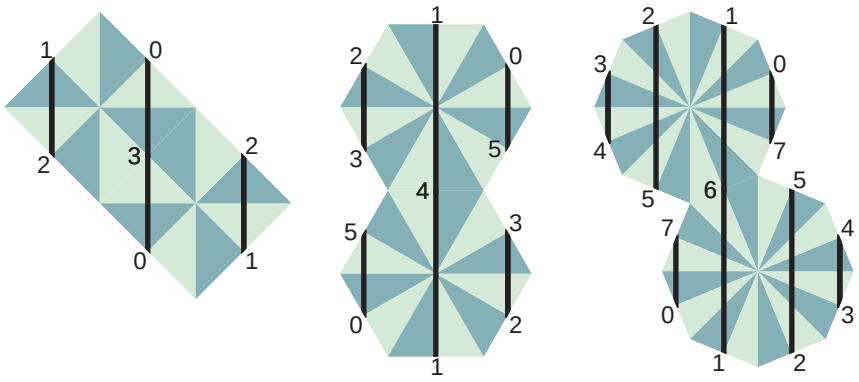

Figure 7.9: The Dehn twist D acts by twists in these curves. Compare to figure 7.3.

We will use this proposition to prove that the diagram

$$\begin{array}{ccc} H_1(MT_{2km} \setminus \Sigma', \mathbb{Z}) & \xrightarrow{\rho_{2km}(D)} & H_1(MT_{2km} \setminus \Sigma', \mathbb{Z}) \\ \psi_k \downarrow & & \psi_k \downarrow \\ H_1(MT_{2m} \setminus \Sigma', \mathbb{Z}) & \xrightarrow{\rho_{2m}(D)} & H_1(MT_{2m} \setminus \Sigma', \mathbb{Z}) \end{array} \tag{7.13}$$

commutes. The curves that $\rho_{2km}(D)$ and $\rho_{2m}(D)$ twist in lie in the center of each of the vertical cylinders. These curves are depicted in figure 7.9. We need a naming scheme for the curves involved. Number the midpoints of the long edge of each triangle in the triangulation of MT_{2km} by the elements of $\mathbb{Z}/2km\mathbb{Z}$ as in the figure. Then, we describe the curves we are interested in by a pair of integers corresponding to the two labeled midpoints that the geodesic passes through. Let $\gamma(a, b)$ denote the geodesic loop on MT_{2km} which travels from a to b in the top $2km$-gon and then from b to a in the bottom $2km$-gon. The curves $\rho_{2km}(D)$ twists in are in the collection

$$\begin{aligned} \gamma = \{ \quad & \gamma(0, -1), \gamma(1, -2), \ldots, \\ & \gamma(km - 2, -km - 1), \gamma(km - 1, -km)\} \end{aligned} \tag{7.14}$$

Similarly, we label the midpoints of the long edges of the triangulation on MT_{2m} by the elements of $\mathbb{Z}/2m\mathbb{Z}$. Name geodesics which pass through the midpoints on MT_{2m}, $\eta(a, b)$, for elements a and b. The Dehn twist $\rho_{2m}(D)$ acts by Dehn twists in the curve family

$$\eta = \{\eta(0, -1), \eta(1, -2), \ldots, \eta(m - 1, -m)\} \tag{7.15}$$

The covering map ψ_k sends midpoints marked t to midpoints marked $t \pmod{2m}$. Therefore,

$$\psi_k([\![\gamma(a, b)]\!]) = [\![\eta(a \mod 2m, b \mod 2m)]\!] \tag{7.16}$$

We cannot apply proposition 7.8 directly, because η is a collection of curves. But we can apply it in pieces. Let $0 \leq a < m$ and let $\eta_a \in \eta$ denote the curve $\eta(a, -1-a)$ on MT_{2m}. Let $\gamma_a \subset \gamma$ be the collection of curves on MT_{2m} given by

$$\gamma_a = \{\gamma(a', -1-a') \text{ such that } a' \equiv a \pmod{2m} \text{ and } 0 \leq a' < 2km \}$$

This is the collection of curves in γ (with modified orientations) whose homology classes are sent to $[\![\eta_a]\!]$ by ψ_k. The curves in γ_a and η_a are shown in figure 7.10 for the parameters $m = 4$, $k = 3$, $a = 0$. I claim that the action of Dehn twisting in the collection of curves γ_a on MT_{2km} corresponds to a Dehn twist in the curve $\eta_a = \eta(a, -1-a) \in \eta$ on MT_{2m} in the sense that the following diagram commutes

$$\begin{array}{ccc} H_1(MT_{2km} \setminus \Sigma', \mathbb{Z}) & \xrightarrow{D_{\gamma_a}} & H_1(MT_{2km} \setminus \Sigma', \mathbb{Z}) \\ \psi_k \downarrow & & \psi_k \downarrow \\ H_1(MT_{2m} \setminus \Sigma', \mathbb{Z}) & \xrightarrow{D_{\eta_a}} & H_1(MT_{2m} \setminus \Sigma', \mathbb{Z}) \end{array} \tag{7.17}$$

To show this, we will verify the conditions of proposition 7.8. First note that by equation 7.16, we know that each curve $\gamma(a', -1-a') \in \gamma_a$ has the property that

$$\psi_k([\![\gamma(a', -1-a')]\!]) = [\![\eta_a]\!]$$

Therefore, to show this diagram commutes, it is enough to show that $[\![\gamma_a]\!] = [\![\psi_k^{-1}(\eta_a)]\!]$.

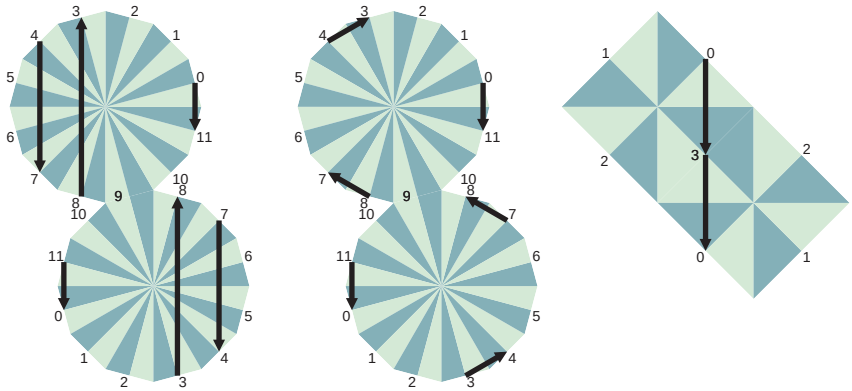

Figure 7.10: ϕ_3 is the covering $MT_{12} \to MT_4$. From left to right we show the curves in γ_0, $\psi_k^{-1}(\eta_0)$, and η_0.

Consider the collection of preimages of the curve $\eta_a = \eta(a, -1-a)$ under the covering ψ_k. η_a enters the top $2m$-gon through the midpoint a and leaves through $-1-a$. Therefore, $\psi_k^{-1}(\eta_a)$ enters the top $2km$-gon through midpoints marked $a' \equiv a \pmod{2m}$ and leaves the top $2km$-gon through midpoints marked $-1-a' \equiv -1-a$

(mod $2m$). Notice that this is the same collection of midpoints points that the curve family γ_a enters and leaves through.

To show that item 2 of proposition 7.8 hold, we will show that $[\![\gamma_a]\!] - [\![\psi_k^{-1}(\eta_a)]\!] = 0$ in $H_1(MT_{2km} \smallsetminus \Sigma', \mathbb{Z})$. Consider walking along a curve in γ_a in the top $2km$-gon until you hit a midpoint. Then we can continue by walking along a curve in $-\psi_k^{-1}(\eta_a)$ in the top $2km$-gon until we hit another midpoint. Then we can turn and walk along γ_a again staying within the top $2km$-gon. Eventually, our walk must close up. We can build a collection of curves in MT_{2km} in this way which is homologically equivalent to $[\![\gamma_a]\!] - [\![\zeta_a]\!]$. Each curve lies in the top or the bottom $2km$-gon, and is therefore contractible in $MT_{2km} \smallsetminus \Sigma'$. Thus $[\![\gamma_a]\!] - [\![\psi_k^{-1}(\eta_a)]\!] = 0$. We have demonstrated that diagram 7.17 holds.

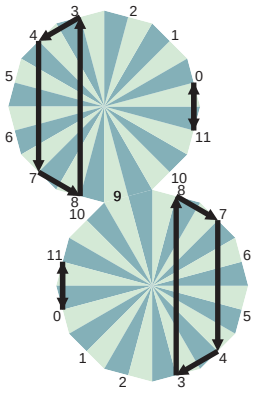

Figure 7.11: Continuing figure 7.10, we show the curves in $\gamma_2 - \zeta_2$.

The original curve collections γ and η of equations 7.14 and 7.15 satisfy

$$\gamma = \bigcup_{0 \le a < m} \zeta_a \quad \textit{and} \quad \eta = \bigcup_{0 \le a < m} \eta_a \tag{7.18}$$

up to sign (which is irrelevant since $D_c = D_{-c}$ for any curve c). Therefore, the commutativity of diagram 7.17 implies the commutativity of diagram 7.13. This concludes the proof of lemma 7.6. $\diamondsuit$

Chapter 8

Another Veech triangle

The goal of this chapter is to demonstrate theorem D from the introduction. The triangle Δ with angles $(\frac{\pi}{12}, \frac{\pi}{3}, \frac{7\pi}{12})$ is a *Veech polygon*. This example fits into an infinite class of examples of Veech surfaces discovered by McMullen [McM].

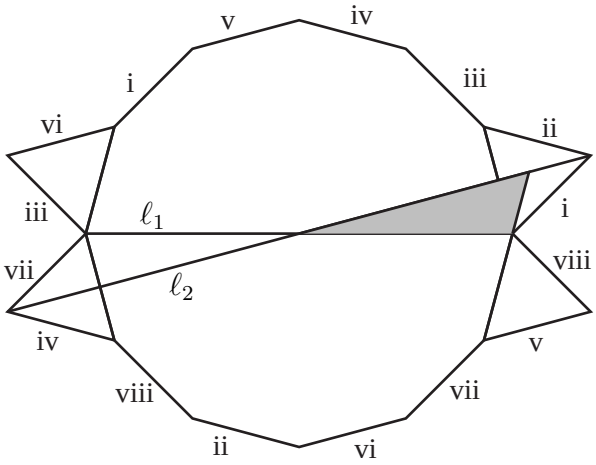

Figure 8.1: The surface MT_Δ together with the triangle $\Delta = (\frac{\pi}{12}, \frac{\pi}{3}, \frac{7\pi}{12})$ which generates it. The Roman numerals indicate edge identifications.

8.1 The translation surface

The translation surface MT_Δ constructed from the triangle $\Delta = (\frac{\pi}{12}, \frac{\pi}{3}, \frac{7\pi}{12})$ has genus 4 and has a single cone singularity with cone angle 14π. The surface is shown with the triangle in figure 8. We can also describe this surface as a regular 12-gon with equilateral triangles glued to every edge. Identify the triples of equilateral triangles which differ by translations.

8.2 The Proof

The group $\widehat{SL}(2,\mathbb{R})$ of equation 6.1 acts on the upper half-plane by hyperbolic isometries in the standard way. The upper half-plane is a subset of the Riemann sphere, $\hat{\mathbb{C}} = \mathbb{C}^2/(\mathbb{C} \smallsetminus \{0\})$. An element of $\widehat{SL}(2,\mathbb{R})$ acts on $\hat{\mathbb{C}}$ as follows:

$$\begin{pmatrix} a & b \\ c & d \end{pmatrix} \begin{pmatrix} z \\ w \end{pmatrix} = \begin{cases} \begin{pmatrix} az+bw \\ cz+dw \end{pmatrix} & \text{if } ad-bc = 1 \\ \begin{pmatrix} a\overline{z}+b\overline{w} \\ c\overline{z}+d\overline{w} \end{pmatrix} & \text{if } ad-bc = -1 \end{cases} \tag{8.1}$$

Note that this action is not faithful because $-I$ acts trivially.

Theorem 8.1. *Let Δ be the triangle with angles $(\frac{\pi}{12}, \frac{\pi}{3}, \frac{7\pi}{12})$. The surface MT_Δ is a Veech surface. A fundamental domain for the action of the Veech group $\Gamma(MT_\Delta)$ acting on the hyperbolic plane is shown in figure 8.2. The Veech group $\Gamma(MT_\Delta)$ is generated by reflections in the sides of this polygon together with $-I$.*

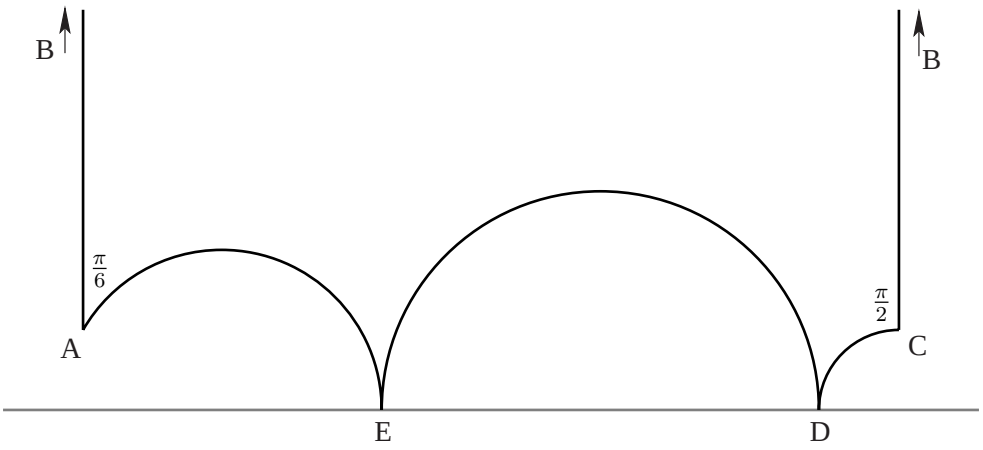

Figure 8.2: The fundamental domain for the action of $\Gamma(MT_\Delta)$ on the upper half-plane is the polygon pictured. The polygon is the hyperbolic convex hull of its vertices: $A = i$, $B = \infty$, $C = 5 + 3\sqrt{3} + i$, $D = 4 + 3\sqrt{3}$, and $E = 2 + \sqrt{3}$

We break up the proof into two lemmas.

Lemma 8.2. *Each of the reflections in the side of the polygon of figure 8.2 is in $\Gamma(MT_\Delta)$. $-I$ is also in $\Gamma(MT_\Delta)$.*

Proof: The surface MT_Δ has several Euclidean automorphisms. The element $-I$ acts on the plane by a Euclidean rotation by π. Thus, it is clear $-I \in \Gamma(MT_\Delta)$. The Euclidean automorphism group is generated by reflections in lines ℓ_1 and ℓ_2 of

figure 8. This gives two of our generators:

$$R_{\overline{AB}} = \begin{pmatrix} 1 & 0 \\ 0 & -1 \end{pmatrix} \quad R_{\overline{AE}} = \begin{pmatrix} \frac{\sqrt{3}}{2} & \frac{1}{2} \\ \frac{1}{2} & -\frac{\sqrt{3}}{2} \end{pmatrix} \tag{8.2}$$

Now we will find a parabolic automorphism of MT_Δ fixing the point B. There is a decomposition of MT_Δ by saddle connections parallel to ℓ_1 of figure 8. This decomposition is depicted in figure 8.3, and cuts the surface into 4 cylinders. The *modulus* of a cylinder is it's length around the central curve divided by its width. It can be verified that these cylinders come in pairs with two possible moduli:

$$5 + 3\sqrt{3} \text{ and } 10 + 6\sqrt{3} \tag{8.3}$$

In particular, note the second modulus is twice the first. Thus, there is a parabolic element of the automorphism group which fixes the horizontal direction and acts as a single Dehn twist on the pair of cylinders with modulus $10 + 6\sqrt{3}$ and a double Dehn twist on the pair of cylinders with modulus $5 + 3\sqrt{3}$. This parabolic is:

$$P_B = \begin{pmatrix} 1 & 10 + 6\sqrt{3} \\ 0 & 1 \end{pmatrix} \tag{8.4}$$

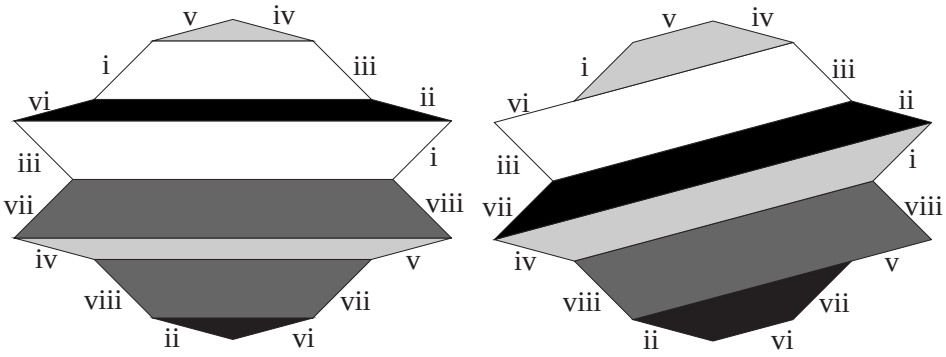

Figure 8.3: Decompositions into cylinders using saddle connections parallel to lines ℓ_1 and ℓ_2 of figure 8.

Both the reflection $R_{\overline{AB}}$ and the parabolic P_B fix the point B, so their composition does as well. Their composition gives another reflection:

$$R_{\overline{BC}} = P_B \circ R_{\overline{AB}} \begin{pmatrix} 1 & -10 - 6\sqrt{3} \\ 0 & -1 \end{pmatrix} \tag{8.5}$$

The same idea will work for generating a reflection preserving points E and D. We decompose MT_Δ into 4 cylinders using segments parallel to ℓ_2 of figure 8. This decomposition is shown on the right in figure 8.3. The moduli of these cylinders

again come in pairs:

$$\frac{6+4\sqrt{3}}{3} \text{ and } 6+4\sqrt{3} \tag{8.6}$$

This means that there is a parabolic inducing a single Dehn twist on the cylinders with moduli $6+4\sqrt{3}$ and a triple Dehn twist on the other cylinders. This parabolic is

$$P_E = \begin{pmatrix} \frac{1}{2}(-1-2\sqrt{3}) & \frac{1}{2}(12+7\sqrt{3}) \\ \frac{1}{2}(-\sqrt{3}) & \frac{1}{2}(5+2\sqrt{3}) \end{pmatrix} \tag{8.7}$$

Again we obtain $R_{\overline{DE}}$ by composition:

$$R_{\overline{DE}} = R_{\overline{AE}} \circ P_E = \begin{pmatrix} \frac{1}{2}(-3-\sqrt{3}) & \frac{1}{2}(13+7\sqrt{3}) \\ \frac{1}{2}(1-\sqrt{3}) & \frac{1}{2}(3+\sqrt{3}) \end{pmatrix} \tag{8.8}$$

We apply the same trick one last time. $R_{\overline{DE}}$ preserves two parallel families of lines on the surface, each corresponding to eigenvectors of the matrix. Of course, one is the family of lines parallel to ℓ_2. The second family has slope $\frac{1}{11}(-4+3\sqrt{3})$. We decompose the surface using saddle connections parallel to this direction (see figure 8.4). Again, these cut the surface into four cylinders whose moduli come in pairs. The moduli are

$$29+17\sqrt{3} \text{ and } 58+34\sqrt{3} \tag{8.9}$$

Therefore, we get a parabolic fixing lines of slope $\frac{1}{11}(-4+3\sqrt{3})$:

$$P_D = \begin{pmatrix} \frac{1}{2}(-11-7\sqrt{3}) & \frac{1}{2}(115+67\sqrt{3}) \\ \frac{1}{2}(-1-\sqrt{3}) & \frac{1}{2}(15+7\sqrt{3}) \end{pmatrix} \tag{8.10}$$

We compose the parabolic with the reflection $R_{\overline{DE}}$:

$$R_{\overline{CD}} = R_{\overline{DE}} \circ P_D = \begin{pmatrix} 5+3\sqrt{3} & -51-30\sqrt{3} \\ 1 & -5-3\sqrt{3} \end{pmatrix} \tag{8.11}$$

One way to check that lines $\overline{BC}$ and $\overline{CD}$ intersect at a right angle is to compute the trace product of reflections in the sides. If this trace is zero, then the sides meet at a right angle. We compute

$$Tr(R_{\overline{BC}} \circ R_{\overline{CD}}) = Tr \begin{pmatrix} -5-3\sqrt{3} & 53+30\sqrt{3} \\ -1 & 5+3\sqrt{3} \end{pmatrix} = 0 \tag{8.12}$$

$\diamondsuit$

Lemma 8.3. *The reflections in the side of the polygon of figure 8.2 together with $-I$ generate the Veech group $\Gamma(MT_\Delta)$.*

Proof: Let G be the group generated by $-I$ and the reflections in the sides of the polygon of figure 8.2, and let G^+ be the index 2 subgroup which preserves the orientation of $\mathbb{H}^2$.

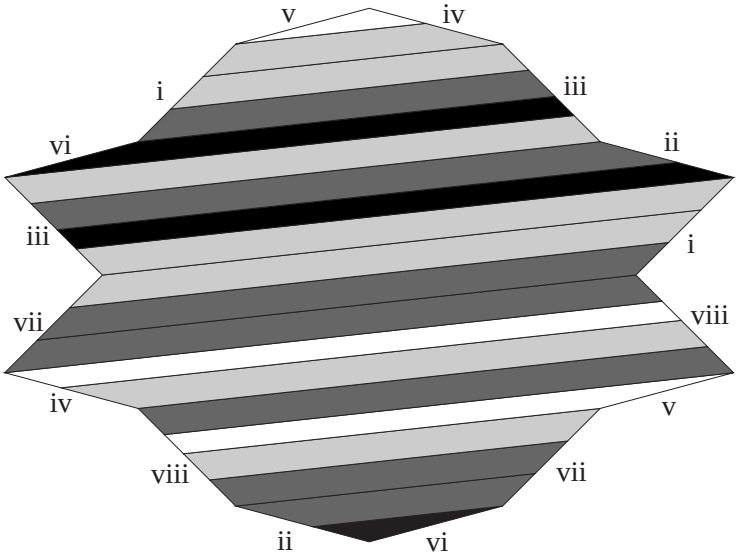

Figure 8.4: Saddle connections with slope $\frac{1}{11}(-4+3\sqrt{3})$ decompose the surface into these cylinders.

Let $X_G = \mathbb{H}^2/G^+$, a sphere with 3 punctures and two cone singularities. One singularity has cone angle π and the other has cone angle $\pi/3$. We can compute the area of X_G using the Gauss-Bonnet formula. Recall the Gauss-Bonnet formula for hyperbolic surfaces with cone singularities tells us that for a surface S of genus g with p punctures and cone singularities of cone angle $\theta_1, \ldots, \theta_n$,

$$area(S) = 2\pi(2g + p - 2) + \sum_{i=1}^{n}(2\pi - \theta_i) \tag{8.13}$$

We compute that $area(X_G) = \frac{14\pi}{3}$.

Now let V be the complete Veech group, V^+ be the orientation preserving subgroup, and $X_V = \mathbb{H}^2/V^+$. We wish to show $\Gamma(MT_\Delta) = G$. The previous lemma showed that G is a subgroup of V. Thus we have a covering map $\psi : X_G \to X_V$. Further we know that

$$[V^+ : G^+] = area(X_G)/area(X_V) \tag{8.14}$$

where $[V^+ : G^+]$ is the index of the subgroup G^+ inside V^+. In order to show that $V^+ = G^+$, it is sufficient to show $area(X_G)/area(X_V) < 2$.

We would like to use Gauss-Bonnet on X_V. First we will show that X_V also has 3 punctures. It is sufficient to show that none of the punctures of X_G can be identified by ψ. We will give affine invariants which distinguish the three decompositions into cylinders mentioned in the previous proof. The ratio of the moduli of the cylinders

associated to vertex E of the polygons is 3, while the ratios of the moduli of cylinders associated to B and D are both 2 (see equations 8.6, 8.3, and 8.9). Thus E can not be identified with B or D. Another affine invariant is the ratio of the widths of the cylinders. We can compute that these ratios are

$$w_B = 1 + \sqrt{3} \quad \text{and} \quad w_D = \tfrac{1+\sqrt{3}}{2} \tag{8.15}$$

Thus, the punctures coming from B and D cannot be identified by the covering ψ. This shows that X_V has 3 punctures.

We also need to show that X_V has at least one cone singularity. The image of a cone singularity in X_G must be a cone singularity in X_V. Further, the image of the cone singularity with cone angle $\pi/3$ must be a cone singularity with cone angle θ which is less than $\pi/3$. Gauss-Bonnet now tells us that

$$\textit{area}(X_V) \geq 2\pi(3-2) + (2\pi - \theta) \geq 4\pi - \pi/3 = 11\pi/3 > \frac{1}{2}\textit{area}(X_G) \tag{8.16}$$

Thus $\textit{area}(X_G)/\textit{area}(X_V) < 2$, so $[V^+ : G^+] = 1$ and $V^+ = G^+$.

Finally, because both V and G contain orientation reversing elements, we know $[V : G] = [V^+ : G^+]$. Thus $V = G$. $\diamondsuit$

Bibliography

[Hoo06] W. P. Hooper, *Periodic billiard paths in right triangles are unstable*, preprint, 2006.

[KS00] Richard Kenyon and John Smillie, *Billiards on rational-angled triangles*, Comment. Math. Helv. **75** (2000), no. 1, 65–108. MR MR1760496 (2001e:37046)

[McM] Curtis T. McMullen, *Prym varieties and Teichmüller curves*, Duke Math. J., To appear.

[MT02] Howard Masur and Serge Tabachnikov, *Rational billiards and flat structures*, Handbook of dynamical systems, Vol. 1A, North-Holland, Amsterdam, 2002, pp. 1015–1089. MR 1928530 (2003j:37002)

[PH92] R. C. Penner and J. L. Harer, *Combinatorics of train tracks*, Annals of Mathematics Studies, vol. 125, Princeton University Press, Princeton, NJ, 1992. MR 1144770 (94b:57018)

[Puc01] Jan-Christoph Puchta, *On triangular billiards*, Comment. Math. Helv. **76** (2001), no. 3, 501–505. MR 1854695 (2002f:37060)

[Sch06a] R. Schwartz, *Obtuse triangular billiards I: Near the (2,3,6) triangle*, to appear, 2006.

[Sch06b] ———, *Obtuse triangular billiards II: 100 degrees worth of periodic trajectories*, preprint, 2006.

[Tab95] Serge Tabachnikov, *Billiards*, Panor. Synth. (1995), no. 1, vi+142. MR 1328336 (96c:58134)

[Vee89] W. A. Veech, *Teichmüller curves in moduli space, Eisenstein series and an application to triangular billiards*, Invent. Math. **97** (1989), no. 3, 553–583. MR 1005006 (91h:58083a)

[VGS92] Ya. B. Vorobets, G. A. Gal′perin, and A. M. Stëpin, *Periodic billiard trajectories in polygons: generation mechanisms*, Uspekhi Mat. Nauk **47** (1992), no. 3(285), 9–74, 207. MR MR1185299 (93h:58088)

[Vor96] Ya. B. Vorobets, *Plane structures and billiards in rational polygons: the Veech alternative*, Uspekhi Mat. Nauk **51** (1996), no. 5(311), 3–42. MR 1436653 (97j:58092)

[War98] Clayton C. Ward, *Calculation of Fuchsian groups associated to billiards in a rational triangle*, Ergodic Theory Dynam. Systems **18** (1998), no. 4, 1019–1042. MR 1645350 (2000b:30065)